LABORATORY STUDY ON PRECIPITATION OF CALCIUM SULPHATE IN BEREA SANDSTONE CORES

Syed Jawwad Ahmed

A Thesis Presented to the
DEANSHIP OF GRADUATE STUDIES

KING FAHD UNIVERSITY OF PETROLEUM & MINERALS

DHAHRAN, SAUDI ARABIA

In Partial Fulfillment of the
Requirements for the Degree of

MASTER OF SCIENCE
In

PETROLEUM ENGINEERING

December, 2004

بسم الله الرحمن الرحيم

In the Name of Allah, Most Gracious, Most Merciful.

KING FAHD UNIVERSITY OF PETROLEUM & MINERALS
DHAHRAN 31261, SUADI ARABIA

DEANSHIP OF GRADUATE STUDIES

This thesis written by **Syed Jawwad Ahmed** under the direction of his thesis advisor and approved by his thesis committee has been presented to and accepted by the Dean of Graduate Studies, in partial fulfillment of the requirements for the degree of **MASTER OF SCIENCE IN PETROLEUM ENGINEERING**.

Thesis Committee

Dr. Sidqi A. Abu-Khamsin (Chairman)

Dr. Hasan S. Al-Hashim (Member)

Dr. Faizur-Rahman (Member)

Dr. Sidqi A. Abu-Khamsin
Department Chairman

Dr. Mohammad A. Al-Ohali
Dean of Graduate Studies

Date

Dedicated to My Beloved Parents whose constant prayers, sacrifice and inspiration led to this wonderful accomplishment

ACKNOWLEDGEMENTS

All praises and thanks are due to Allah (subhana wa taala) for bestowing me with health, knowledge and patience to complete this work. Thereafter, acknowledgement is due to KFUPM for the support given to this research through its tremendous facilities and for granting me the opportunity to pursue graduate studies with financial support.

I would like to acknowledge, with deep gratitude and appreciation, the inspiration, encouragement, valuable time and continuous guidance given to me by my thesis advisor Dr. Sidqi Ahmad Abu-Khamsin. My deep thanks are offered to my thesis committee members Dr. Faizur Rahman and Dr. Hasan S. Al-Hashim for their contribution and their critical review of this thesis.

I also acknowledge the sincere and invaluable help of Engr. Abdul Rahim Muhammadin in the experimental set-up, Mr. Khurshid Alam of CRP in the Research Institute for atomic absorption analysis, and Mr. Abdul Rashid of the Material Section in RI for SEM analysis utilized in this study.

Many thanks to the faculty and staff members of the Department of Petroleum Engineering for all the facilities and cooperation extended to me during my stay. I m especially indebted to the laboratory Staff, Mr. Mansour Al-Dhafeer, Mr. Abukari Iddris, Mr. AbdulSamad, Mr. Ahmad Al-Shuwaikhat and Mr. Mousa. Thanks to the Department secretary, Mr. Masroor Bakht, for his help and assistance.

Special thanks are due to my colleagues and friends at the University and my uncle Mr. Nasim Akhtar, who were always there to help me in my work and made my stay at the University memorable and source of valuable experience.

Finally, I am grateful to my dearest parents and all family members for their extreme moral support throughout my academic career and also for their love, patience, encouragement and prayers.

TABLE OF CONTENT

CHAPTER FIVE EXPERIMENTAL APPARATUS, MATERIALS AND PROCEDURE …………... 38

LIST OF TABLES

LIST OF FIGURES

NOMENCLATURE

s	Solubility (m^2)
m	Molality (moles / kg of solvent)
M	Molarity (mole/ liter of solution)
PPM	Parts per million (mg / liter of solution)
IP	Ionic Product (m^2 or M^2)
K_{sp}	Solubility Product (m^2 or M^2)
AS	Absolute Supersaturation (%)
PS	Percent Supersaturation (%)
SR	Supersaturation Ratio
Is	Ionic Strength (m or M)
TDS	Total Dissolved Solids (PPM)
γ	Activity Coefficient
K_{sp}^{o}	Thermodynamic Solubility Product (m^2 or M^2)
k	Kinetic rate constant
A	Frequency or Pre-Exponential Factor in Arrhenius Equation
E_A, E	Energy of Activation (kJ/mole)
R	Universal Gas Constant (J/mole.K)
T	Absolute Temperature (K)
SI, SS	Scaling Index (supersaturation level)
q	Reaction Rate (m/sec or M/sec)
Q	Injection Flow Rate (ml/min)

C_{Ca}	Concentration of Ca^{++} in the Solution (m or M or PPM)
C_{SO4}	Concentration of SO_4^{--} in the Solution (m or M or PPM)
Δt	Residence Time (min or sec)
V_p	Pore Volume (ml)
Co	Injected Concentration of Calcium (m or M or PPM)
ϕ	Porosity (%)
PVI	Pore Volume Injected
SEM	Scanning Electron Microscope
EDS	Energy Dispersive Spectrum
BEI	Backscattered Electron Image
L	Length of core (cm or inches)
D	Diameter of core (cm or inches)

THESIS ABSTRACT

Name of Researcher:	**Syed Jawwad Ahmed**
Title of Research Study:	**Laboratory Study on Precipitation of Calcium Sulphate in Berea Sandstone Cores**
Major Field:	**Petroleum Engineering**
Date of Degree:	**December 2004.**

Scale deposition is one of the most serious oil field problems that inflict water injection systems primarily when two incompatible waters are involved. Two waters are called incompatible if they interact chemically and precipitate minerals when mixed. Typical examples are sea water, with high concentration of SO_4^{-2}*, and formation waters, with high concentrations of* Ca^{+2}*,* Ba^{+2} *and* Sr^{+2}*. Mixing of these waters, therefore, could cause precipitation of* $CaSO_4$*,* $BaSO_4$*, and/or* $SrSO_4$*.*

Due to the lack of reaction kinetics data, the rate of calcium sulphate deposition in porous rock was measured through flooding Berea core samples of uniform properties with super-saturated brine. The brine was formulated at the core inlet by mixing two solutions containing Ca^{+2} *and* SO_4^{-2} *ions, separately. The rate of* $CaSO_4$ *scale formation was estimated by monitoring the core effluent's* Ca^{+2} *ion concentration. SEM & BMI analyses were also used to examine the nature of scale deposition throughout the core. Several parameters were varied including temperature, pressure, degree of brine super-saturation, and flooding velocity.*

The results indicated increased rate of $CaSO_4$ *precipitation at higher temperatures, higher flood velocities, and greater brine super-saturation, whereas pressure had a slight effect on* $CaSO_4$ *deposition. The results were utilized to build a general reaction rate equation to predict* $CaSO_4$ *deposition in Berea sandstone for a given temperature, brine super-saturation, and flooding velocity. The equation was validated by more experimental data with reasonable accuracy.*

Master of Science Degree
King Fahd University of Petroleum & Minerals
Dhahran-31261, Saudi Arabia
December 2004

ملخص البحث

الإسم : سيد جواد أحمد
عنوان البحث : دراسة مخبرية في ترسب كبريتات الكالسيوم في صخور بيريا الرملية
التخصص : هندسة البترول
تاريخ التخرج : ديسمبر 2004م

يعتبر ترسب القشرة المعدنية من أكثر مشاكل حقول الزيت جدية و التي تبتلى بها أنظمة حقن المياه ، خاصة عندما يختلط نوعان غير متساوقان من الماء . وينعت أي نوعين من المياه بأنهما غير متساوقين اذا أحدث مزجهما تفاعلاً كيميائياً ينتج عنه راسب معدني . و من الأمثلة التقليدية لذلك مياه البحر التي تحتوي على تركيزاً عالياً من أيون الكبريتات ، ومياه المكامن التي تحتوي على تركيزاً عالياً من أيونات الكالسيوم والباريوم والسترونشيوم . لذا فإن إختلاط هذه المياه قد يسبب ترسب كبريتات الكالسيوم اوكبريتات الباريوم أو كبريتات السترونشيوم .
ونظرا لندرة المعلومات المتوفرة عن كينتكية التفاعل ، تم قياس معدل ترسب كبريتات الكالسيوم في الصخور المسامية من خلال غمر عينات قورية من صخور البيريا ذات خواص منتظمة بأجاج فوق المشبع . و لقد تم توليف الأجاج عند مدخل القور عن طريق مزج محلولين يحتوي احدهما على أيون الكالسيوم والأخر على أيون الكبريتات . وتم تقدير معدل ترسب قشرة كبريتات الكالسيوم بمتابعة تركيز ايون الكالسيوم في الدفق الخارج من القور . و أستخدم ايضاً مجهر و مسبار الكترونيان لفحص طبيعة الراسب المعدني عبر العينة القورية . كما تم دراسة أثر تغيير عدة عوامل كالحرارة والضغط ودرجة فوق تشبع الأجاج وسرعة الازاحة .
اظهرت النتائج ازدياد معدل ترسب كبريتات الكالسيوم مع ازدياد كلا من درجة الحرارة وسرعة الازاحة ودرجة فوق تشبع الأجاج ، بينما كان للضغط تأثيرا طفيفا على ترسب كبريتات الكالسيوم . ولقد استخدمت هذه النتائج في استحداث معادلة عامة لمعدل التفاعل للتنبؤ بترسب كبريتات الكالسيوم في صخور بيريا الرملية عند ظروف معطاة من درجة الحرارة ودرجة فوق تشبع الأجاج وسرعة الازاحة . ولقد تم التثبت من صحة هذه المعادلة و بدقة معقولة باستخدام نتائج تجارب أخرى .

درجة الماجستير في العلوم
جامعة الملك فهد للبترول والمعادن
ديسمبر 2004م

Chapter 1

INTRODUCTION

Scale is inorganic mineral solids deposited out of a salt solution. For example, calcium carbonate scale forms when a calcium ion (Ca^{2+}) and a carbonate ion (CO_3^{2-}) dissolved in water react to form solid calcium carbonate ($CaCO_3$). The reaction is triggered when the product of the calcium and carbonate ion concentrations, known as the ionic product, exceeds the solubility product (K_{sp}) of calcium carbonate in water. The water is then characterized as supersaturated with respect to calcium carbonate and precipitation could occur.

$[Ca^{2+}][CO_3^{2-}] > K_{sp} \rightarrow$ Supersaturated Solution $\rightarrow$ $CaCO_{3\,(s)}$

There are other reasons why scale forms, and the amount and location of which are influenced by several factors. Yet, supersaturation is the most important reason behind mineral precipitation.

A supersaturated solution contains more ions than is thermodynamically possible, meaning that sooner or later a salt will precipitate. The degree of supersaturation, also known as the scaling index, is the driving force for the precipitation reaction and a high supersaturation, therefore, implies high possibilities for salt precipitation. The degree of supersaturation of a given salt is defined as:

$$\text{Degree of supersaturation} = \frac{IP}{K_{sp}} \times 100$$

where, IP is the ionic product and K_{sp} is the solubility product of the salt.

Changes in temperature, pressure, pH, and CO_2/H_2S partial pressure could also contribute in forming a scale [4, 5, 7, 9].

While supersaturation is a good indicator of the scaling tendency of a solution, it does not predict when and how fast scale will form. For such an exercise, the kinetics of scale formation must be known.

The kinetics of a reaction determine how fast a reaction proceeds in order to take the reacting system towards thermodynamic equilibrium. The kinetics are influenced by several factors with temperature being the most important. The precipitation rates for different salts vary significantly. Sodium chloride, NaCl, will precipitate spontaneously if it is supersaturated as compared to $CaCO_3$ and Ferrous Carbonate, $FeCO_3$, which could take several hours or days, even at high temperatures. Thus, the degree of supersaturation determines if a salt will precipitate or not, the kinetics will tell us how fast the precipitation reaction proceeds. It is therefore, necessary to include kinetic considerations when evaluating the scaling potential of a system.

The most common oil field scales are listed in Table1, along with the primary variables that affect their solubility [9]. These scales are typically the sparingly soluble sulphates and carbonates of calcium, strontium, and barium, and they include strontium

Table 1.1: Most Common Oilfield Scales

Name	Chemical Formula	Primary Variables
Calcium Carbonate	$CaCO_3$	Partial pressure of CO_2, temperature, total dissolved salts, pH
Calcium Sulphate:		Temperature, total dissolved salts, pressure
Gypsum	$CaSO_4.2H_2O$	
Hemi hydrate	$CaSO_4.1/\ 2H_2O$	
Anhydrite	$CaSO_4$	
Barium Sulphate	$BaSO_4$	Temperature, pressure total dissolved salts
Iron Compounds:		Corrosion , dissolved gases, pH
Ferrous Carbonate	$FeCO_3$	
Ferrous Sulphide	FeS	
Ferrous Hydroxide	$Fe(OH)_2$	
Ferric Hydroxide	$Fe(OH)_3$	

sulphate ($SrSO_4$), barium sulphate ($BaSO_4$), calcium sulphate ($CaSO_4.2H_2O$) and calcium carbonate ($CaCO_3$).

Scale deposition is one of the most important and serious problems that inflict oil field water injection systems. Scale limits and sometimes blocks oil and gas production by plugging the oil-producing formation matrix or fractures and perforated intervals. It can also plug production lines and equipment and impair fluid flow. The consequence could be production-equipment failure, emergency shutdown, increased maintenance cost, and overall decrease in production efficiency. The failure of these equipments could result in safety hazards. In case of water injection systems, scale could plug the pores of the formation and results in injectivity decline with time [3, 4, 6, 8, 11, 13, 14, 15, 17].

The chief source of oil field scale is mixing of incompatible waters. Two waters are called incompatible if they interact chemically and precipitate minerals when mixed. A typical example of incompatible waters are sea water with high concentration of SO_4^{-2} and low concentrations of Ba^{+2}/Sr^{+2}, and formation waters with very low concentrations of SO_4^{-2} but high concentrations of Ca^{+2}, Ba^{+2} and Sr^{+2}. Mixing of these waters, therefore, causes precipitation of $CaSO_4$, $BaSO_4$, and/or $SrSO_4$. Field produced water (disposal water) can also be incompatible with seawater. In cases where disposal water is mixed with seawater for re-injection, scale deposition is possible [3, 10, 12, 13, 14].

Scale deposition has been studied in the laboratory in numerous experiments to evaluate the scaling potential in a reservoir. On the basis of these laboratory experiments, different models that quantitatively evaluate scaling behavior have been developed and tested. The experiments include core flooding, core analysis [1, 2, 6, 8, 10], the use of glassware bead packs [1, 6] and the use of sand-packs [7].

On the basis of these experiments, theoretical models have been developed that estimate scaling potential using the available solubility data and thermodynamics. Models have been developed to predict the sulphate scaling tendency in oil-field operations15], to evaluate $BaSO_4$ scale [17], and to predict the presence of scale in production and injection processes based on kinetic data and thermodynamics [16, 18, 19].

In the next chapter, a detailed literature review is presented on problems related to scale in oil fields and on various scale prediction methods which are based on laboratory testing and modeling analysis.

Chapter 2

LITERATURE REVIEW

Considerable work has been conducted to study the problem of scaling in oil fields. In this chapter, laboratory investigations of scale in different media and procedures used to predict scale are presented. In addition, existing models on scale prediction are reviewed.

2.1. The Scaling Problem

Scale formation is a major problem in the oil industry. The costs due to the problem are high because scaling results in oil and gas production decline, frequently pulling of down-hole equipment for replacement, re-perforation of the producing intervals, re-drilling of plugged oil wells, stimulation of plugged oil-bearing formations, and other remedial workovers through production and injection wells. The following is a brief account of scaling cases reported in the literature.

Bayona [3] mentioned two major problems with seawater injection in the North Uthmaniyah section of the Ghawar field in Saudi Arabia. The first is maintenance of acceptable water quality and the second is control of plugging in the pores and corrosion in the equipment due to which excessive losses of well injectivity occur. The only cause of these losses is the deposition of scales due to the presence of salts in the injection water.

Asghari and Kharrat [6] reported water injectivity loss in the Siri field in Iran of over 75% within six years of injection. Field and laboratory data indicated that this loss of injectivity is the result of permeability reduction caused by fine particles migration and deposition in the rock pores.

Voloshin, et al. [8] described the problems of scale in some Western Siberian fields where formation pressure is maintained by injecting water (fresh water, Senoman reservoir water, and Podtovarnaya reservoir water). Electric submersible pumps (ESPs) and rod pumps are used to lift reservoir fluids to surface. Within the past two years, scale problems have increased greatly resulting in the failure of ESPs, which are widely used in the West Siberian oil fields. Investigation showed that carbonate deposit (calcite) is the main culprit, along with mechanical impurities. Iron deposits were present too. In 2003, the number of wells compromised by scale was approximately 1000.

Paulo, et al. [13] reported that a common problem in the Alba field in the North Sea resulted from injected seawater mixing with aquifer brines. Here, sulphate scale deposition is most severe in and around the injection and production well bores and can cause considerable disruption to hydrocarbon production after water breakthrough.

Moghadasi, et al. [9] investigated scale in the Iranian oilfields and found it to be a major operational problem causing formation damage either at injection or producing wells. It also contributes to equipment wear and corrosion and flow restrictions, thus resulting in a decrease in oil and gas production.

2.2 Scale Prediction

2.2.1 Laboratory Evaluation

Scale formation can be predicted by laboratory experiments. Several experimental studies have been conducted to determine the scaling potential in different oil-fields.

Peter and Jon [1] described a series of laboratory tests designed to evaluate the extent of formation damage which could result from scales formed within the porous rock. These tests were performed in glassware, bead packs, and synthetic alumina cores. Initially, the formation water and seawater were analyzed. Analyses showed that mixtures of these waters could precipitate both strontium and barium sulphate. The weights of these salts were calculated based on solubility products. To confirm these calculations, blends of both waters were mixed in glassware and the total amount of precipitate was determined by filtering and weighing. As a check, the precipitate was also re-dissolved in dilute HC1 and the concentrations of calcium, strontium, and barium were determined by atomic absorption analysis. These mixing tests were also conducted in a pack of 4 mm glass beads and in synthetic alumina cores that were 4 inches in length and $1\frac{1}{2}$ inches in diameter. No pressure was applied during a test but reservoir temperature of $70^{o}C$ was maintained. The core was first saturated with formation water and base permeability determined. Core flooding was done in varying proportions of seawater and formation water and pressure differential was continuously recorded throughout the flow. From the experimental results, it was found that formation damage occurred with highest amount of precipitation for lower proportion of seawater. At 10% seawater, rapid blocking was observed due to scale deposition, as there was a dramatic increase in the differential pressure.

Asghari and Kharrat [6] conducted core flooding experiments on 3 cm long and 2.5 cm diameter cores extracted from the Siri field in Iran. The core was dried and seawater filtered through a 10µ filter was injected at flow rates of 0.04 cm^3/s and 0.07 cm^3/s. In both cases, significant damage occurred during injection. Permeability loss was more than 50% for the injection rate of 0.04 cm^3/s and around 70% for the case of 0.07 cm^3/s injection rate. This indicated that filtration through a 10µ filter did not prevent permeability loss which occurred due to foreign particles from the seawater entering into the core and blocking the pore throats.

Voloshin, et al. [8] also performed core flooding tests for western Siberian oil fields. From their experiments they concluded that injected water salinity and the mineralogical composition of formation rock played an important role in the process of scaling in the reservoirs and the wells. During interaction with the rock, the injected water changed its ionic composition by becoming richer in either carbonates or sulphates, or both. Analysis showed that carbonates (calcium and magnesium), quartz, chlorite, and gypsum were present in the mineral composition of the scale deposits. While carbonates were amongst the main components of the deposits, chloride and gypsum were present in negligible quantities in every sample. In some deposits, siderite and iron oxide were present too.

Mitchell, et al. [21] performed an experiment to study the effect of incompatibility of injected water and formation water. They used a core with six injectors at one end and one outlet at the other end to simulate a production well. The flow rate was kept constant with a ratio of injected water to formation water of 1:10. They found that the injection pressure remained constant and then increased rapidly just before the core became completely blocked. They stated that scale deposition occurred around the surfaces of the pores. As more scale was deposited, the pore-throat flow area was reduced.

Lindlof and Stoffer [23] conducted a study on seawater injection incompatibility in Saudi Arabia. The laboratory tests showed no measurable reduction in permeability due to incompatibility effects between Arab-D formation water and seawater when the two waters mix in the pore channels during displacement of one water by the other. They reported that mixing of Arab-D water with seawater in various proportions demonstrated that strontium sulphate could be precipitated.

Betero, et al. [22] evaluated quantitatively the permeability reduction caused by scale formation in reservoir rock pores. They designed a piece of equipment that enabled two water streams to be continuously mixed in the pores of a core sample. One incompatible water was simulated with diluted sodium sulphate, the other was reservoir brine. The two waters were pumped simultaneously through the core at constant rates and at a constant ratio and the differential pressure between the inlet and outlet was measured. [26] At regular intervals, the core sample was withdrawn and weighed to determine the amount of scale present in the pores. They stated that the practice of running water-flood tests to evaluate the compatibility of injected water with reservoir brine was of limited value as only first contact phenomena were produced. Hence such test must be used for screening only.

Al-Mumen [26] performed compatibility tests at temperature of 90°C and overburden pressure of 1500 psia using Berea core and Arabian light crude oil. They showed that when connate Arab-D water was mixed with sea water, calcium sulphate precipitated. However, no kinetic data was reported.

McElhiney, et al. (2001) [31] conducted core flooding experiments at frontal velocities of 0.31 m/day in Berea sandstone cores to evaluate in-situ barium sulphate precipitation at ambient temperature (~ 70°F) and atmospheric pressure. Synthetic raw seawaters containing low and high sulphate contents were mixed with formation water containing dissolved barium ions before injection. The precipitation loss of $BaSO_4$ was observed by the measurement of the effluent profiles of sulphate ion. The results indicated that for low sulphate seawater, the barium sulphate scaling potential was reduced, which was also verified by SEM analysis.

Zhang and Farquhar [29] performed tube blocking tests using the conventional flooding method. Two separate solutions, one containing an anionic scaling ion (HCO_3^-) and the other containing a cationic scaling ion (Ca^{2+}), were injected through tubes of bore diameters ¼ inch and $^1/_{16}$ inch to obtain different flow velocities. As a result of this study the kinetic model for $CaCO_3$ scale prediction was updated to high temperatures (up to 180^oC), high pressures (up to 100 bar) and flow velocities up to 1.3 m/s. It was determined that $CaCO_3$ scaling rate was influenced by water flow velocity; i.e., in the low flow velocity range it increased sharply with an increase in flow velocity. The influence of pressure on $CaCO_3$ scaling rate was investigated and was found to decrease very slightly with an increase in pressure.

2.2.2 Model Development

Along with laboratory experiments, several models and, in later years, computer programs for scale prediction have been presented in the literature [9, 12, 13, 15, 16, 17, 18, 19].

Early models were fairly simple, they neglected various aspects that affect scaling, and as a result, large errors may occur in scale prediction at certain conditions. These models did not consider the pressure effect on scaling [24, 25]. Another shortcoming of these models lies in the assumption that salt solubility is a unique function of sodium chloride concentration or ionic strength [4, 24, 25]. Previous models considered the specific ion effect on solubility and predicted scale formation of only one mineral without considering the effect of potential scale formation of other minerals in the same solution.

Vetter et al. [24] reported a model for predicting simultaneous precipitation of $BaSO_4$, $SrSO_4$ and $CaSO_4$. They showed the effect of scaling of a less soluble sulphate, such as $BaSO_4$, on the precipitation of more soluble salts such as $SrSO_4$ and $CaSO_4$. The scale component having the smallest solubility product (K_{sp}), e.g. $BaSO_4$, precipitates first, thus removing some SO_4 ions from the solution. This is followed by the precipitation of the second component having the next larger K_{sp}, e.g. $SrSO_4$. The ionic product required for calculating this new precipitation is adjusted for the previous $BaSO_4$ precipitation. Finally the last component of this series, $CaSO_4$, will precipitate. The entire process is repeated for each set of thermodynamic conditions at which precipitation can occur.

Bertero, et al. [43] presented a numerical model which couples a reservoir fluid flow / thermal equilibrium simulator with a chemical equilibrium computer code. The code, derived from the EQ3/EQ6 software package developed by the Lawrence Livermore Laboratory, was used to calculate the chemical equilibrium between aqueous solution and minerals. The reservoir simulator, called AGIPS, is a finite-difference numerical model which calculates the evolution in time of the amount of scale formed in any point of the reservoir and inside the wells when changes occur in the temperature of the injected water and when the injection water mixes with reservoir brine. The model also calculates temperature and pressure profiles in the reservoir, together with their evolution in time, taking into account the permeability reduction caused by scale formation. For validation of their model, mixtures with different proportions of injection and reservoir water (taken from North African oil fields) were prepared and kept in a pressure vessel at reservoir conditions. The results obtained from the experiment matched the values predicted by the model, thus validating the numerical model.

Yuan and Todd [15] developed a model for predicting sulphate scaling problems caused by commingling of chemically incompatible waters as well as by temperature and pressure changes. This model is based on the Pitzer equation and has proved to be successful in calculating sulphate solubilities over wide ranges of solution compositions and temperature. The model is capable of predicting the scaling tendencies of $BaSO_4$, $SrSO_4$, and $CaSO_4$ at various water compositions, temperature, and pressures covering oil field conditions. The simultaneous co-precipitation of $BaSO_4$, $SrSO_4$, and $CaSO_4$, which is a common phenomenon in oilfield scale formation, is reflected in the model, allowing the effect of one sulphate scale formation on another to be taken into account. The experiments also determined whether the $CaSO_4$ scale was in the form of anhydride or gypsum and their corresponding sulphate scaling tendencies. The experiments determined which samples of injected water were likely to result in $SrSO_4$ deposition. This model was used in evaluating the sulphate scaling potentials resulting from mixing North Sea injection water with Forties formation water. The predicted scaling precipitation was substantiated by field observations.

Atkinson, et al. [46] developed a comprehensive scale prediction program for the prediction of oil field scales in single brines or brine mixtures. The effects of temperature, pressure, and ionic strength were considered using the classical thermodynamic approach. In all cases, the Pitzer equation with a semi-empirical extension was used. The effect of pressure was small and was ignored under most practical considerations.

All models mentioned above [4, 15, 17, 24, 25] are based on thermodynamics and use either solubility or thermo-chemical data. In most cases, the effect of ion pairs is ignored. The solubility data used are often limited and based on low temperature and pressure data. The following works do contain an element of kinetics.

Yeboah et al. [16] developed Oilfield Scale Prediction Model (OSPMod) which predicts the potential and deposition profile based on extensive thermodynamic and kinetic data. The first major step of the model is to use the input data (water analysis and thermo-chemical data) to determine the thermodynamic scaling potential. If scale is predicted to form, the next step is to use kinetic and well data to determine the scale deposition profile from bottom-hole to the surface. Thus, it computes the deposition profile as a function of position and time if a well is predicted to scale. In addition to the highly informative and attractive graphic display of results, the model provides extensive tabulation of the results including calculation of densities, activity coefficients, solubilities, supersaturations, solubility product constants, pH, saturation indices, velocity, amount and type of scale, and available cross sectional area at different positions and times. The model, however, does not predict scale formation within rocks.

Thomas, et al. [18] developed an expert system for prediction and analysis of the damage potential in the oil field during production and injection because of interactions between the fluids and the solid phase. These interactions are due to hydro-mechanical processes and/or changes in physiochemical conditions of the fluid (pH, temperature, ionic strength) and cause a reduction in the permeability of the reservoir rocks and technical equipment. The expert system FROCKI (Fluid-Rock-Interactions) is written in LISP as an object-oriented computer language to manage all these problems of oil fields.

Moghadasi, et al. [9] developed a model which is based on experimental data and empirical correlations, which perfectly match Iranian oil-field conditions where water injection is being performed. The first step of the model is to use the water analysis and physical conditions (temperature and Pressure) to determine the scaling potential. If scale is expected to form, the next step is to use kinetic and well data to compare the scale deposition. This model can be applied to predict scaling due to commingling of chemically incompatible waters within the system. The model predicted the effect of temperature, pressure and pH on scale formation. It was found that $CaCO_3$ scale formation increased with increase in temperature, a decrease in pressure and an increase in pH. The results obtained from the model were compared with field observations from Iranian oil fields and the model was found to be valid. The precision of the results was found to be affected only by the occurrence of water sampling and water analyzing. Calcium sulphate is not covered by the model.

Rousseau, et al. [19, 30] applied a thermo-kinetic model to predict scale in Angolan reservoirs which are dolomitic with temperatures ranging from 150 to 164^{o}C with a constant pressure (320 bar). Here, the kinetic module of the SCALE2000 software was used to explain the scaling phenomenon.

Mackay [38] developed a model for scale deposition, which was an extension of his work on mixing of injected, connate, and aquifer brines in water flooding and its relevance to oilfield scaling [40]. In this model, the location of maximum scale deposition and the resulting brine compositions at the production wells are calculated for a range of sensitivities, including reservoir geometry (1D, 2D aerial and vertical, and 3D), well geometry and the reaction rate. Limitation to his modeling work is lack of kinetic reaction rates. Mixing of brines in the well bore was not been discussed either.

From the above survey of the literature, it can be seen that most of the scaling models are based on the conventional thermodynamic approach. There is not enough data available to include kinetic aspects in predicting scale deposition with time. In addition, most of the flooding experiments conducted used different media like bead packs, sand packs, and alumina cores and were run at either low or specific temperatures and pressures.

Chapter 3

STATEMENT OF THE PROBLEM AND STUDY OBEJCTIVE

Seawater injection into Saudi Arabian reservoirs has been going on for decades for the purpose of pressure maintenance. Seawater contains significant concentrations of sulphate ion (greater than 4000 ppm) while reservoir water is rich in divalent cations such as Ca^{++} (greater than 7000 ppm). When these two incompatible waters mix, an unstable, supersaturated brine is created which precipitates calcium sulphate within the reservoir rock. Such scale deposition could have adverse effects on reservoir performance, primarily through damaging reservoir permeability.

To predict the formation of scale in a reservoir in time and space, a reservoir simulator must employ a sound kinetic model along with flow equations. In the literature review it has been observed that earlier attempts at scale prediction have not been good on kinetic grounds and do not have enough data for kinetic modeling.

Therefore, this study is focused on the measurement of the amount and rate of scale deposition in porous rock as a result of flowing a supersaturated brine through core samples at various conditions. The goal is to generate sufficient kinetic data that will help develop an empirical model for $CaSO_4$ scale formation considering kinetics and hydrodynamic parameters.

The methodology used to meet the objectives of this study shall employ a combination of experimental, theoretical and empirical techniques.

Chapter 4

THEORETICAL CONSIDERATIONS

This chapter presents the theoretical background of topics relevant to this study such as solubility and the kinetics and mechanism of scale formation. It also covers factors on which solubility depends. In addition, mixing of incompatible waters and its effect on scaling are also discussed.

4.1 Solubility and the Solubility Product (K_{sp})

When a sufficiently large amount of solute is maintained in contact with a limited amount of solvent, dissolution occurs continuously till the solution reaches a state when the reverse process becomes equally important. This reverse process is the return of dissolved species (atoms, ions, or molecules) to the undissolved state, a process called precipitation. When dissolution and precipitation occur continuously and at the same rate, the amount of dissolved solute present in a given amount of solvent remains constant with time. The process is one of dynamic equilibrium and the solution in this state of equilibrium is known as a saturated solution. The concentration of the saturated solution is referred to as the solubility of the solute in the given solvent. Thus solubility of a solute is defined as its maximum concentration which can exist in solution under a given set of conditions of temperature, pressure and concentration of other species in the solution. A solution that contains less solute than required for saturation is called an unsaturated solution. A solution, whose concentration is higher than that of a saturated solution due to any reason, such as change in other species concentration, temperature, etc., is said to be supersaturated. When the temperature or concentration of a solvent is increased, the solubility may increase, decrease, or remain constant depending on the nature of the system. For example, if the dissolution process is exothermic, the solubility decreases with increased temperature; if endothermic, the solubility increases with temperature. [60, 56].

Both unsaturated and saturated solutions are stable and can be stored indefinitely whereas supersaturated solutions are generally unstable. However, in some cases, supersaturated solutions can be stored for a long time without exhibiting any change and the period for which a supersaturated solution can be stored depends on the degree of departure of such a solution from the saturated concentration and on the nature of the substances in the solution [56].

The degree of supersaturation can be defined in two ways. One method is to measure the **absolute supersaturation (AS)** which can be represented as:

$$AS = C - C_{eq} \tag{4-1}$$

where C is the concentration of the dissolved substances in a given supersaturated solution and C_{eq} is its normal equilibrium saturation concentration.

The other method of expressing the degree of supersaturation is in terms of the **percent supersaturation (PS)**:

$$PS(\%) = \left[\frac{\left(C - C_{eq} \right)}{C_{eq}} \right] * 100 \qquad (4\text{-}2)$$

and the supersaturation ratio (SR):

$$SR = \frac{C}{C_{eq}} \qquad (4\text{-}3)$$

Solubility data of solutes provides a basis to establish saturation condition. A convenient method of discussing the solubility of a solute is by means of a solubility product (K_{sp}). Consider the addition of a solute MX $_{(s)}$ to distilled water. At the limit of solubility, there is a dynamic equilibrium which can be represented as follows:

$$MX_{(s)} \rightleftharpoons M^{+}{}_{(aq)} + X^{-}{}_{(aq)} \qquad (4\text{-}4)$$

and the equilibrium constant, $K_{sp}°$, for the solubility process is given as

$$K_{sp}{}^{o} = \frac{a\left[M^{+} \right] a\left[X^{-} \right]}{a\left[MX \right]} \qquad (4\text{-}5)$$

Since the activity, a, of a pure solid MX(s) is unity, the equilibrium expression simplifies to

$$K_{sp}{}^{o} = a\left[M^{+} \right] a\left[X^{-} \right] \qquad (4\text{-}6)$$

$K_{sp}°$ is known as the Solubility Product or sometimes the ‘Thermodynamic Solubility Product’ and it is a function of temperature and invariant with the ionic strength of the solution [47].

In any aqueous solution containing M^+ and X^- ions, as long as the activities $a[M^+]$ and $a[X^-]$ are such that their product is greater than $K_{sp}{}^{o}$ then some solid $MX_{(s)}$ should precipitate until the product of $a[M^+]$ and $a[M^-]$ becomes equal to $K_{sp}{}^{o}$.

For a general case:

$$M_pX_{q(s)} \rightleftharpoons pM^{q+}{}_{(aq)} + qX^{p-}{}_{(aq)} \tag{4-7}$$

$$K_{sp}{}^{o} = a\left[M^{q+}\right]^{p} a\left[X^{p-}\right]^{q} \tag{4-8}$$

$$K_{sp}{}^{o} = \left[C\left[M^{q+}\right]^{p} C\left[X^{p-}\right]^{q}\right]\left[\gamma\left[M^{q+}\right]^{p} \gamma\left[X^{p-}\right]^{q}\right] \tag{4-9}$$

where $\gamma[M^{q+}]^p$ and $\gamma[X^{p-}]^q$ are the activity coefficient of species M and X. If C $[M^{q+}]$ and C $[X^{p-}]$ are the concentrations, the mean activity coefficient of $M_p X_q$ is denoted as γ^{p+q} then

$$K_{sp}{}^{o} = \left[C\left[M^{q+}\right]^{p}\ C\left[X^{p-}\right]^{q}\right]\ \gamma^{(P+q)} \tag{4-10}$$

The solubility product expression can now be modified as follows

$$K_{sp} = \left[C\left[M^{q+}\right]^{p}\ C\left[X^{p-}\right]^{q}\right] \tag{4-11}$$

where K_{sp} is known as the Apparent Solubility Product and is related to the Thermodynamic Solubility Product as follows:

$$K_{sp} = \frac{K_{sp}{}^{o}}{\gamma^{p+q}} \tag{4-12}$$

If the ionic strength of the aqueous environment is low, the activity coefficient (γ) is unity (i.e. ideal behavior of solution is approached, in which activity and concentration can be equated) and the above expression reduces to an approximate form:

$$K_{sp}{}^{o} \approx K_{sp} \tag{4-13}$$

$$K_{sp} \approx \left[C \left[M^{q+} \right]^{p} C \left[X^{p-} \right]^{q} \right] \quad (4\text{-}14)$$

This form is frequently used in practice, where the true solubility product is expressed simply in terms of the concentrations of the ions.

4.2. Review of $CaSO_4$(Gypsum) Solubility Literature

Madgin and Swales [8] determined solubility of anhydrite ($CaSO_4$) in NaCl solutions at 25°C and of gypsum ($CaSO_4.2H_2O$) at 25 and 35 °C. They also studied the effect of Na_2SO_4 on solubility of gypsum in NaCl solutions. The solubility was found to peak at about 2.25 molal concentration of NaCl. Na_2SO_4, because of the well known common ion (SO_4^{--}) effect, significantly lowered the solubility of gypsum.

Marshall and Slusher [13] evaluated solubility of various forms of $CaSO_4$ (including gypsum) in NaCl solutions at various temperatures. They used the extended Debye-Huckel equation to correlate their gypsum data:

$\log K_{sp} = \log K_{sp}^{o} + 8A\sqrt{(I_s)} / (1 + Ba\sqrt{(I_s)}) + B (I_s) - C (I_s)^2$

The agreement between the predicted and experimental solubilities was quite good.

Power, et al. [9] extended their work on transition behavior of various forms of calcium sulphate and reported solubility data on gypsum in NaCl solution for temperatures ranging from 25 to 95 ^{0}C.

Ostroff and Metler [6] presented gypsum solubility data in the solutions of NaCl and $MgCl_2$ for the 28-90 ^0C temperature range. They correlated their data using the following regression equation:

$S = a + b\,[m\ NaCl] + c\,[m\ NaCl]^2 + d\,[m\ NaCl]^3 + e\,[m\ NaCl]^4$

Where,

S : gypsum solubility (gm/kg H_2O)

NaCl : molal conc. of NaCl solution

m : molal conc. of $MgCl_2$ solution

a, b, c, d, e : regression coefficients listed at several temperatures.

Their data showed that, for the same molal concentration or ionic strength, the gypsum solubility in $MgCl_2$ solution was significantly higher than in NaCl solution.

4.3. Factors Affecting Solubility of $CaSO_4$

The precipitation of calcium sulphate from water can be expressed as:

$Ca^{++} + SO_4^{--} \rightarrow CaSO_4$

and the solubility product is given by:

$K_{sp} = [Ca^{2+}]\,[SO_4^{2-}]$

The solubility product is a number which varies with temperature and concentration of total dissolved solids in the solution but is not appreciably affected by pressures encountered in oilfield operations. When the product of the calcium and sulphate ion concentrations exceeds this number, calcium sulphate precipitates until the product of the ion concentrations equals the solubility product.

The solubility of $CaSO_4$ is influenced by the following parameters:

1. Temperature
2. Pressure
3. Ionic strength

4.3.1 Effect of Temperature

The influence of temperature on the solubility of gypsum in distilled water is shown in Figure 4.1. This graph shows a slight increase in solubility up to about 40°C and then it decreases with increasing temperature. Above 50°C, the decrease in $CaSO_4$ solubility becomes more pronounced.

4.3.2 Effect of Ionic Strength

The concentration of a brine is typically represented by the brine's total dissolved solids (TDS). However, for matters relating to solubility and scaling, a more appropriate representative of the brine concentration is its ionic strength (I_s). I_s is defined as:

$$\mathbf{I_s = \Sigma \tfrac{1}{2} m z_i^2}$$

where, z_i : charge on each component in the solution

m : molal conc. of each component in the solution in molal

Figure 4.2 shows a strong influence of brine I_s on the $CaSO_4$ solubilities of Marshall and Slusher (1966) [13]. At low brine I_s, the solubility is seen to increase significantly with higher brine I_s. For all temperatures as shown in Figures 4.2, 4.3 and 4.4, the solubility first increases with brine I_s but tends to decrease or stabilize at low temperatures whereas at high temperatures the solubility tends to increase.

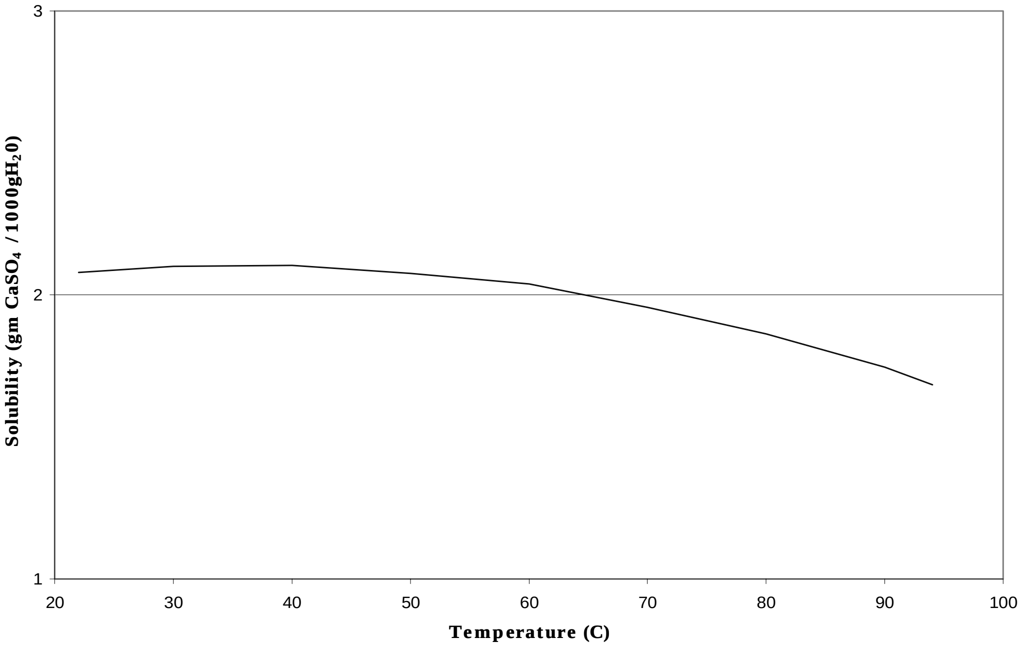

Figure 4.1: Effect of temperature on gypsum solubility [50]

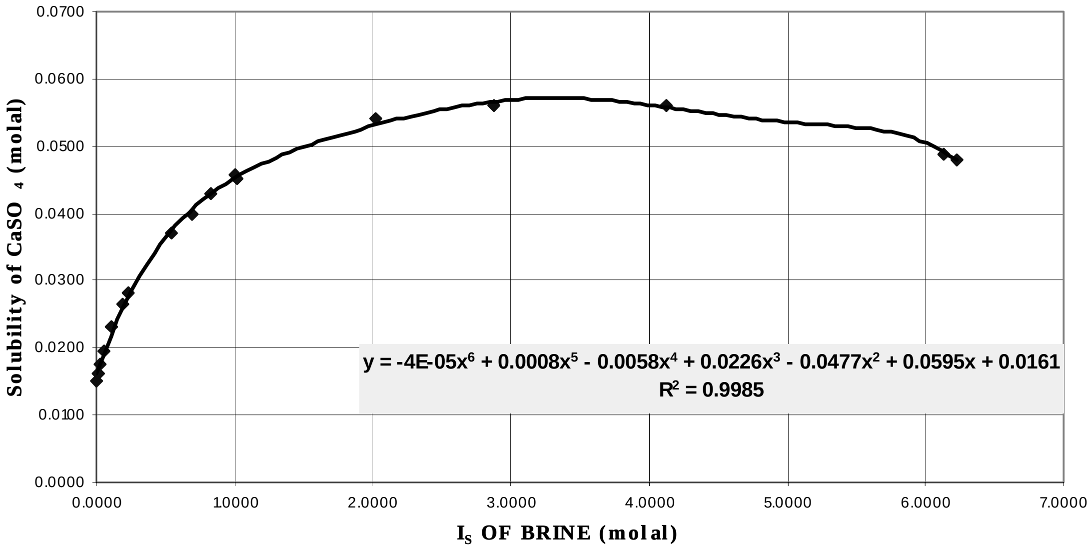

Figure 4.2: Effect of brine ionic strength on $CaSO_4$ solubility ($T = 25^oC$) [13]

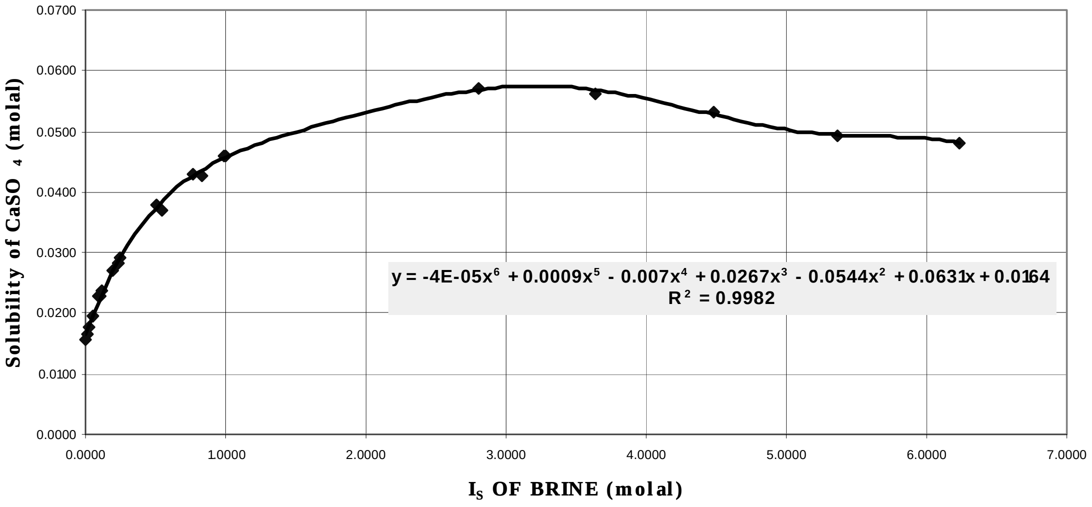

Figure 4.3: Effect of brine ionic strength on $CaSO_4$ solubility (T = 40^{o}C) [13]

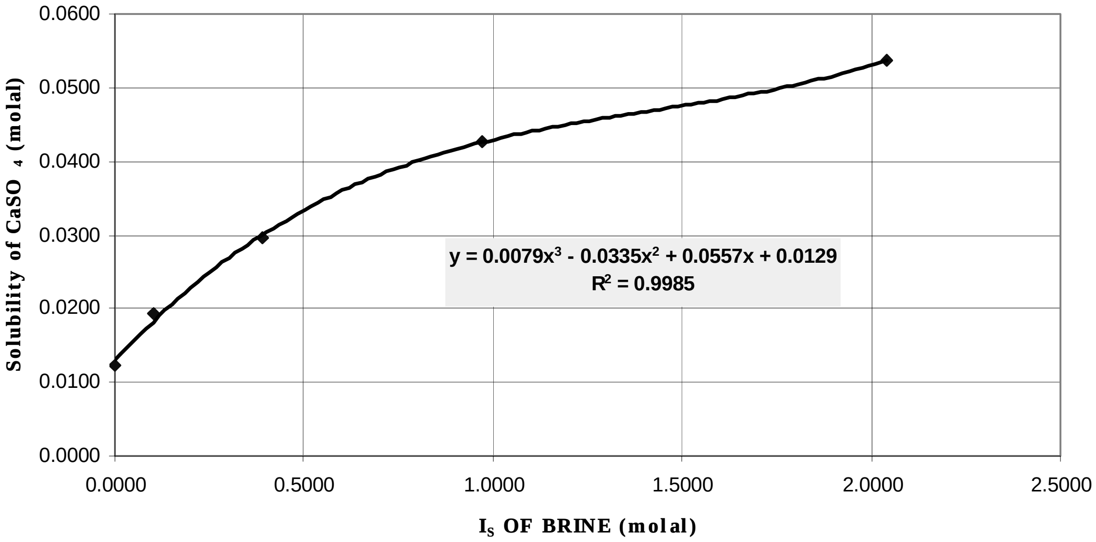

Figure 4.4: Effect of brine ionic strength on $CaSO_4$ solubility (T = 95^{o}C) [13]

4.3.3 Effect of Pressure

A drop in pressure can cause calcium sulphate deposition. The reason is quite different from that for calcium carbonate. The presence or absence of CO_2 in solution has little to do with calcium sulphate solubility.

Generally speaking, the solubility of $CaSO_4$:

- Decreases with temperature,
- slightly increases with pressure,
- increases with total salt concentration up to a certain point and then tends to decrease.

4.4. Scaling Potential

Solubility data obtained from various literature sources are presented in Appendix-A. Among these, the data of Marshall and Slusher [13] shall be used as the standard $CaSO_4$ solubility at temperatures of 40, 70 and 95 ^{0}C, as shown in Figures 4.2, 4.3 and 4.4. From these figures, for any ionic strength of the solution, the corresponding value of solubility can be read at the required temperatures. The solubility value can then be used to predict the scale potential for a given brine. To demonstrate this method, five example brines shall be examined as shown below.

Five Example Brines

Analyses of disposal water from a Saudi field and seawater are listed in Table 4.1. Five brines produced by mixing the two fluids at different ratios are also shown in the same table.

Table 4.1: Solubility Analysis of Five Disposal water / Sea water Brines

Component	Weight	*Disposal water*			*Sea water*		
		PPM	***(M)***	***(m)***	***PPM***	***(M)***	***(m)***
Ca	40	7535	0.1884	0.1802	606	0.0152	0.0146
Mg	24.31	1129	0.0464	0.0442	2043	0.0840	0.0809
Na	23	20680	0.8991	0.8710	16537	0.7190	0.7022
Sr	87.62	276	0.0031	0.0030	9.3	0.0001	0.0001
SO_4	96	740	0.0077	0.0073	4010	0.0418	0.0403
HCO_3	61	263	0.0043	0.0041	126	0.0021	0.0020
Cl	35.5	45518	1.2822	1.2727	29477	0.8303	0.8214
Sp.Gr.		1.0538			1.0404		
TDS		76141			52808.3		
pH		6.2			7.1		
Ionic Strength		1.54318			1.03462		

Molality : m (moles / kg of Solvent)

Molarity : M (moles / litre of Solution)

Weight Fraction : PPM (moles / kg of Solution)

Ratios (DW:SW)		**(0.2 : 0.8)**			**(0.4 : 0.6)**			**(0.5 : 0.5)**			**(0.6 : 0.4)**			**(0.8 : 0.2)**		
Component	Weight	Disposal water	Sea water	Mixture	Disposal water	Sea water	Mixture	Disposal water	Sea water	Mixture	Disposal water	Sea water	Mixture	Disposal water	Sea water	Mixture
Ca	*40*	0.0360	0.0117	0.0477	0.0721	0.0087	0.0808	0.0901	0.0073	0.0974	0.1081	0.0058	0.1139	0.1441	0.0029	0.1471
Mg	*24.31*	0.0088	0.0647	0.0736	0.0177	0.0486	0.0662	0.0221	0.0405	0.0625	0.0265	0.0324	0.0589	0.0353	0.0162	0.0515
Na	*23*	0.1742	0.5618	0.7360	0.3484	0.4213	0.7697	0.4355	0.3511	0.7866	0.5226	0.2809	0.8035	0.6968	0.1404	0.8372
Sr	*87.62*	0.0006	0.0001	0.0007	0.0012	0.0001	0.0013	0.0015	0.0001	0.0015	0.0018	0.0000	0.0018	0.0024	0.0000	0.0024
SO_4	*96*	0.0015	0.0322	0.0337	0.0029	0.0242	0.0271	0.0037	0.0202	0.0238	0.0044	0.0161	0.0205	0.0059	0.0081	0.0139
HCO_3	*61*	0.0008	0.0016	0.0024	0.0016	0.0012	0.0028	0.0020	0.0010	0.0030	0.0025	0.0008	0.0033	0.0033	0.0004	0.0037
Cl	*35.5*	0.2545	0.6571	0.9116	0.5091	0.4928	1.0019	0.6363	0.4107	1.0470	0.7636	0.3285	1.0922	1.0181	0.1643	1.1824
Ionic Strength				1.136			1.238			**1.289**			1.340			1.44
Ionic Product of $CaSO_4$				0.002			0.002			0.002			0.002			0.00
Ksp At T= 25^{0}C				0.002			0.002			0.002			0.002			0.00
S.I.(Scaling Index) At T= 25^{0}C				0.727			0.947			0.982			0.970			0.82
Ksp At T= 40^{0}C				0.002			0.002			0.002			0.002			0.00
S.I.(Scaling Index) At T= 40^{0}C				0.728			0.958			0.997			0.990			0.84
Ksp At T= 95^{0}C				0.002			0.002			**0.002**			0.002			0.00
S.I.(Scaling Index) At T= 95^{0}C				0.811			1.058			**1.098**			1.086			0.92

Ionic Product

The ionic product (IP) can be computed by the following formula

$$\mathbf{IP = C_{Ca}.\ C_{SO4}}$$

where:

C_{Ca} : Average concentration of Ca^{++} ions in the supersaturated solution

C_{SO_4} : Average concentration of SO_4^{--} ions in the supersaturated solution

For each mixing ratio, the molar concentration of each component in the available base solution is multiplied by the corresponding ratios and added together to get the mixture concentration of the desired ratio. Then, the ionic strength and ionic product are found and are also shown in the Table 4.1.

K_{sp} Values from Literature Data

Plots are generated from the data of Marshall and Slusher [13] between ionic strength and solubility of the mixture at different temperatures. The ionic strengths are then used to find the corresponding solubilities (S) of the mixtures ($CaSO_4$ in NaCl) of different ratios with the help of the plots at each temperature.

Since $CaSO_4$-in-NaCl is an example of **equimolar systems** (systems where the molar concentrations of Ca^{++} and SO_4^{--} are equal, i.e. $\mathbf{C_{Ca} = C_{SO4}}$),

K_{sp} is calculated from the solubility (S) data using the following equation:

$$\mathbf{K_{sp} = S^2}$$

K_{sp} values obtained from the equation for the mixtures of different ratios are also shown in Table 4.1. For example at a temperature of 95^oC, K_{sp} for the ratio of 0.5:0.5 is 0.0021 $moles^2/kg^2$.

Evaluation of Scaling Index (S.I.)

The scaling index of a solution is defined as:

S.I. = Ionic Product / Solubility Product

S.I. = IP / K_{sp}

The scaling indices of the five brines are then calculated and presented in Table 4.1

Scaling Potential from the Scaling Index (S.I.)

If:

- The mixture's ionic product (IP) is less than the mixture's solubility product (K_{sp}) of $CaSO_4$, the brine will be undersaturated with respect to $CaSO_4$ and it will not form scale. The S.I. in this case will be less than 1.
- IP = K_{sp}, the brine will be saturated and S.I. will be 1.
- IP > K_{sp}, the brine will be supersaturated and may from scale. The S.I. will be greater than 1.

To summarize:

S.I. = I.P. / K_{sp} → < 1; no scale
→ = 1; saturated
→ > 1; scale potential

These criteria are used to predict the scaling potential of $CaSO_4$ for the five brines as shown in Table 4.1.

Observation: Saturation or scaling index values greater than 1 indicate a scaling potential in the mixture. The scaling potential varies with different mixing ratios and with different temperatures. For the worst case, the table shows a value of SI = 1.098 at a temperature of 95°C and a mixing ratio of 0.5:0.5 of the two incompatible waters indicating maximum scaling potential

4.5. Kinetics of Scale Precipitation

4.5.1 Reaction Kinetics

For a homogenous reaction,

$A + B \rightarrow C$

the rate is defined as the change in concentration of a reactant per unit time per unit volume of the reaction mixture.

$$Rate = \frac{-dC_A}{dt}$$

For a simple one step reaction, the rate of a reaction is found to be proportional to the concentrations of the reactants raised to a power. For a first-order reaction, the rate of the reaction is proportional to the product of the molar concentrations of two reactants A and B, i.e.,

$$\mathbf{Rate = k\ [C_A]\ [C_B]}$$

The coefficient k is called the rate constant for the reaction and depends upon temperature, pressure, and other factors such as the presence of a catalyst. An experimentally determined equation of this kind is called the rate law of the reaction. More formally, a rate law is an equation that expresses the rate of reaction as a function of the concentrations of all species present in the overall chemical equation [70].

4.5.2 Arrhenius equation

The rate constant of most reactions increases as the temperature is raised. The relationship between a reaction rate constant (k) and the absolute temperature (T) is given by the Arrhenius equation:

$$k = Ae^{\left(\frac{-E}{RT}\right)} \qquad (4\text{-}17)$$

Where,

A : Frequency or pre-exponential factor

E : Activation Energy, J/mole or cal/mol

R : Universal gas constant = 8.314 kJ mole^{-1} K^{-1} = 1.987 cal mole^{-1} K^{-1}

T : Absolute temperature, K

If the Arrhenius equation applies, a plot of *ln* k versus 1/T should give a straight line of slope $\left(\frac{-E}{R}\right)$ and intercept *ln* A. The fact that E is given by the slope means that, the higher the activation energy, the stronger is the temperature dependence of the rate constant (that is, the steeper the slope). The pre-exponential factor could depend on the temperature, but is mainly the function of total pressure, ionic strength and catalyst. [70, 76]

4.5.3 Rate Laws for $CaSO_4$ Precipitation

Many rate laws for the precipitation of $CaSO_4$ were proposed in the literature [72, 73]. These are:

$$q = k\ C_{Ca} C_{SO_4} \tag{4.18}$$

$$q = k\left[\frac{C_{Ca} C_{SO_4}}{K_{sp}} - 1\right] \tag{4.19}$$

$$q = k\left(C_{Ca} C_{SO_4}\right)^2 \tag{4.20}$$

$$q = k \exp\left[\frac{\left(C_{Ca} C_{SO_4}\right)}{K_{sp}} - 1\right] \tag{4.21}$$

$$q = k\ \frac{C_{Ca} C_{SO_4}}{K_{sp}} \tag{4.22}$$

$$q = k\left\lfloor C_{Ca} C_{SO_4} - K_{sp}\right\rfloor \tag{4.23}$$

Where,

k : Rate Constant

q : Rate of the reaction (precipitation)

K_{sp} : Solubility Product

C_{Ca} : Average concentration of Ca^{++} ions in the supersaturated solution

C_{SO_4} : Average concentration of SO_4^{--} ions in the supersaturated solution

Obviously, the rate of precipitation becomes zero when one of the reactant concentrations reaches zero. Among the six laws, equs. 4.19, 4.21 and 4.23 will give non-zero values for the rate at a zero concentration of any reactant. On the other hand, among equations 4.18, 4.20 and 4.22, Equ. 4.22 is believed to be the most appropriate since it includes the K_{sp} (solubility product), while the other equations neglect the effect of solubility.

In this study, the reaction shall be modeled according to Equ. 4.22. However, the other proposed rate laws (4.18-4.23) are also studied and compared with the equation 4.22.

4.6 Synthetic Brines

To study the kinetics of $CaSO_4$ precipitation, a wide range of super saturations (scaling indices) need to be examined. For this purpose, synthetic brines containing Ca^{++} and SO_4^{--} need to be prepared at various concentrations. Only Na^+ and Cl^- ions are present in these brines to isolate the effect of other anions and cations that are present in natural brines.

In this section, three such synthetic brines are studied and their scaling potentials are presented.

Synthetic Brine of SI = 2.834

A 50:50 mixture of 0.15 M (6000 PPM) $CaCl_2$ in distilled water and a solution of 0.036 M (3566 PPM) Na_2SO_4 produces a brine with the following scaling potential at T = **95**°C:

Ionic Product = 0.0014 m^2.

Ionic Strength = 0.18755 and corresponding $K_{sp} = 0.000494\ m^2$

Thus, Scaling Index for this synthetic brine = ***2.834.***

Synthetic Brine of SI = 1.235

A 50:50 mixture of 0.1 M (4000 PPM) $CaCl_2$ in distilled water and a solution of 0.025 M (2400 PPM) Na_2SO_4 produces a brine with the following scaling potential at T = **25**°C:

Ionic Product = 0.000662 m^2.

Ionic Strength = 0.13138 and corresponding $K_{sp} = 0.000536\ m^2$

Thus, Scaling Index for this synthetic brine = ***1.235.***

Synthetic Brine of SI = 3.890

A 50:50 mixture of 0.163 M (6520 PPM) $CaCl_2$ in distilled water and a solution of 0.027 M (2592 PPM) Na_2SO_4 produces a brine with the following scaling potential at T = **50**°C:

Ionic Product = 0.00409 m^2.

Ionic Strength = 0.4617 and corresponding $K_{sp} = 0.001052\ m^2$

Thus, Scaling Index for this synthetic brine = ***3.89.***

Chapter 5

EXPERIMENTAL APPARATUS, MATERIALS AND PROCEDURE

In this chapter the materials, apparatus and experimental procedures employed in this study are described.

5.1 MATERIALS

Porous Medium

In all flooding experiments, Berea sandstone cores of 2” length and of diameters around 1.5” with an average porosity of 22% and of absolute permeability around 200 md were used. All the cores were dried in a vacuum oven at 100^oC for 3 to 4 hours before use. Table 5.1 lists the physical properties of all core samples used in this study.

Scanning Electron Microscope analysis of one dried core sample showed the core to be highly porous and consists mainly of quartz crystals and clay particles as shown in

Table 5.1: Physical Properties of Berea Cores used in this Study

Core of Run #	Length (inch)	Diameter (inch)	Dry Weight (gm)	Porosity (%)	Absolute Permeability (md)
1	12	1.485	730.5	22.0	194.0
2	12	1.481	721.2	22.1	191.0
3	12	1.482	720.6	22.0	241.7
4	12	1.500	720.5	22.4	216.0
5	2	1.487	120.0	22.7	213.4
6	2	1.484	118.2	24.7	212.3
7	2	1.489	122.6	22.9	168.0
8	2	1.481	124.5	23.2	241.0
9	2	1.495	117.7	23.6	208.0
10	2	1.489	123.5	25.5	217.0
11	2	1.486	123.2	24.4	215.2
12	2	1.487	122.1	25.1	218.3
13	2	1.481	124.3	23.3	213.9
14	2	1.482	119.0	23.1	205.1
15	2	1.491	122.5	22.5	229.0
16	2	1.487	122.4	22.2	216 .3
17	2	1.485	118.7	24.7	214.0
18	2	1.491	119.9	22.4	209.5
19	2	1.487	120.9	26.1	205.1
20	2	1.482	122.6	20.7	181.1
21	2	1.482	120.6	21.0	225.6

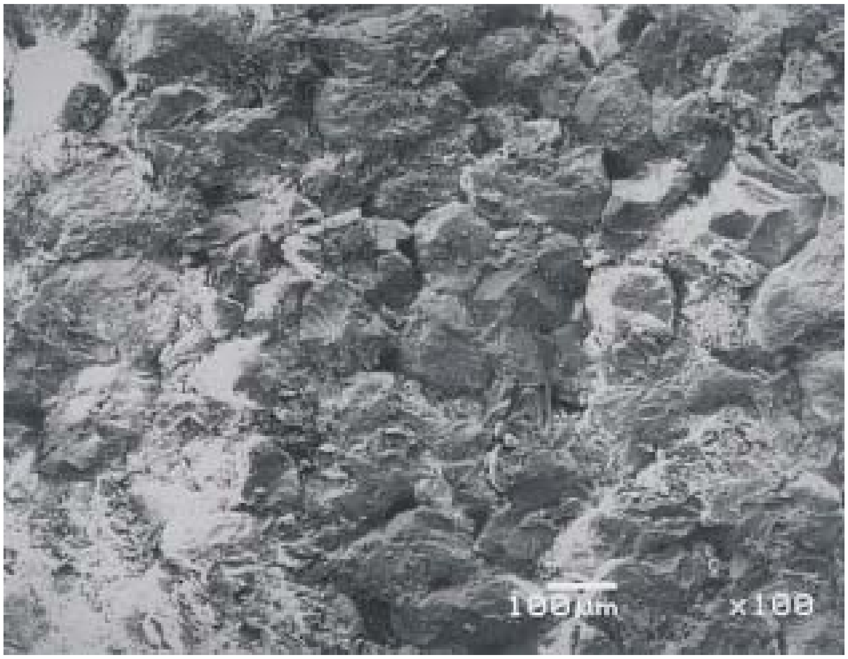

Fig. 5.1: Scanning Electron Microscope Photo of a Berea Core Sample

Fig. 5.2: Magnification of Clay Particles in a Berea Core Sample

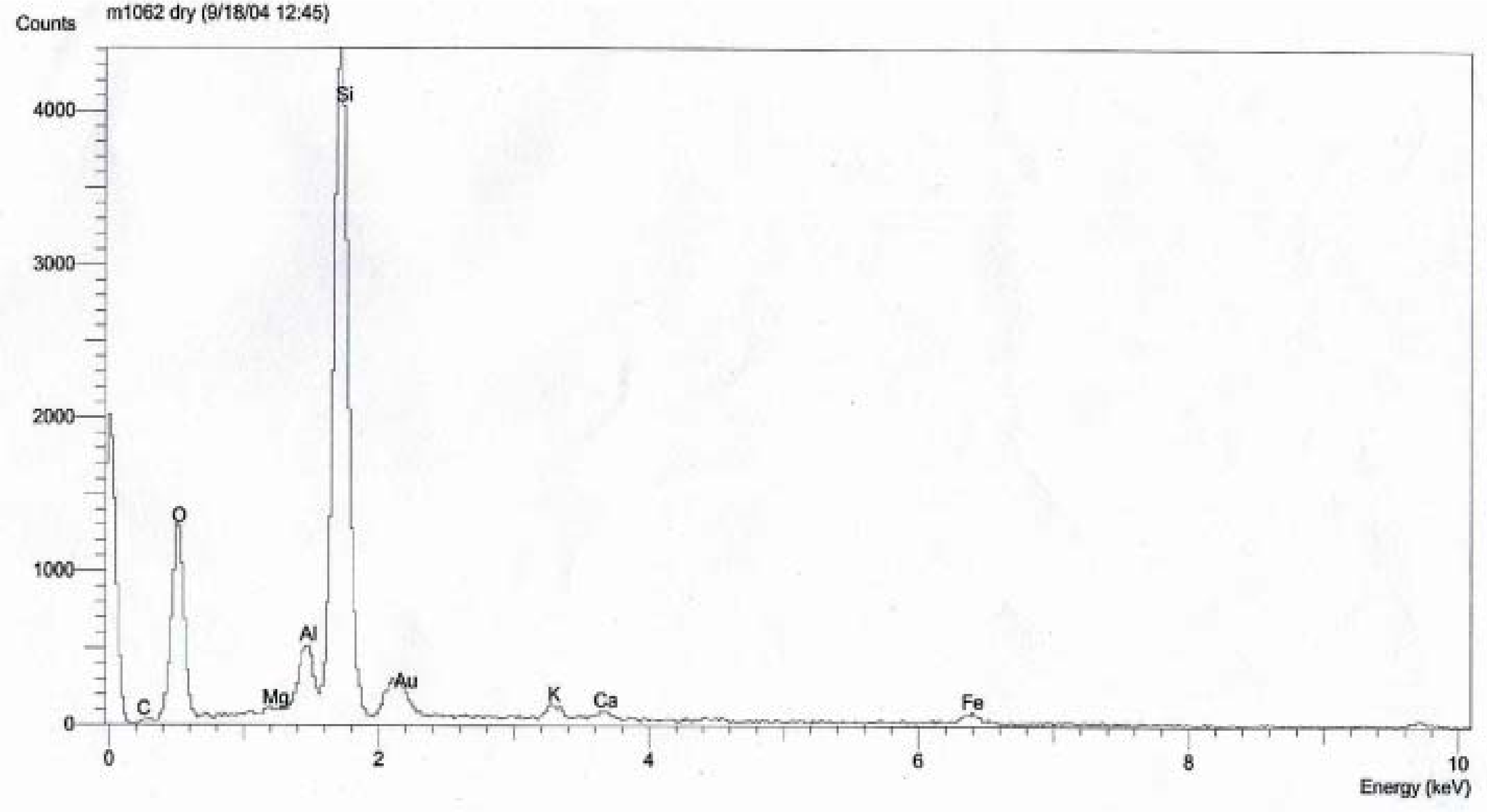

Fig. 5.3: EDS of the Clay Particles of a Berea Core Sample

Figs. 5.1 and 5.2. The Energy Dispersive Spectrum (EDS) of a clay particle showed the presence of mainly aluminum, oxygen and silicon as seen in Fig. 5.3.

Salts

Three salts were used for the preparation of the solutions. These are:

a. Sodium Chloride ~ BDH AnalaR NaCl (M. Wt. = 58.44, 99.9% Purity) ~ Manufactured by BDH Chemical Limited, England.

b. Sodium Sulphate (Anhydrous) ~ Baker Analyzed Reagent Na_2SO_4 (M. Wt. = 110.99, 96.5% purity) ~ manufactured by J.T.Baker Chemical Co., NJ.

c. Calcium Chloride (Anhydrous) ~ Panreac $CaCl_2$ (M. Wt. = 142.04) ~ manufactured by PRS Montplet & Estaban SA, Spain.

Distilled Water

Analytical grade distilled water with conductivity of 1 mili Siemens and a pH value of 7.0 was used to prepare all solutions.

Solutions

Three different types of solutions were used in this study. These are:

1. A solution of 1.0-1.5 % NaCl concentration was used to saturate the core and allow porosity and absolute permeability measurements.

2. Solutions of pure calcium chloride ($CaCl_2$) dissolved in distilled water at various concentrations were used as injection brine ingredients for all runs as shown in Table 5.2.
3. Solutions of pure sodium sulphate (Na_2SO_4) in distilled water at various concentrations were used as injection brine ingredients for all runs as shown in Table 5.2.

Various combinations of the $CaCl_2$ and Na_2SO_4 solutions were injected simultaneously in the cores to create scaling brines of the desired level of supersaturation.

Table 5.2: Solution Concentrations used in all Runs

Run No.	**$CaCl_2$ Solution* Concentration**			**Na_2SO_4 Solution* Concentration**		
	Molarity (M)	Molality (m)	$CaCl_2$ PPM	Molarity (M)	Molality (m)	Na_2SO_4 PPM
1	0.1500	0.14660	6000	0.03600	0.03580	3566
2	0.1500	0.14660	6000	0.03600	0.03580	3566
3	0.1950	0.19060	7800	0.05000	0.04972	4800
4	0.2000	0.19540	8000	0.05000	0.04972	4800
5	0.2000	0.19540	8000	0.05000	0.04972	4800
6	0.2000	0.19540	8000	0.05000	0.04972	4800
7	0.2000	0.19540	8000	0.05000	0.04972	4800
8	0.1000	0.09770	4000	0.02500	0.02486	2400
9	0.1500	0.14670	6000	0.03750	0.03729	3600
10	0.1500	0.14670	6000	0.03750	0.03729	3600
11	0.1500	0.14670	6000	0.03750	0.03729	3600
12	0.1500	0.14670	6000	0.03750	0.03729	3600
13	0.0768	0.07513	3060	0.01875	0.01864	1800
14	0.0920	0.08900	3640	0.02250	0.02237	2160
15	0.0768	0.07513	3060	0.01875	0.01864	1800
16	0.0768	0.07513	3060	0.01875	0.01864	1800
17	0.0768	0.07513	3060	0.01875	0.01864	1800
18	0.0775	0.07574	3100	0.01900	0.01870	1800
19	0.0163	0.15930	6520	0.02700	0.02670	2592
20	0.0750	0.07460	3000	0.02400	0.02380	2304
21	0.0600	0.05460	2400	0.01400	0.01380	1344

* Both solutions were injected at equal rates to produce a 50:50 mixture at the core inlet.

5.2 APPARATUS

A schematic diagram of the experimental setup used in this study is shown in Fig. 5.4. It consists of the following:

5.2.1 Core Holder

A Hassler type, stainless steel core holder model HCH-1.5 designed for consolidated core samples up to 12” in length and 1.5” in diameter was used. The holder was manufactured by TEMCO, Inc., Tulsa, USA and can withstand pressures upto 10,000 psia. A cross-section and photograph of the core holder are shown in Fig. 5.5.

The core sample is housed inside a viton rubber sleeve, which is held in place by two ferrules. Each ferrule rests on one end of the core holder body where an ‘O’ ring is placed in a groove around the rim of the body. These ferrules are pressed against the holder’s body by two screw-on end caps.

An end plug made of stainless steel is inserted into each end of the sleeve and is pressed against the core sample by a retaining screw, which threads through the end cap. Both end plugs have circular grooves to ensure fluid injection into and production from the entire cross-section of the core as shown in Fig. 5.6. The outlet plug has one production port at the center. However, the inlet plug has two ports with two separate delivery tubes (one for each solution directly from the pump) to allow delivery of the two solutions to the core face separately without prior contact. That is the two solutions come into contact and mix only at the last possible point, the inlet plug grooves before entry into the core. This is to prevent any scale formation inside the inlet piping and to confine the reaction to within the pore space of the core. A sectional view of the inlet end plug is shown in Fig. 5.7.

The annular space between the sleeve and the core holder body is filled with a confining fluid and is pressurized up to the desired pressure. This pressure prevents fluid by-pass around the core and ensures good sealing between the ferrules and sleeve. The confining pressure was applied using a hand pump model A39/18 manufactured by Core Lab Inc.

5.2.2 Fluid Injection Pumps

Two Double-piston positive-displacement pumps (Models 260D and 500D), also known as Syringe Pumps, manufactured by Isco, Inc., with minimum capacity of 0.001 ml / min, were used to inject the two solutions during flooding at different flowrates.

5.2.3 Transfer Cells

Two stainless steel transfer cells, manufactured by Core Lab Inc., which can withstand pressures up to 10,000 psia, were used to store and transfer the injection solutions to the core holder. Each cell with a capacity of 1000 ml has a free-floating piston, which separates the pump fluid (distilled water) from the injection fluid. The pump fluid was pumped into a transfer cell to displace the solution into the core.

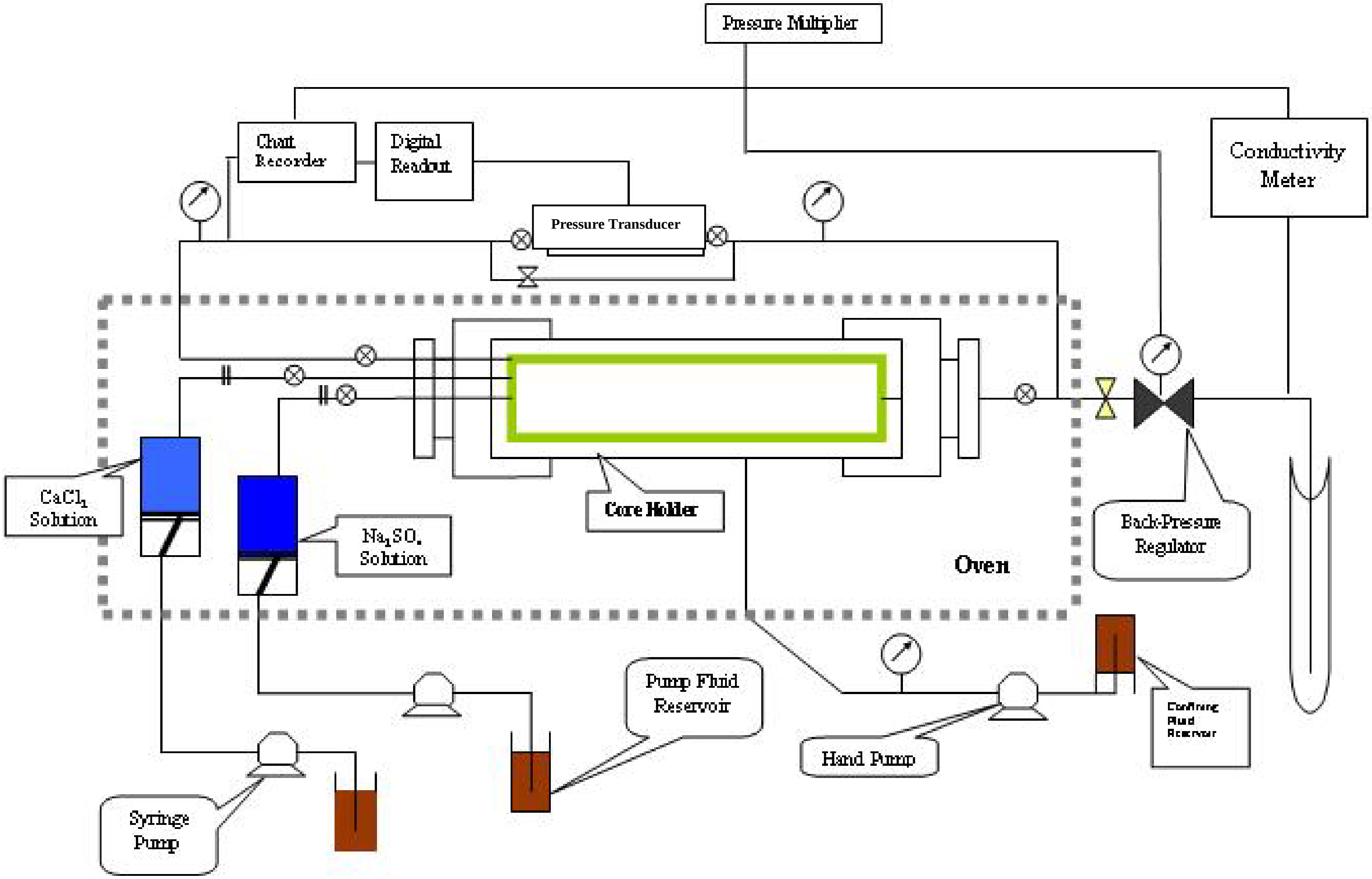

Fig. 5.4: Schematic of the Core Flooding Apparatus

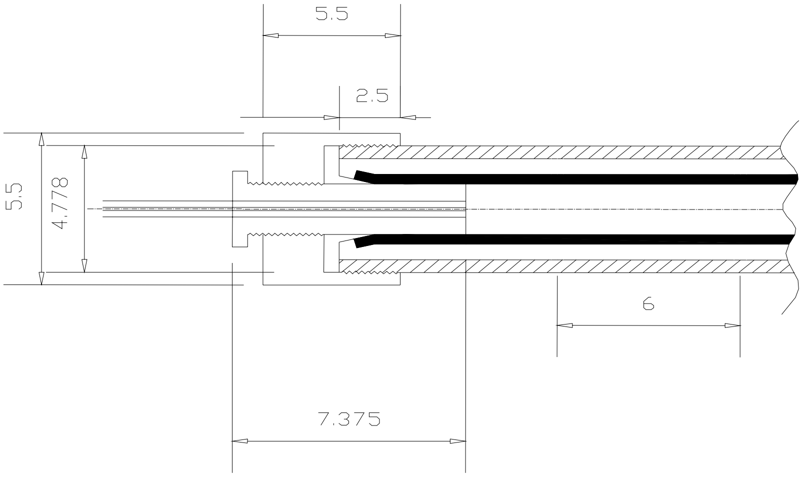

Fig. 5.5: Sectional and Physical Views of the Core Holder used in this study

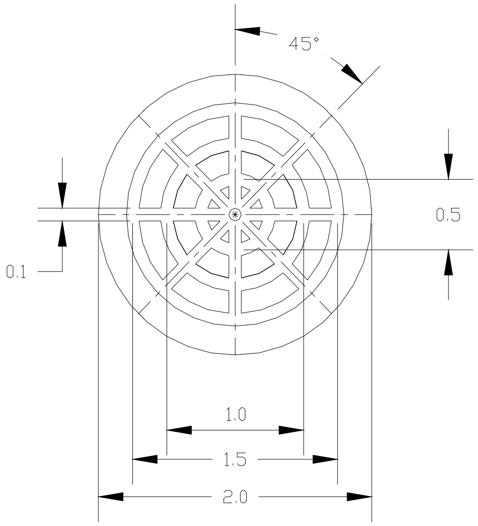

Fig. 5.6: Cross-Sectional View of the Inlet End Plug of the Core Holder

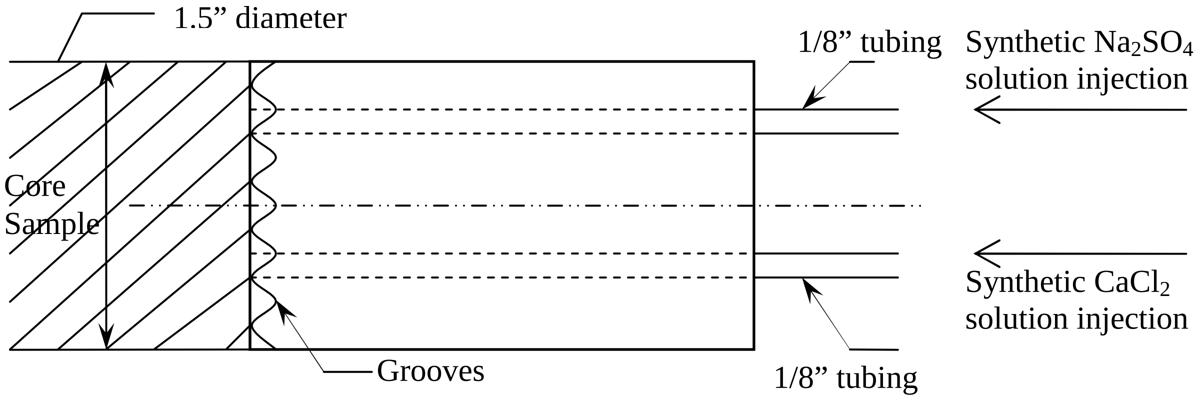

Fig. 5.7: Sectional View of the Inlet End Plug of the Core Holder

5.2.4 Vacuum Pump

A Welch vacuum pump 1.5 model 8906A, manufactured by Thomas Industries Inc., was used for air evacuation during core saturation.

5.2.5 Back Pressure Regulator

A dome loaded back-pressure regulator, manufactured by Temco, Inc., was used to apply a constant back pressure to the core during all flooding experiments. Its pressure limit is 5000 psia.

5.2.6 Back Pressure Multiplier

A pressure multiplier, manufactured by Core Lab Inc., operating with mineral oil was used to provide the required confining pressure to the back-pressure regulator from a low pressure source (low pressure Nitrogen cylinder).

5.2.7 Oven

During all flooding runs, the core holder and the transfer cells were placed inside a temperature controlled oven (Memmert, model D-6072) manufactured by Karl Kolb Co. This oven has a temperature range from 5^{o}C above room temperature to 270^{o}C with natural convection and half full sight glass doors. It also has two ducts at the sides to allow access to the oven chamber.

5.2.8 Pressure Measurement System

The differential pressure across the core during flooding runs was measured using a Validyne model DP 303 pressure transducer with a digital display model CD23. The working range of the transducer can be varied using different diaphragms. The output signal of the transducer was continuously recorded by a Soltec strip-chart recorder model 1243. The pressure transducer with the appropriate diaphragm was calibrated using either a dead weight tester or a pressure gauge calibrated by a dead weight tester. Before using the transducer, bleed ports were bled off to ensure the cavities of the diaphragm are completely filled with liquid.

5.2.9 Conductivity Measurement System

The electric conductivity of the core holder effluent was measured using a conductivity meter model 101 manufactured by Orion Research Inc., with ranges from 10μS to 100mS. The probe of the conductivity meter was dipped in the effluent solution downstream from the back pressure regulator. The output signal of the conductivity meter was continuously recorded by the strip-chart recorder.

5.2.10 Viscometer

A Plate-Cone type, Contraves low shear 30 viscometer equipped with a HAAKE M circulated temperature oil bath was used for measuring injected solution viscosities at various temperatures.

5.2.11 Auxiliary Equipment and Tools

Many other pieces of equipment and tools were used during this study. These include: pressure gauges, vacuum oven, pyro-magnestir with hot plate, weighing balance, vernier caliper, stainless steel fittings and tubings, valves, glass test tubes, conical and round bottom flasks of different capacities, micro pipette of 0.8 & 0.2 ml and plastic bottles for sampling…. Etc.

5.3 EXPERIMENTAL PROCEDURE

5.3.1 Core Saturation

Before each run, the core sample was dried in a vacuum oven at 100^{o}C. The core was then saturated with 1.5 % NaCl solution at room temperature. The saturation procedure starts with loading the core in the heat resistant rubber sleeve. This assembly was then placed in the core holder with the end pieces clamped over the sleeve and caps were fixed. A confining pressure of 1000 psia was applied to the core holder. Vacuum was then applied to the core sample for several hours. A known amount of solution was then injected to saturate the core, while the evacuation was continuing. After the appearance of NaCl solution at the outlet, vacuum was stopped immediately while flooding was continued long enough to ensure 100% saturation.

5.3.2 Porosity Measurements

The porosity of a core sample was measured in conjunction with the saturation step described above. Porosities were determined from the initial and remaining volumes of the solutions, dead volumes, and the dimensions of the cores. Porosities of all the cores used in this study are listed in Table 5.1.

5.3.3 Absolute Permeability Measurement

After porosity measurement, the core holder with the saturated core sample was connected to the flooding apparatus (Figure 5.4). The annulus between the rubber sleeve and the core holder body was then filled with confining fluid (distilled water) to a confining pressure of 4500-5000 psia. The back pressure was set to 3000 psia. The absolute permeability was measured by flooding the core with the 1.5% NaCl solution. Variable flow rates were used and the corresponding differential pressures were recorded to calculate absolute permeability using Darcy's Law. Table 5.1 lists the absolute permeabilities of the cores used in this study.

5.3.4 Flooding Experiment

The system consisting of the core holder assembly and transfer cells containing the two incompatible solutions ($CaCl_2$ and Na_2SO_4) were then placed inside the oven and heated to the desired temperature of the run. The system was left overnight for temperature equilibrium to be attained. The required back pressure, usually 3000 psig, was then set and the confining pressure was adjusted to be approximately 500 psia above the back pressure.

A flooding run was started by setting both syringe pumps at the same rate (ranging from 0.06 to 7.5 ml/min), then turning them on. Thus, the two solutions were always injected into the core sample at a mixing ratio of 50:50, and the total flow rate through the core was twice the rate of each pump.

At regular intervals of time, a small sample of the core effluent (0.8 or 0.2 ml) was collected using a micro-pipette and was then immediately diluted in a conical flask (50 or 25 ml) containing chilled distilled water. This great dilution was intended to prevent further precipitation reaction outside the core. The diluted sample was then preserved under chilled condition until the time of analysis.

The differential pressure and conductivity of the effluent were also recorded continuously by the chart recorder.

A run was terminated when the electric conductivity of the core effluent stabilized at a given level for a sufficiently long time. This signaled the attainment of a steady-state Ca^{++} concentration profile across the core sample.

5.3.5 Calcium Content Measurement

The concentration of Ca^{++} ions present in each diluted effluent sample was determined by atomic absorption apparatus model Analyst-100. After multiplying with the dilution factor, the exact concentration of Ca^{++} in the effluent at the sampling time was computed.

5.3.6 Scanning Electron Microscopy (SEM)

For selected runs, the core sample was removed at the end of flooding and broken into sections. These sections were then examined by SEM to reveal the nature of $CaSO_4$ crystals which had precipitated and the degree of pore plugging that had taken place.

Chapter 6

RESULTS AND DISCUSSION

In this chapter, the experimental results are presented, analyzed and discussed. A total of **21** runs were performed, out of which **4** were preliminary runs, **2** failed due to plugging of tubing, **11** were considered successful and **4** were used to validate the kinetic model. The operating conditions of the first 17 runs are presented in Table 6.1 including the concentrations of $CaCl_2$ and Na_2SO_4 solutions used for injection. The detailed experimental data are presented in Appendix-**B**.

The coreflood experiments were designed to investigate the effect of temperature (45 to 95^oC), pressure (100-3000 psia), flow velocity (1-10 m/s), and concentration (2180-4175 ppm of Ca^{++}) on the scaling tendency of brines.

First, a typical run is described and analyzed in detail to explain the method employed in estimating the rate of scale precipitation and rate constant. Later in this chapter, the effect of temperature, concentration, pressure, and flow velocity on reaction rate kinetics shall be discussed along with graphical representations.

Table 6.1: Operating Parameters for Core Flooding Runs

Run #		**Berea Sandstone Core Properties**			**Operating Conditions**					**Injected Brine Concentrations ***					
		L inch	**d inch**	**Φ (%)**	**k (md)**	**Total Flow Rate (Q) (ml /min)**	**Total Injection Time**	**Pressure (P) (Psig)**	**Temp. (^{o}C)**	**Ca^{++}**			**SO_4^{--}**		
										PPM	M	m	PPM	M	m
Preliminary	1	**12**	1.5	22.4	216	**0.242**	167 hrs	3000	95	3053	0.075	0.0733	1783	0.018	0.0179
	2	12	1.5	22.1	191	0.242	90 hrs	3000	95	**3053**	0.075	0.0733	**1783**	0.018	0.0179
	3	12	1.5	22	241	0.242	74.5 hrs	3000	94	**3900**	0.0975	0.0953	**2400**	0.025	0.02486
	4	**2**	1.5	22.4	216	**0.12**	74 hrs	3000	95	**4000**	0.1	0.09773	**2400**	0.025	0.02486
Failed	5	2	1.5	22.6	213	10	15 min	3000	95	4174	0.104	0.1016	2400	0.025	0.02486
	6	2	1.5	24.7	212	10	20 min	3000	95	4174	0.104	0.1016	2400	0.025	0.02486
Successful Runs	7	2	1.5	22.9	168	**10**	47 min	3000	95	**4174**	0.104	0.1016	**2400**	0.025	0.02486
	8	2	1.5	25.5	241	10	198 min	3000	95	**2180**	0.0545	0.05326	**1200**	0.0125	0.01243
	9	2	1.5	23.6	208	**10**	190 min	**3000**	**95**	**3060**	0.0768	0.07513	**1800**	0.01875	0.018645
	10	2	1.5	25.5	217	10	188 min	3000	**70**	3060	0.0768	0.07513	1800	0.01875	0.018645
	11	2	1.5	24.4	215	10	179 min	3000	**45**	3060	0.0768	0.07513	1800	0.01875	0.018645
	12	2	1.5	25.1	218	10	93 min	**500**	95	3060	0.0768	0.07513	1800	0.01875	0.018645
	13	2	1.5	23.3	214	10	113 min	**100**	95	3060	0.0768	0.07513	1800	0.01875	0.018645
	14	2	1.5	23.1	205	10	160 min	3000	95	**3640**	0.0920	0.08900	**2160**	0.02250	0.022370
	15	2	1.5	22.5	229	**5**	340 min	3000	95	3060	0.0768	0.07513	1800	0.01875	0.018645
	16	2	1.5	22.2	216	**15**	127 min	3000	95	3060	0.0768	0.07513	1800	0.01875	0.018645
	17	2	1.5	24.7	214	**1**	27.25 hrs	3000	95	3060	0.0768	0.07513	1800	0.01875	0.018645

* Computed for the injected 50:50 mixture of $CaCl_2$ and Na_2SO_4 solutions.

6.1 Detailed Results of Coreflooding Run # 8

This run was conducted at T = 95^{o}C and P = 3000 psig. A Berea core sample of length 2 inches and diameter of 1.5 inch with a porosity of 25.5 %, permeability of 241 md, and pore volume (V_p) of 14.97 cc, was first saturated with 1% NaCl solution. Solutions of 2180 ppm $CaCl_2$ (0.053 m) and 1200 ppm Na_2SO_4 (0.0124 m) were injected into the core at a rate of 5 ml/min each. Total injection volume of each solution was 1 liter.

During the run, differential pressure across the core (ΔP), temperature of the oven, and conductivity of the effluent were measured and plotted versus time. Detailed data for Run # 8 is shown in Table 6.2 and is also presented in Appendix-B.

6.1.1 Effluent Ca^{++} Concentration History

The effluent calcium concentration for Run # 8 is plotted against injection time in Figure 6.1. Also, the normalized Ca^{++} concentration (measured effluent concentration divided by the injected concentration of calcium, Co) is plotted vs. pore volumes of injected brine in Figure 6.2. As can be detected from Figure 6.1, breakthrough of Ca^{++} occurs within 2 minutes as a result of the small pore volume of the core and high injection rate. The Ca^{++} effluent concentration reached 2000 ppm within 20 minutes of injection and fluctuated around this level for the rest of the run. Such fluctuations are due to error in analysis of the effluent samples. We can, therefore, assert that the steady-state effluent Ca^{++} concentration is 2000 ppm and the steady-state drop in Ca^{++} concentration across the core is then = 2180 - 2000 = 180 ppm.

Table 6-2: Experimental Data of Core Flood Run # 8

Effluent Sample #	Time Collected	Cumulative Injection Time (min)	No. of PV's Injected	Effluent Conductivity in ms	ΔP	T	P_{inlet}	P_{Back}	P_{OB}	Effluent Ca^{++} Conc.	
	am				psig	C	psig	psig	psig	PPM	Mole/lit
1	5:51 AM	1	0.78	8.8	7.2	89	3068	3000	4500	1625	0.041
2	6:00 AM	10	3.54	4.7	7.4	90	3073	3000	4500	1750	0.044
3	6:10 AM	20	6.68	4.5	7.6	92	3079	3000	4500	2000	0.050
4	6:20 AM	30	10.09	4.4	7.8	92	3082	3000	4500	2000	0.050
5	6:30 AM	40	12.91	4.2	7.8	92	3087	3000	4500	1937.5	0.048
6	6:40 AM	50	16.28	4.1	7.9	92	3092	3000	4500	1875	0.047
7	6:50 AM	60	19.49	3.9	8	92	3096	3000	4500	2062.5	0.052
8	7:00 AM	70	23.05	3.9	8.1	92	3099	3000	4500	2062.5	0.052
9	7:10 AM	80	26.87	3.9	8.3	92	3112	3000	4500	2000	0.050
10	7:20 AM	90	29.83	3.8	8.4	92	3122	3000	4500	1750	0.044
11	7:30 AM	100	32.82	3.9	8.5	92	3122	3000	4500	1875	0.047
12	7:40 AM	110	36.41	4.3	8.6	92	3126	3000	4500	1937.5	0.048
13	7:50 AM	120	39.75	4.4	8.7	92	3130	3000	4500	2125	0.053
14	8:00 AM	130	42.95	4.3	8.8	92	3134	3000	4500	2000	0.050
15	8:10 AM	140	46.29	4	8.9	92	3139	3000	4600	2000	0.050
16	8:20 AM	150	50.30	4.2	9	92	3143	3000	4600	2000	0.050
17	8:28 AM	158	53.11	4.2	9	92	3151	3000	4800	2000	0.050
18	8:35 AM	165	55.18	4.2	9.1	92	3157	3000	4800	2000	0.050
19	8:42 AM	172	57.52	4.2	9.2	92	3160	3000	4800	2062.5	0.052
20	8:49 AM	179	59.92	4.3	9.3	92	3162	3000	4800	2125	0.053
21	8:57 AM	187	62.99	4.2	9.4	92	3167	3000	4800	1812.5	0.045
22	9:08 AM	198	66.40	3.8	9.4	92	3173	3000	4800	1875	0.047

* Flooding started at 5:50 AM. * Injected brine Ca^{++} concentration = 2180 ppm

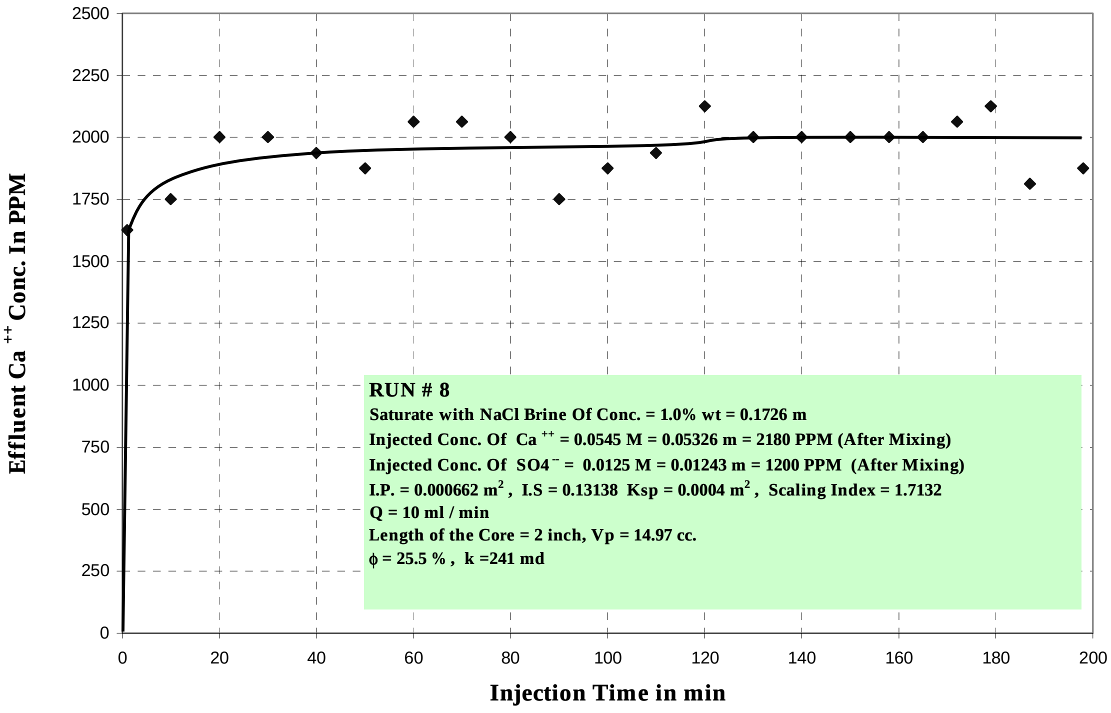

Figure 6.1: Effluent Calcium Concentration versus Injection Time

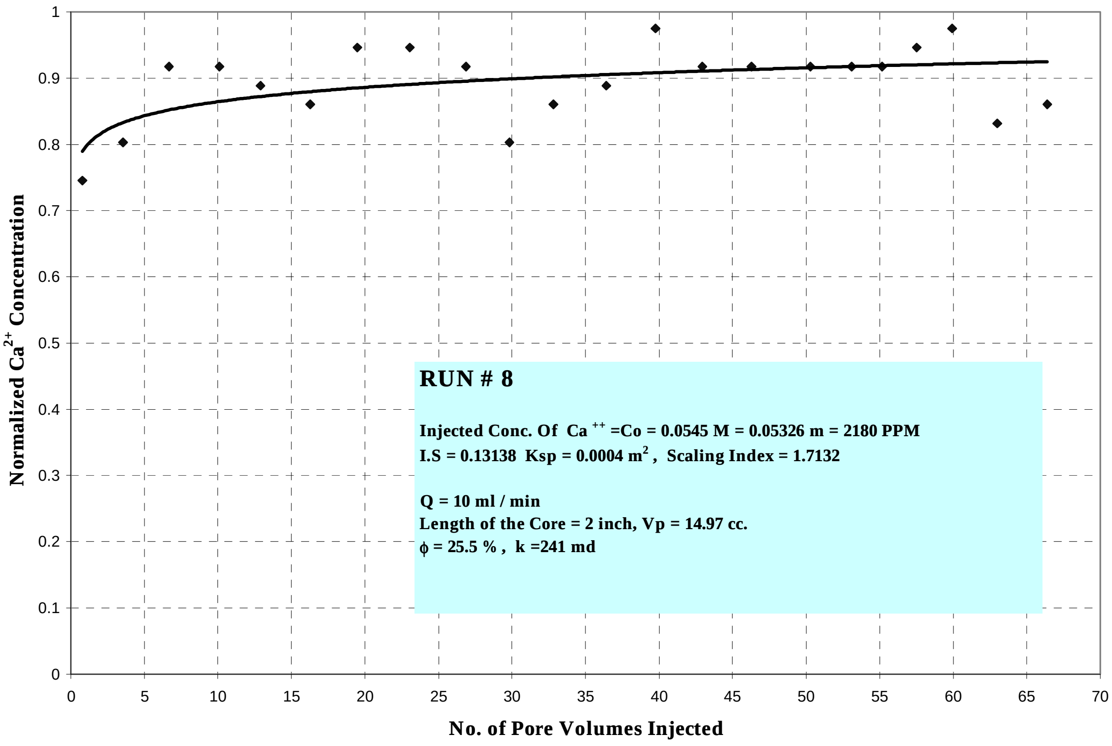

Figure 6.2: Normalized (Effluent / Injection) Calcium Concentration versus Pore Volumes Injected

6.1.2 Effluent Electric Conductivity History

The effluent electric conductivity with respect to time is shown in Figure 6.3. The initial high conductivity (8.8 mS) is that of NaCl solution, which saturated the core initially. As the injected brine / NaCl solution mixing zone is produced, the conductivity drops drastically. Ultimately, the conductivity stabilized at a value of 4.0 mS, which should correspond to a 2000 ppm concentration of Ca^{++}.

6.1.3 Differential Pressure Plot versus Pore Volumes Injected (PVI)

Differential pressure across the core is plotted versus the PVI in Figure 6.4. The pressure drop (ΔP) continuously increased from 7.2 psi to a final value of 9.4 psi after injection of 67 pore volumes. This net rise of 2.2 psi is due to precipitation of the $CaSO_4$ inside the core with the consequent reduction in its permeability and porosity.

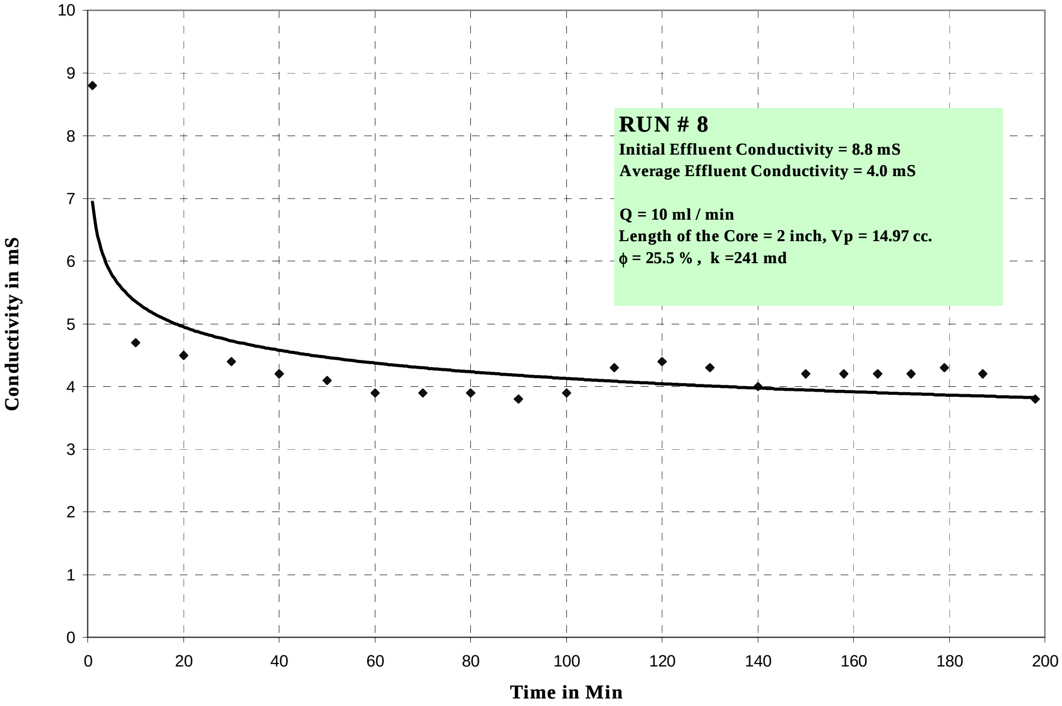

Figure 6.3: Effluent Electric Conductivity vs. Injection Time

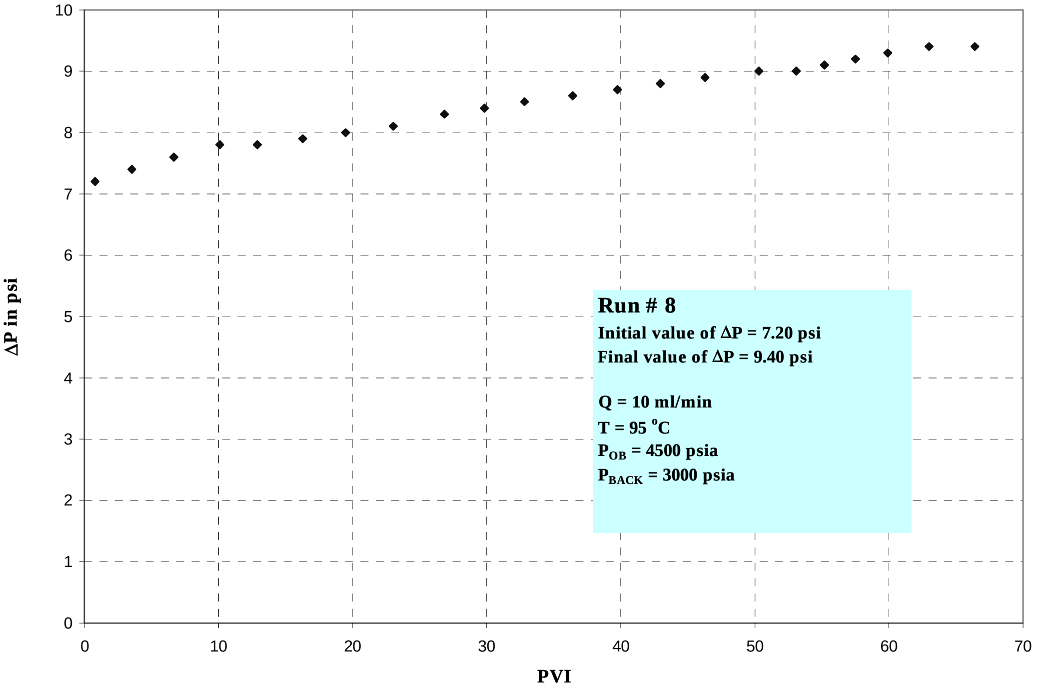

Figure 6.4: Differential Pressure vs. Pore Volumes Injected

6.1.4 Reduction in Core Permeability

The core permeability retention (current k / initial k) is plotted versus PVI in Figure 6.5. The data shows more than 23% loss in absolute permeability after 66 PVI. Considering the mass of $CaSO_4$ precipitated (3.58 gm), the resulting loss in porosity is estimated at 8%.

6.1.5 Supersaturation level across the Core

The supersaturation level of the brine decreased from 1.7132 at the inlet of the core to steady state values of 1.0059 at the core's outlet.

The steady-state outlet SS indicates that the brine has lost almost all its scaling potential through the core and has emerged in an almost stable state. Yet, its exit SS value above 1 reveals that the precipitation reaction was not complete. This observation is an important pre-requisite for reaction rate calculations that follow.

6.1.6 Scanning Electron Microscope Analysis

Scanning electron microscopy (SEM) micrographs revealed the formation of crystals at the inlet face (Figure 6.6) and outlet face (Figure 6.7) of the core in Run # 8.

EDS analysis and BEI (Back Scattered Imagining) of these crystals (Figure 6.8-6.11) showed the high percentage of calcium and sulfur, which confirmed the composition of these crystals to be $CaSO_4$.

At the inlet face, the amount of crystals of $CaSO_4$ is high as compared to the outlet face indicating more precipitation at the inlet face.

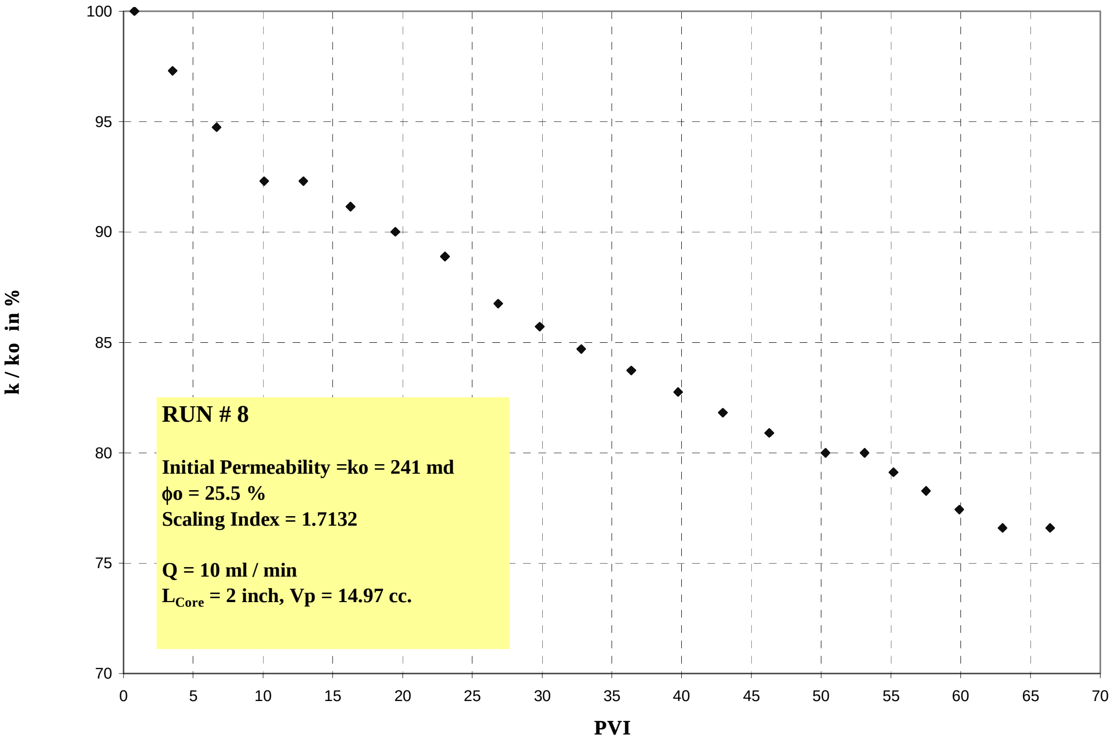

Figure 6.5: Core Permeability Retention vs. Pore Volume Injected

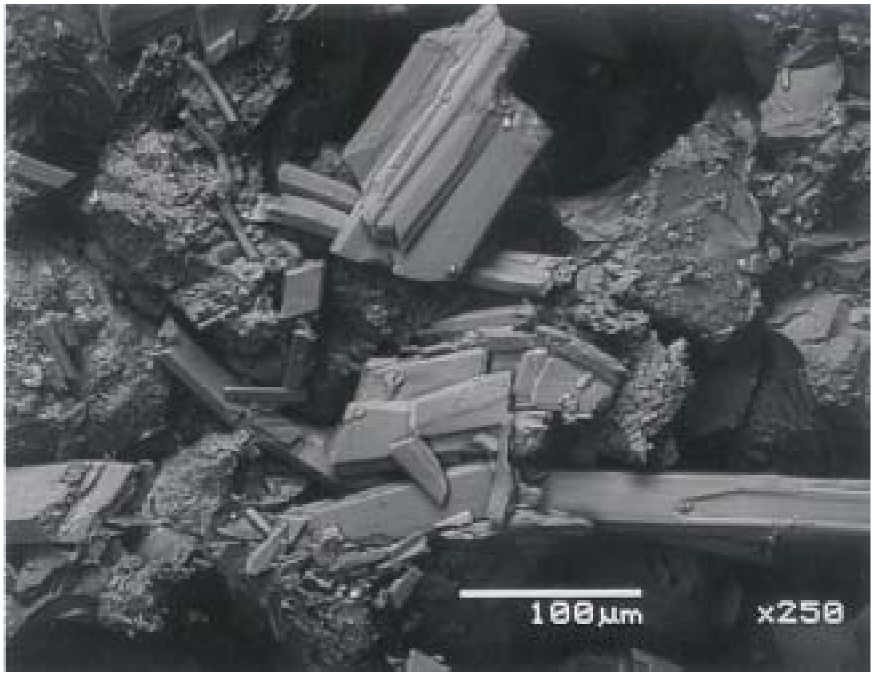

Figure 6.6: SEM of the Inlet face of the Core (Run # 8)

Figure 6.7: SEM of the Outlet face of the core (Run # 8)

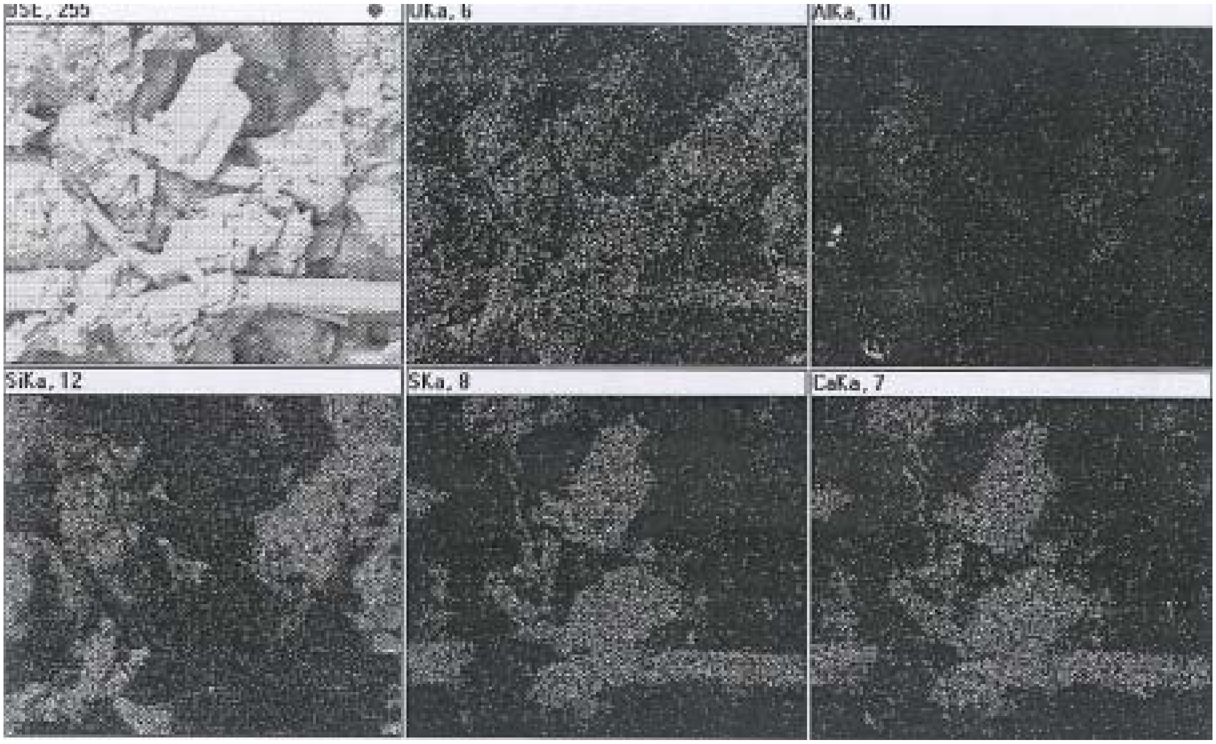

Figure 6.8: BEI of the Inlet face of the Core (Run # 8)

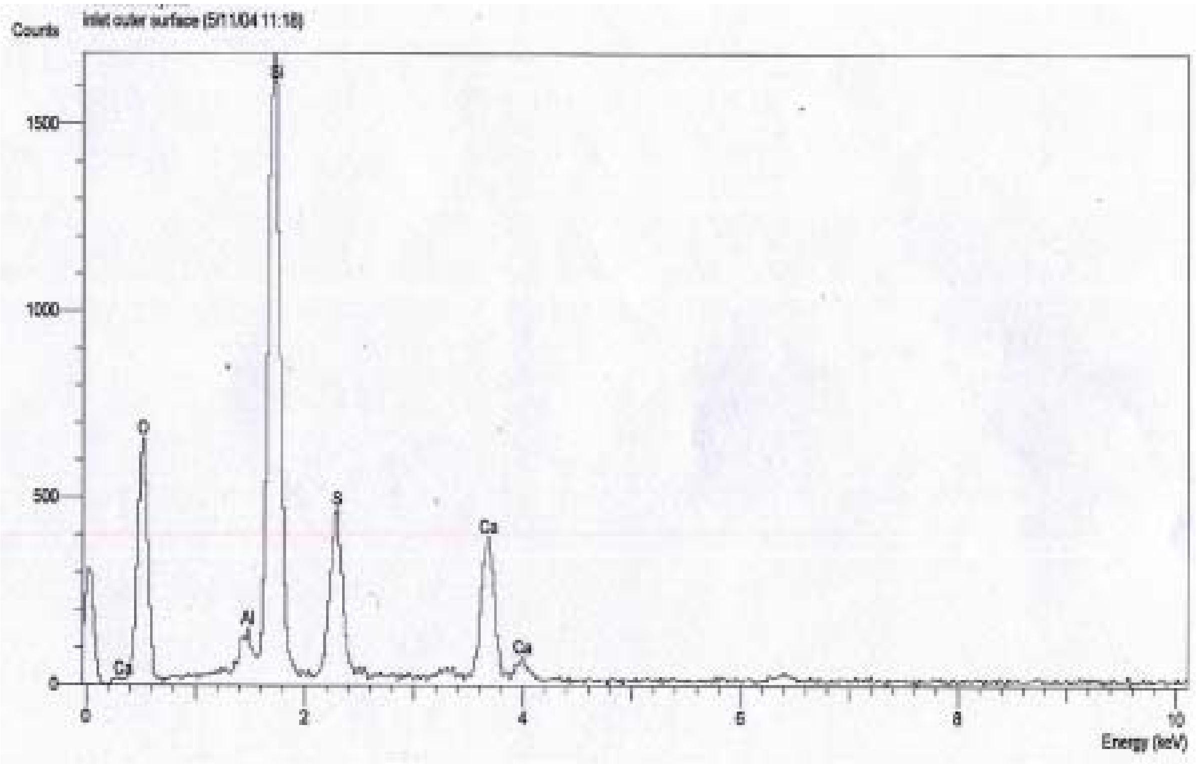

Figure 6.9: EDS Analysis at the Inlet face of the Core (Run # 8)

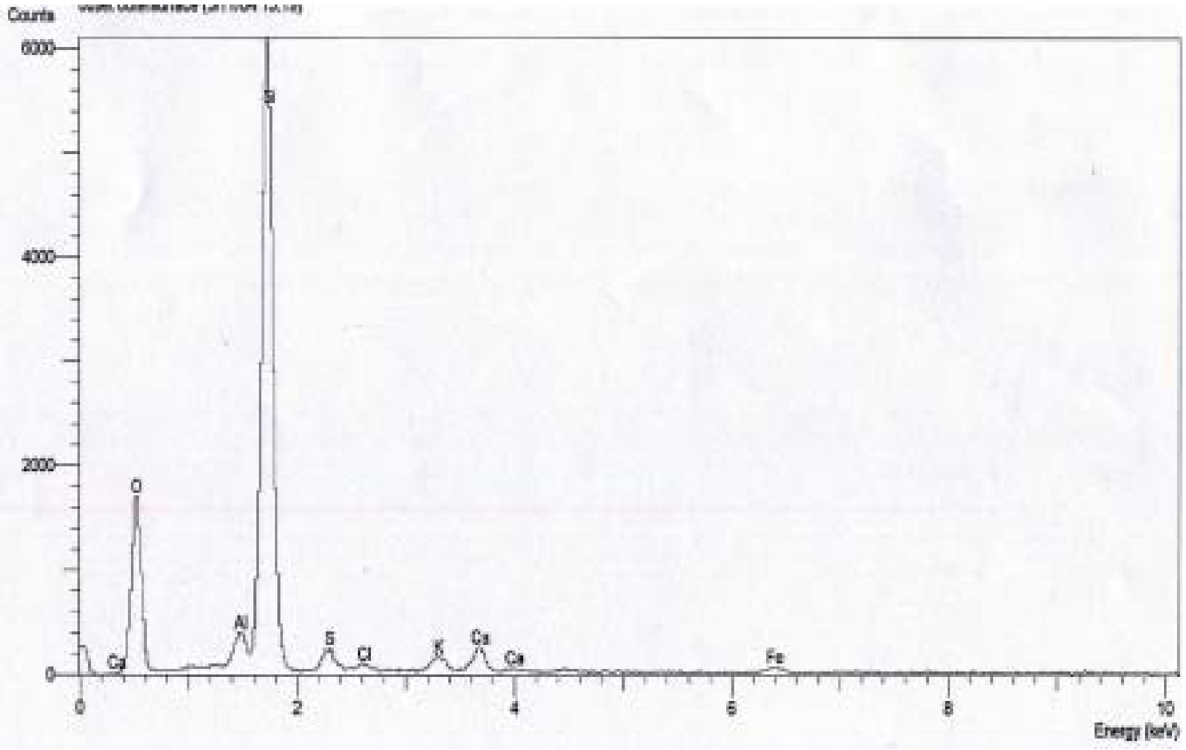

Figure 6.10: EDS Analysis at the Outlet face of the Core (Run # 8)

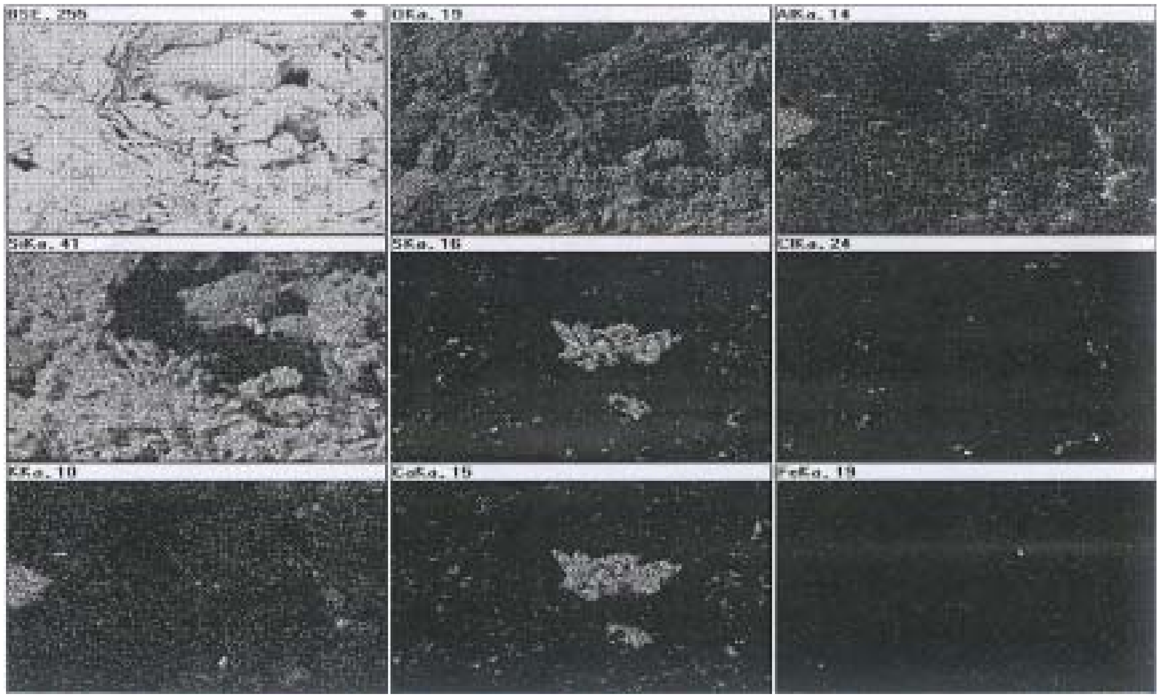

Figure 6.11: BEI of the Outlet face of the Core (Run # 8)

6.1.7 Average Rate of Precipitation of $CaSO_4$

The instantaneous rate of precipitation of $CaSO_4$ at any point within the core is given by,

$$Rate = \frac{-d\,C_{Ca}}{d\,t} \quad \text{(m/min)}$$

where,

dC_{Ca} : Infinitesimal change in the concentration of Ca^{++} within the core. (m)

dt : Infinitesimal contact time between Ca^{++} and SO_4^{--} within the core. (min)

Since Ca^{++} concentration profile across the core is not available, the average reaction rate across the core is calculated by:

$$Rate = -\frac{\Delta C_{Ca}}{\Delta t} = -\frac{C_{Ca\,out} - C_{Ca\,in}}{\Delta t} = -\frac{C_{Ca\,in} - C_{Ca\,out}}{\Delta t}$$

Δt is the residence time of the brine in the core as given by:

$$\Delta t = \frac{V_p}{Q}$$

where,

Q : Brine injection flow rate (ml/min)

V_p : Pore volume of the core sample (ml)

The above simplification is warranted by the short length of the core, which allows the Ca^{++} concentration profile to be nearly linear. Therefore, for Run # 8

ΔCa^{++} = 2180 - 2000 = 180 PPM = 0.0044 m

where 2000 ppm is the steady-state concentration of Ca^{++} in the effluent as estimated from Fig. 6.1.

$$\Delta t = \frac{V_p}{Q} = \frac{14.97 ml}{10 ml/\min} = 1.497 \min \approx 1.5 \min$$

Thus, $q = \dfrac{180PPM}{1.5\min} = 120PPM\,\min^{-1} = 0.00294m\,\min^{-1}$

where q is the average rate of the reaction.

6.1.8 Rate Constant (K_a) Calculations

Among the different reaction law expressions presented in Chapter 4 and represented by equations 4.18 to 4.23, the following form (Equ. 4.22) shall be used for illustration pursposes:

$$q = k\left[\frac{C_{Ca}\ C_{SO_4}}{K_{sp}}\right] \tag{4.22}$$

Where,

k : Kinetic rate constant (m. $\min^{-1}$)

q : Rate of the $CaSO_4$ precipitation reaction (m/min)

$\overline{C_{Ca}}$, $\overline{C_{SO_4}}$: Average steady-state concentrations of the ions across the core (m)

$\overline{K_{sp}}$: Solubility Product based on the average steady-state concentrations. (m^2)

From the experimental data of Run # 8;

$$\overline{C_{Ca}} = \frac{(2180+2000)}{2} = 2090PPM = 0.05106m$$

$$\overline{C_{SO_4}} = \frac{(1200+768)}{2} = 984PPM = 0.01019m$$

$\overline{K_{sp}} = 0.000432\ m^2$

Substituting the experimentally estimated value of q in Equ. 4.22, the average kinetic rate constant is computed as:

$$k = \frac{q \times \overline{K_{sp}}}{\overline{C_{Ca}}\ \overline{C_{SO_4}}} = \frac{0.00294\, m \min^{-1} \times 0.000432\, m^2}{(0.05106)(0.0102)\, m^2} = 0.00244 \text{ m min}^{-1}$$

k = 0.0024 m min^{-1} = 4.0644 M Sec^{-1}

6.2 Effect of Various Parameters on CaSO$_4$ Precipitation

Various operating parameters such as temperature, pressure, concentration and flow velocity (injection rate) are known to effect the scaling potential of a brine. In this section, the influence of each parameter on the reaction rate constant is investigated.

6.2.1 Effect of Temperature

To study the effect of temperature on the rate constant, core flood Runs # 9, 10 and 11 were performed at temperatures of 95, 70 and 45 ^{o}C, respectively. All other parameters were maintained constant such as P_{Back} = 3000 psig, Q= 10 ml/min, L_{Core} = 2”, D_{Core} = 1.5”, and the injected brine concentrations are also identical: Ca^{++} = 3060 PPM (0.075 m); SO_4^{--} = 1800 PPM (0.019 m). Average values of K_{sp}, SS, and rate of reaction for these runs are listed in Table 6.3. Also listed in Table 6.3 are values of k computed using the six rate laws.

Literature data shows calcium sulphate solubility increasing with temperature up to about 15^{o}C (that is below room temperature), then decreasing with further increase in temperature. [74] Since the three runs were conducted above 15^{o}C, drop in solubility with increase in temperature should favor more scale formation inside the core.

A plot of k (using Equ. 4.22) vs. temperature shows an increasing trend between 45 to 95^{o}C as shown in Figure 6.12. Since the Arrhenius equation (eqn. 4.17) stipulates that k varies semi-logarithmically with 1/T, a plot of these two parameters is shown in Figure 6.13 for the 3 runs.

The best straight line fit of Figure 6.13 produces the following value:

E_A (Activation Energy) = 42.8 kJ/mole

Table 6.3: Experimental Data and Results at Different Temperature Runs

Run #	**Berea Sandstone Core Properties**			**Operating Conditions**			**Ionic Strength**								**Supersaturation**			
	V_p cc	**Φ (%)**	**k md**	**(P) Psig**	**(Q) ml/min**	**T °C**	**Ca^{++} Conc.**				**SO_4^{--} Conc.**				**Average Ionic Prod (m^2)**	**Average Is (m)**	**Average K_{sp} (m^2)**	**Average SS**
							Inlet		**Outlet (Steady State.)**		**Inlet**		**Outlet (Steady State)**					
							PPM	m	PPM	m	PPM	m	PPM	m				
9	13.5	23.6	208	3000	10	95	3060	0.075	2770	0.068	1800	0.019	1104	0.0114	0.00108	0.2201	0.000558	1.9292
10	15	25.5	217	3000	10	70	3060	0.075	2870	0.0705	1800	0.019	1344	0.0139	0.00119	0.2250	0.000702	1.6885
11	13.9	24.4	215	3000	10	45	3060	0.075	3030	0.0744	1800	0.019	1728	0.0179	0.00137	0.2330	0.000800	1.7070

Average Rate of Reaction $\Delta C_{Ca} / \Delta t$ (m/min)	**Average Rate Constant (k)**					
	$k = q / C_{Ca} C_{SO4}$	**$k = q / ((C_{Ca} C_{SO4} / K_{sp}) - 1)$**	**$k = q /(C_{Ca} C_{SO4})^2$**	**$k = q / \exp[((C_{Ca} C_{SO4} / K_{sp}) - 1)]$**	**$k = q * K_{sp} / C_{Ca} C_{SO4}$**	**$k = q / (C_{Ca} C_{SO4} - K_{sp})$**
0.00529	0.0818	0.000095	76.0	0.0000348	0.0000457	0.1699
0.00312	0.0438	0.000075	37.0	0.0000261	0.0000308	0.1074
0.00053	0.0065	0.000012	4.7	0.0000044	0.0000052	0.0156

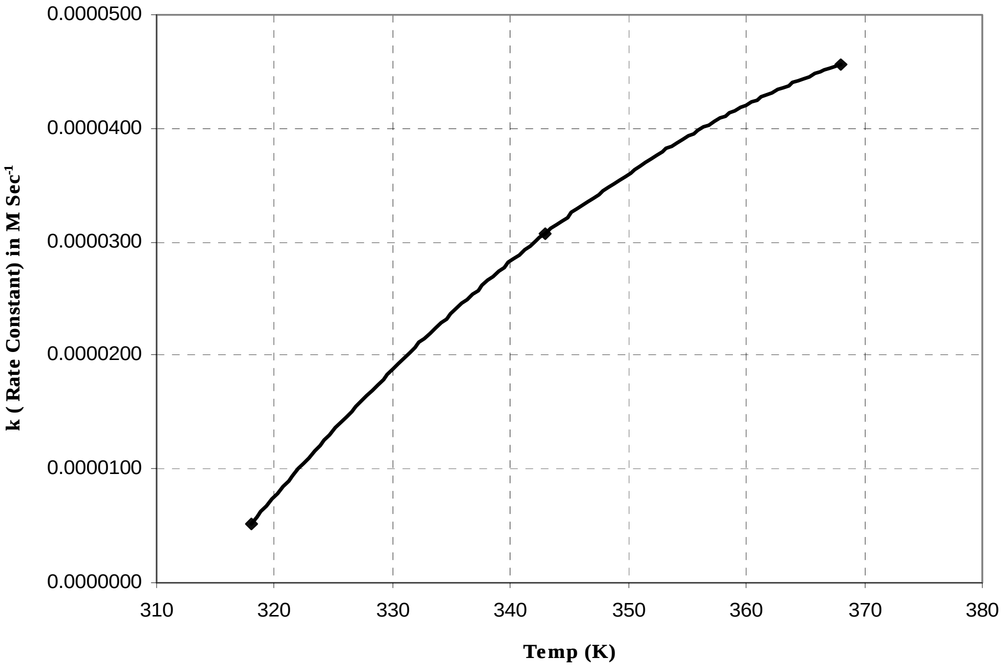

Figure 6.12: Rate Constant vs. Temperature

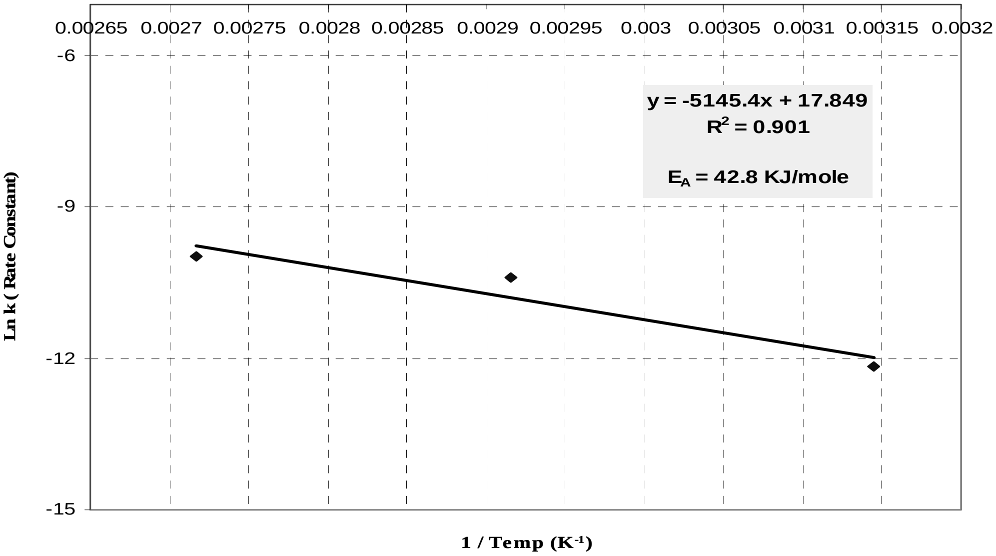

Figure 6.13: Ln k vs. Reciprocal of Temperature

It should be noted that this value of E_A is only a first estimate. A more refined value will be reported later in section 6.3.

6.2.2 Effect of Pressure

To study the effect of pressure on the reaction kinetics, core flood Runs # 9, 12 and 13 were performed at pressures of 3000, 500 and 100 psig, respectively. The other parameters were maintained constant, such as T = 95 ^{o}C, Q= 10 ml/min, L_{Core} = 2", D_{Core} = 1.5" and the ionic strength of the injected brine concentrations are: Ca^{++} = 3060 PPM = 0.075 m; SO_4^{--} = 1800 PPM = 0.019 m.

From the experimental data, the values of K_{sp}, Supersaturation (SS), q, and k (six rate laws) were computed and listed in Table 6.4.

From the literature, it was inferred that the precipitation rate decreases steadily but slightly with increasing pressure, but the differences were not significant. [29, 74] In our case, since the injected brine is an incompressible fluid, the change in density due to change in pressure is negligible. Also, no gaseous components are involved in the precipitation reaction of $CaSO_4$. This explains the insensitivity of the reaction rate constant (as computed by Equ. 4.22) with respect to the pressure as depicted in Fig. 6.14.

Table 6.4: Experimental Data and Results of Different Pressure Runs

Run #	Berea Sandstone Core Properties			Operating Conditions			Ionic Strength								Supersaturation			
	V_p (cc)	Φ (%)	k (md)	Pressure (P) (Psig)	Flow Rate (Q) (ml/min)	Temp. (^oC)	Ca^{++} Conc.				SO_4^{--} Conc.				Average Ionic Prod (m^2)	Average Is (m)	Average Ksp (m^2)	Average SS
							Inlet		Outlet (Steady State.)		Inlet		Outlet (Steady State)					
							PPM	m	PPM	m	PPM	m	PPM	m				
9	13.5	23.6	208	3000	10	95	3060	0.075	2770	0.068	1800	0.019	1104	0.01144	0.001076	0.2201	0.0005580	1.9292
12	14.5	25.1	218	500	10	95	3060	0.075	2775	0.0681	1800	0.019	1116	0.01156	0.001082	0.2204	0.0005585	1.9371
13	14	23.3	214	100	10	95	3060	0.075	2770	0.068	1800	0.019	1104	0.01144	0.001076	0.2201	0.0005580	1.9292

Average Rate of Reaction $\Delta C_{Ca} / \Delta t$ (m/min)	Average Rate Constant (k)					
	$k = q / C_{Ca} C_{SO4}$	$k = q / ((C_{Ca} C_{SO4} / K_{sp}) - 1)$	$k = q /(C_{Ca} C_{SO4})^2$	$k = q / \exp[((C_{Ca} C_{SO4} / K_{sp}) - 1)]$	$k = q * K_{sp} / C_{Ca} C_{SO4}$	$k = q / (C_{Ca} C_{SO4} - K_{sp})$
0.00529	0.0818	0.000095	76.0	0.0000348	0.0000457	0.16992
0.00484	0.0750	0.000086	68.9	0.0000316	0.0000416	0.15400
0.00509	0.0790	0.000091	73.2	0.0000335	0.0000439	0.16349

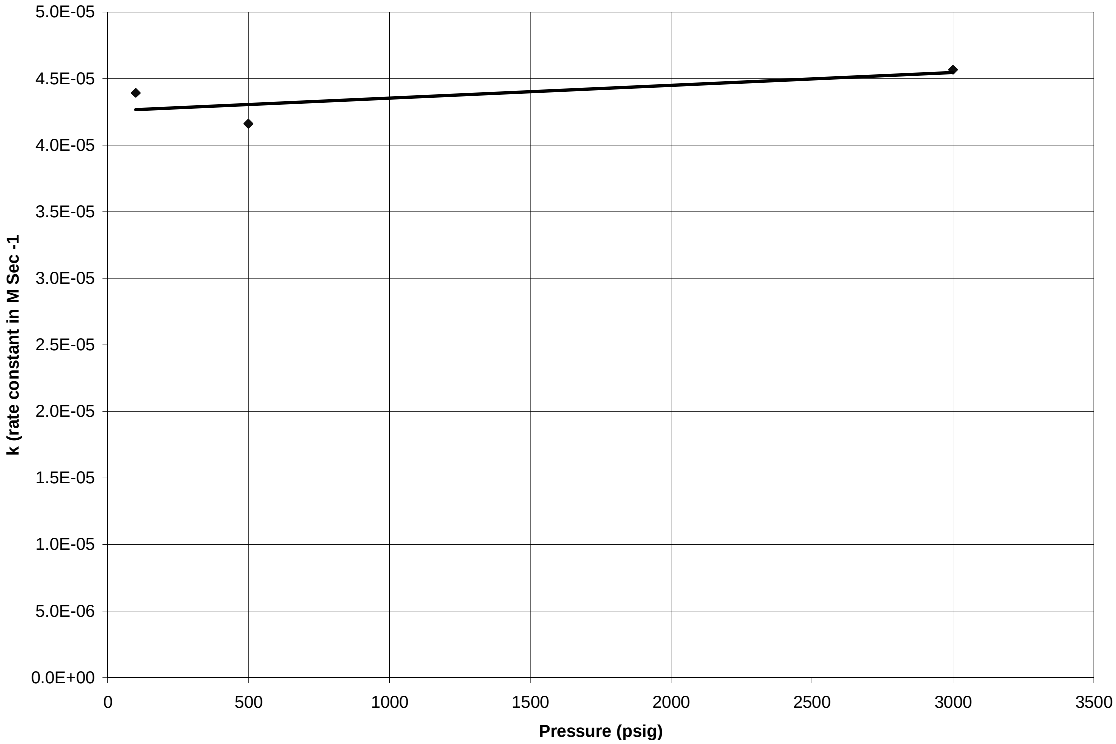

Figure 6.14: Rate Constant vs. Pressure

6.2.3 Effect of Supersaturation (scaling index)

To study the effect of Ca^{2+} and SO_4^{2-} concentrations on the precipitation reaction, core flood Runs # 7, 14, 9 and 8 were performed at the average brine supersaturation of 3.24, 2.9, 2.31 and 1.41, respectively, based on average ionic strength of the inlet and outlet concentrations. The other parameters remained constant, such as T = 95 ^{o}C, Q= 10 ml/min, L_{Core} = 2”, D_{Core} = 1.5” and back pressure P = 3000 psig.

From the experimental data, the values of K_{sp}, supersaturation (SS), q and k (six rate laws) were determined and listed in Table 6.5.

As expected, the rate of precipitation increased as supersaturation level increased. However, a plot of k (Equ. 4.22) vs. SS (Fig. 6.15) shows no distinct variation in k with SS confirming insensitivity of the rate constant to supersaturation.

Table 6.5: Experimental Data and Results of Different Supersaturation (Scaling Index) Runs

Run #	Berea Sandstone Core Properties			Operating Conditions			Ionic Strength								Supersaturation			
	V_p (cc)	Φ %	k md	(P) Psig	(Q) ml/min	T (°C)	Ca^{++} Conc.				SO_4^{--} Conc.				Average Ionic Prod (m^2)	Average Is (m)	Average Ksp (m^2)	Average SS
							Inlet		Outlet (Steady State.)		Inlet		Outlet (Steady State)					
							PPM	m	PPM	m	PPM	m	PPM	m				
7	14	22.9	168	3000	10	95	4175	0.102	3750	0.0913	2400	0.0249	1380	0.0142	0.00189	0.2952	0.000709	2.6624
14	13	23.1	205	3000	10	95	3640	0.089	3300	0.0807	2160	0.022	1344	0.0139	0.00154	0.2617	0.000641	2.4013
9	13.5	23.6	208	3000	10	95	3060	0.075	2770	0.068	1800	0.019	1104	0.0114	0.00108	0.2201	0.000558	1.9292
8	15	25.5	241	3000	10	95	2180	0.053	2000	0.0489	1200	0.012	768	0.0079	0.00052	0.1554	0.000432	1.2059

Average Rate of Reaction $\Delta C_{Ca} / \Delta t$ (m/min)	Average Rate Constant (k)					
	$k = q / C_{Ca} C_{SO4}$	$k = q / ((C_{Ca} C_{SO4} / K_{sp}) - 1)$	$k = q /(C_{Ca} C_{SO4})^2$	$k = q / \exp[((C_{Ca} C_{SO4} / K_{sp}) - 1)]$	$k = q * K_{sp} / C_{Ca} C_{SO4}$	$k = q / (C_{Ca} C_{SO4} - K_{sp})$
0.00740	0.0654	0.0000742	34.6	0.00002340	0.00004634	0.1047
0.00641	0.0694	0.0000762	45.0	0.00002631	0.00004450	0.1189
0.00529	0.0818	0.0000948	76.0	0.00003479	0.00004567	0.1699
0.00294	0.0941	0.0002377	180.8	0.00003985	0.00004060	0.5509

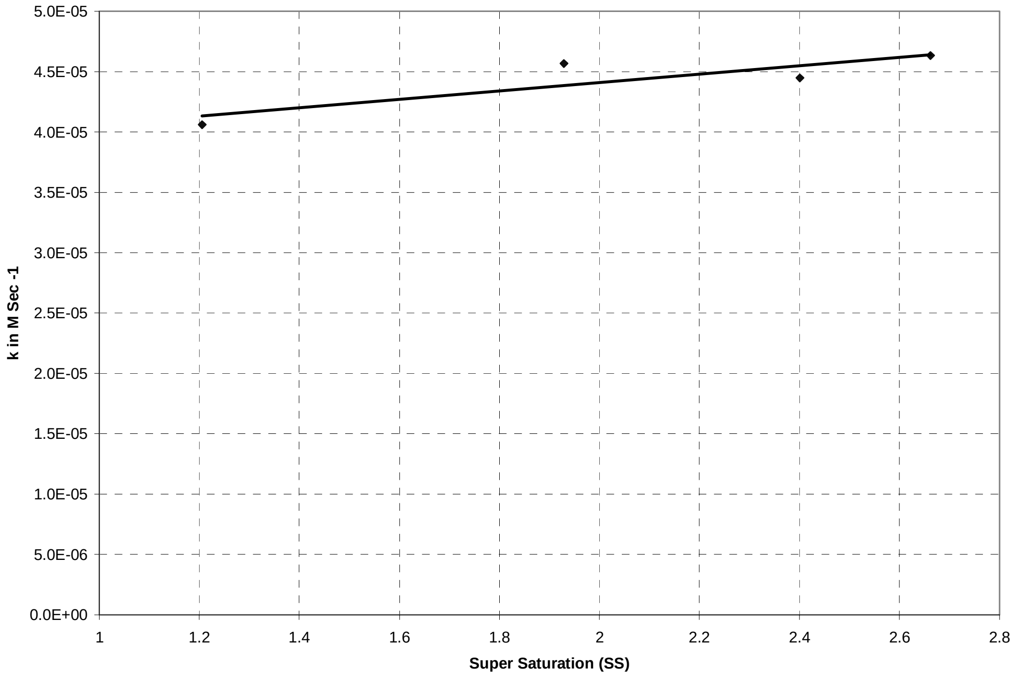

Figure 6.15: Rate Constant vs. Supersaturation

6.2.4 Effect of Flow Rate

To study the effect of flow rate on the scaling reaction, core flood Runs # 17, 15, 9 and 16 were performed at the flow rates of 1, 5, 10 and 15 ml/min, respectively. The other parameters remained constant such as T = 95 ^{o}C, P = 3000 psig, L_{Core} = 2", D_{Core} = 1.5" and the initial injected brine concentrations are also identical (Ca^{++} = 3060 PPM = 0.075 m; SO_4^{--} = 1800 PPM = 0.019 m).

From the experimental data, the values of K_{sp}, supersaturation (SS), rate of reaction and rate constant (k) were determined and listed in Table 6.6. A plot of k (Equ. 4.22) versus Q (Fig. 6.16) shows a nearly linear increase, which has been observed in the literature [29, 72, 73].

The reaction rate constant obtained from chemical reactor test is independent of flow dynamics since it is taken at the so called stirring rate. But in the case of flow through porous media like Berea sandstone, the reaction rate constant had been found to depend on the flow velocity (injection rates of the brines)[72, 73]. This was explained by the fact that as the flow rate increased there were more collisions between the dissolved ions (due to the tortuous nature of the flow paths) which promote the reaction. Hence, the value of the kinetic constant increased.

Employing the Arrhenius equation with E_A = 42.8 kJ/mole, values of A for those 4 runs were computed and plotted in Fig. 6.17. The trend is described by:

$$A = 3 \times 10^{6} Q^{1.189} \qquad (6.1)$$

It is interesting to note that if $Q = 0$, the above equation yields $A=0$ which means no reaction. Naturally, this is not realistic; the equation only shows that when $Q=0$, the flow-rate dependency of A ceases.

Once again, this equation serves only as a component in the model that will be built and refined in the following section.

Table 6.6: Experimental Data and Results of Different Injection Flow Rate Runs

Run #	Berea Sandstone Core Properties			Operating Conditions			Ionic Strength								Supersaturation			
	V_p (cc)	Φ %	k md	(P) Psig	(Q) ml/min	T (°C)	Ca^{++} Conc.				SO_4^{--} Conc.				Average IP (m^2)	Average Is (m)	Average K_{sp} (m^2)	Average SS
							Inlet		Outlet (Steady State.)		Inlet		Outlet (Steady State)					
							PPM	m	PPM	m	PPM	m	PPM	m				
17	14	24.7	229	3000	1	95	3060	0.075	2850	0.07	1800	0.019	1296	0.0134	0.00116	0.2241	0.000566	2.0560
15	13	22.3	214	3000	5	95	3060	0.075	2840	0.0697	1800	0.019	1272	0.0131	0.00115	0.2236	0.000565	2.0402
9	13.5	23.6	208	3000	10	95	3060	0.075	2775	0.0681	1800	0.019	1116	0.0115	0.00108	0.2204	0.000558	1.9371
16	13	22.2	216	3000	15	95	3060	0.075	2755	0.0676	1800	0.019	1068	0.0110	0.00106	0.2194	0.000556	1.9054

Average Rate of Reaction $\Delta C_{Ca} / \Delta t$ (m/min)	Average Rate Constant (k)					
	$k = q / C_{Ca} C_{SO4}$	$k = q / ((C_{Ca} C_{SO4} / K_{sp}) - 1)$	$k = q / (C_{Ca} C_{SO4})^2$	$k = q / \exp[((C_{Ca} C_{SO4} / K_{sp}) - 1)]$	$k = q * K_{sp} / C_{Ca} C_{SO4}$	$k = q / (C_{Ca} C_{SO4} - K_{sp})$
0.00037	0.0053	0.0000058	4.5	0.00000214	0.00000299	0.01029
0.00208	0.0301	0.0000334	26.1	0.00001226	0.00001701	0.05907
0.00519	0.0800	0.0000924	74.0	0.00003392	0.00004469	0.16543
0.00866	0.1361	0.0001594	128.4	0.00005837	0.00007575	0.28647

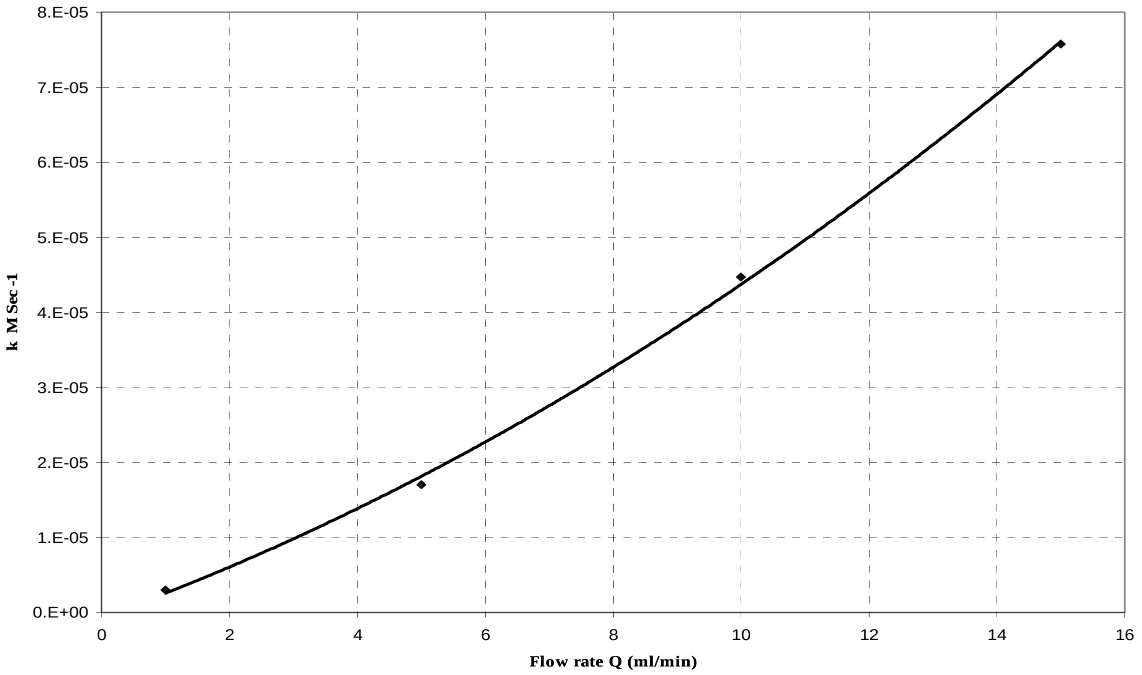

Figure 6.16: Rate Constant vs. Injection Flow rate

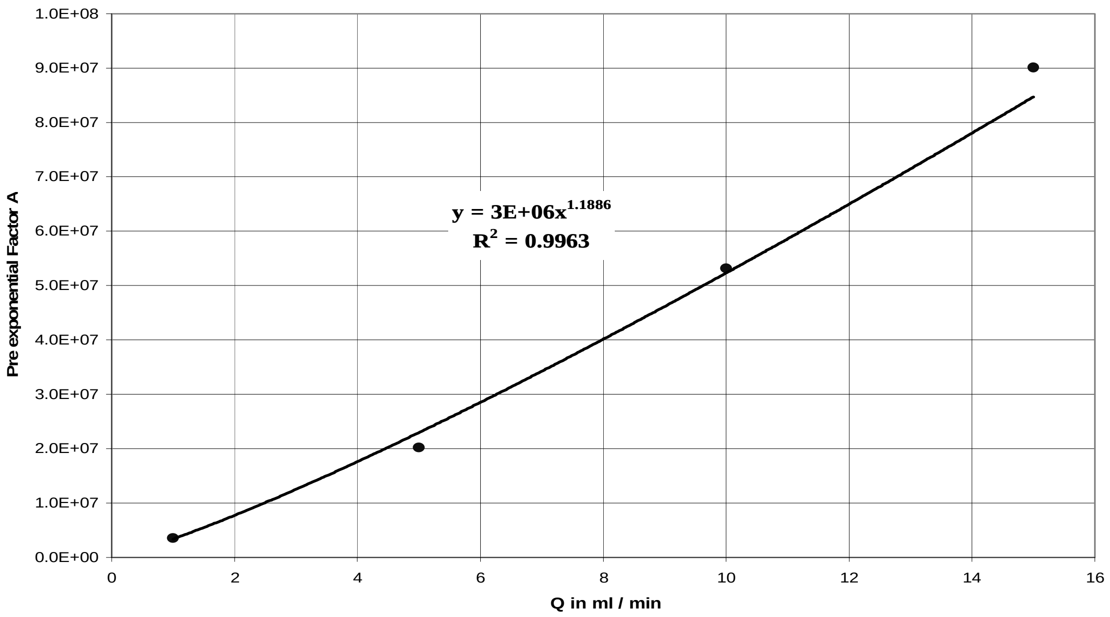

Figure 6.17: Pre-Exponential Factor (A) vs. Injection Flow Rate

6.3 General Equation for the Reaction-rate Constant

In this section, a general equation for the reaction rate constant is developed utilizing the isolated dependencies of k on T and Q derived in the previous sections. Combining Equs. 4.17 and 6.1, the general equation should have the following form:

$$\mathrm{k} = \left[\, a\, \mathrm{Q}^{\,b} + c \,\right] \mathrm{e}^{-\mathrm{E_A}/\mathrm{R\,T}} \qquad (6.2)$$

where a, b, c, and E_A are constants. While values of these constants were obtained in the previous sections, one cannot generalize those values to all runs. Therefore, non-linear regression analysis was used to refine the values of the 3 coefficients plus E_A to fit all 11 runs with minimum error in k.

The regression results were as follows:

a = 0.011

b = 1.323

c = 2.376×10^{-3}

E_A = 26.175 kJ/mole,   R = 8.314 J/mole.K

and Equ. 6.2 becomes:

$$\mathrm{k} = \left[0.011\,\mathrm{Q}^{\,1.323} + 2.376\times10^{-3}\,\right] \mathrm{e}^{-26175/\mathrm{RT}} \qquad (6.3)$$

Table 6.7 lists the values of the kinetic rate constant for the 11 successful runs as predicted by Equ. 6.3. Those values were obtained by substituting the operating parameters of each run (Q, T) into that equation.

Table 6.7: Comparison among Rate Constant Values of 11 Runs

Run #	**Operating Conditions**					**Average Super-saturation**	**Ka From Experiment (M Sec $^{-1}$)**	**Ka From Model (M Sec $^{-1}$)**	**Absolute Percentage Error**
	P (Psig)	**Q (ml/min)**	**Flow Vel V (m/sec)**	**Temp (°C)**	**Temp (K)**		$k = \frac{q \times \overline{K_{sp}}}{\overline{C_{Ca}}\ \overline{C_{SO_4}}}$		
Effect of Supersaturation									
7	3000	10	1.5E-04	95	368	3.245	4.63E-05	4.47E-05	3.49
14	3000	10	1.5E-04	95	368	2.906	4.45E-05	4.47E-05	0.50
9	3000	10	1.5E-04	95	368	2.311	4.57E-05	4.47E-05	2.08
8	3000	10	1.5E-04	95	368	1.407	4.06E-05	4.47E-05	10.15
Effect of Flow Rate									
17	3000	1	1.5E-05	95	368	2.457	2.99E-06	2.56E-06	14.37
15	3000	5	7.4E-05	95	368	2.438	1.70E-05	1.82E-05	6.71
9	3000	10	1.5E-04	95	368	2.320	4.47E-05	4.47E-05	0.07
16	3000	15	2.2E-04	95	368	2.283	7.58E-05	7.61E-05	0.51
Effect of Temperature									
9	3000	10	1.5E-04	95	368	2.311	4.57E-05	4.47E-05	2.08
10	3000	10	1.5E-04	70	343	1.977	3.08E-05	2.40E-05	22.07
11	3000	10	1.5E-04	45	318	2.024	5.17E-06	1.16E-05	125.15

Since the data point of maximum error was obtained with Run # 11, which was performed at the lowest temperature, non-linear regression was repeated on the other 10 runs and gave the following values.

$a = 0.00031$

$b = 1.341$

$c = 9.986 \times 10^{-5}$

$E_A = 15.437$ kJ/mole, $R = 8.314$ J/mole.K

and Equ. 6.2 becomes:

$$k = \left[0.00031\,Q^{\,1.341} + 9.986 \times 10^{-5}\right] e^{-15437/RT} \tag{6.4}$$

A plot of the equation-predicted values against the experimentally-derived values is shown in Fig. 6.18. The average absolute percent error, maximum absolute percent error and the root mean square percent error were found to be 3.73 %, 11.73 % and 5.37 %, respectively.

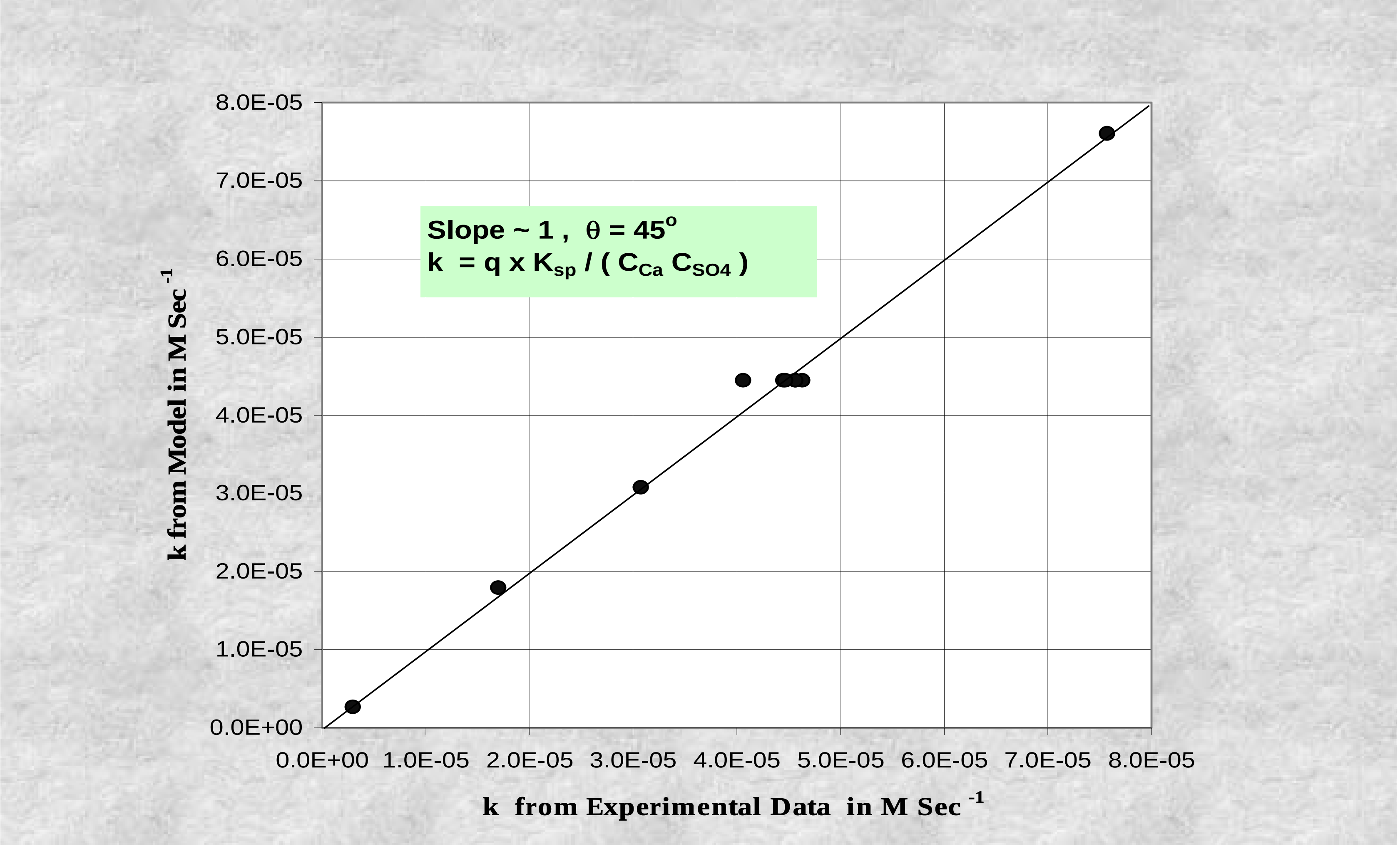

Figure 6.18: Comparison between Measured & Predicted Kinetic Rate Constants for 10 Runs

6.4 Validation of the Model

For validation of the derived model, 4 more runs (18-21) with random values of the parameters (supersaturation level, temperature and injection flow rate) were conducted. The operating parameters included concentrations of Ca^{2+} and SO_4^{2-} ions, K_{sp} values at the test temperatures from the data available in literature and supersaturation level based on average concentration of inlet and outlet. The experimental data for those runs is presented in Table 6.8. The detailed validation run data are also included in Appendix-B.

The experimentally-determined values of kinetic rate constant ($k_{Experimental}$) for the 4 runs are also listed in Table 6.8 along with model-predicted values (k_{Model}). The average absolute % error between $k_{Experimental}$ and k_{Model} for all validation runs is 12.85 % (excluding the worst error run also at the lowest temperature).

Fig. 6.19 is a plot of the model vs. experimental k values (estimated by Equ. 4.22) for the validation runs. From Fig. 6.19, it can be seen that all the values lied very close to the line of unit slope ($\theta = 45^o$) indicating good predictability by the model.

Table 6.8: Validation Runs Data

Run #	Berea Sandstone Core Properties			Operating Conditions					Ionic Strength							
									Ca^{++} Conc.				SO_4^{--} Conc.			
									Inlet		Outlet (Steady State.)		Inlet		Outlet (Steady State)	
	V_p cc	ϕ %	k md	P Psig	Q ml/min	Flow Vel m/sec	Temp °C	Temp K	PPM	m	PPM	m	PPM	m	PPM	m
18	12.97	22.4	210	3000	**20**	3E-04	**90**	363	3100	0.07574	2850	0.06963	1800	0.019	1200	0.0124
19	14.97	26.1	205	3000	**25**	4E-04	**50**	323	6520	0.1593	6440	0.15735	2592	0.027	2400	0.0249
20	11.97	20.67	181	3000	**7**	1E-04	**85**	358	3000	0.075	2795	0.06988	2304	0.024	1812	0.0189
21	11.97	21.03	226	3000	**15**	2E-04	**110**	383	2400	0.06	2105	0.05263	1344	0.014	636	0.0066

Scaling Potential				q = $\Delta C_{Ca^{++}} / \Delta t$ (m/min)	k in M Sec $^{-1}$	k $_{\text{From Model}}$ (M Sec^{-1})	Absolute Percent Error
IP (m^2)	Is (m)	K_{sp} (m^2)	S I		$k = \frac{q \times \overline{K_{sp}}}{\overline{C_{Ca}}\ \overline{C_{SO_4}}}$		
0.00113	0.2236	0.000587	**1.92**	0.00942	0.00008162	0.00009883	21.09
0.00409	0.4614	0.001052	**3.89**	0.00326	0.00001398	0.00004531	224.10
0.00155	0.2373	0.000687	**2.26**	0.00300	0.00002210	0.00002210	0.03
0.00058	0.1703	0.000356	**1.63**	0.00924	0.00009443	0.00010644	12.72

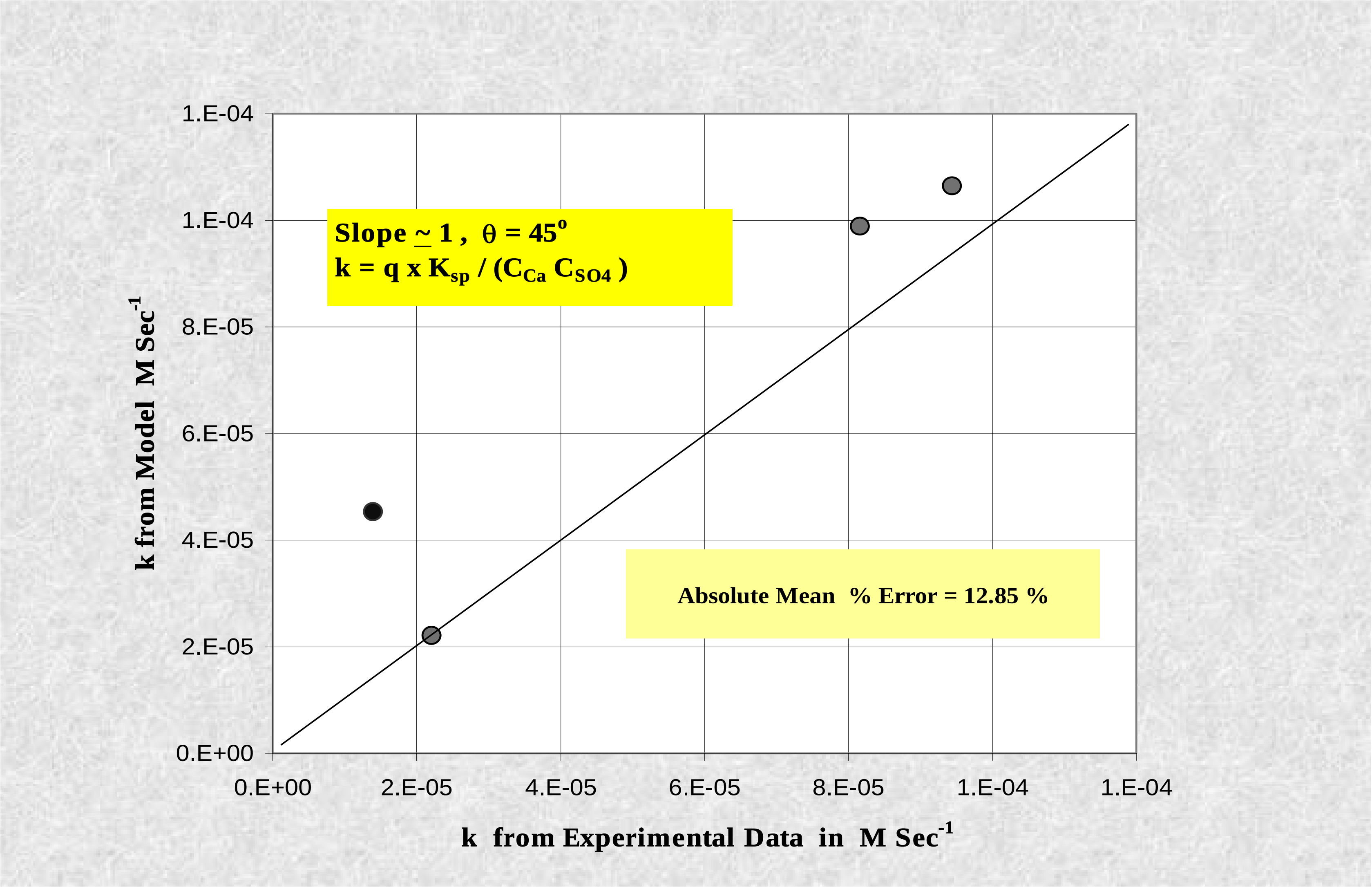

Figure 6.19: Comparison between Experimental & Model Kinetic Rate Constants for Validation Runs

6.5 Further Refinement of the Model

k values estimated from experimental data using the 6 different rate laws (Equ. 4.18 - 4.23) were fitted with Equ. 6.2. The resulting errors are reported in Table 6.9 for the 11 runs and Table 6.10 for the 3 validation runs. The error analyses indicate that Equ. 4.22 is indeed the most appropriate for this reaction.

Further improvement was made by adding the 3 validation data points to the group of 10 runs to increase data span for the derived equation and to minimize the absolute % error. Non-linear regression analysis for all 13 runs yielded the following values:

$a = 0.0083$

$b = 1.021$

$c = -6.56 \times 10^{-3}$

$E_A = 22.9$ kJ/mole, $R = 8.314$ J/mole.K

and Equ. 6.4 is refined to:

$$k = \left[\, 0.0083\, Q^{\,1.021} - 6.56 \times 10^{-3} \,\right] e^{-22903/RT} \qquad \textbf{(6.5)}$$

A plot of the equation-predicted values vs. the experimentally-derived values (based on Equ. 4.22) is shown in Fig. 6.20. The average absolute percent error and the root mean square percent error were improved to 11.16 % and 20.6 %, respectively.

Table 6.9: Approximate Error Analysis for 11 Runs

	$k = q / C_{Ca} C_{SO4}$	**$k = q / ((C_{Ca} C_{SO4} / K_{sp}) - 1)$**	**$k = q / (C_{Ca} C_{SO4})^2$**	**$k = q / \exp[((C_{Ca} C_{SO4} / K_{sp}) - 1)]$**	**$k = q * K_{sp} / C_{Ca} C_{SO4}$**	**$k = q / (C_{Ca} C_{SO4} - K_{sp})$**
Avg. Absolute Percent Error	19.9	43.9	46.9	24.05	**17.02**	56.13
Max. Abs. Percent Error	130.1	128.31	136.13	137.3	**125.15**	126.13
Point less than 15.1% Error	63.64	9.09	45.45	54.55	**81.82**	9.09

Table 6.10: Approximate Error Analysis for Validation Runs

	k = q / $C_{Ca}\,C_{SO4}$	**k = q / (($C_{Ca}\,C_{SO4}$ / K_{sp}) - 1)**	**k = q / ($C_{Ca}\,C_{SO4}$)^2**	**k = q / exp[(($C_{Ca}\,C_{SO4}$ / K_{sp}) - 1)]**	**k = q *K_{sp} / $C_{Ca}\,C_{SO4}$**	**k = q / ($C_{Ca}\,C_{SO4}$ - K_{sp})**
Avg. Absolute Percent Error	40.32	46.5	38.24	59.78	**12.85**	32.65
Max. Abs. Percent Error	127.62	102.6	73.75	88.85	**27.5**	80.73
Root Mean Square %Error	64.69	61.67	47.25	69.83	**16.8**	44.22

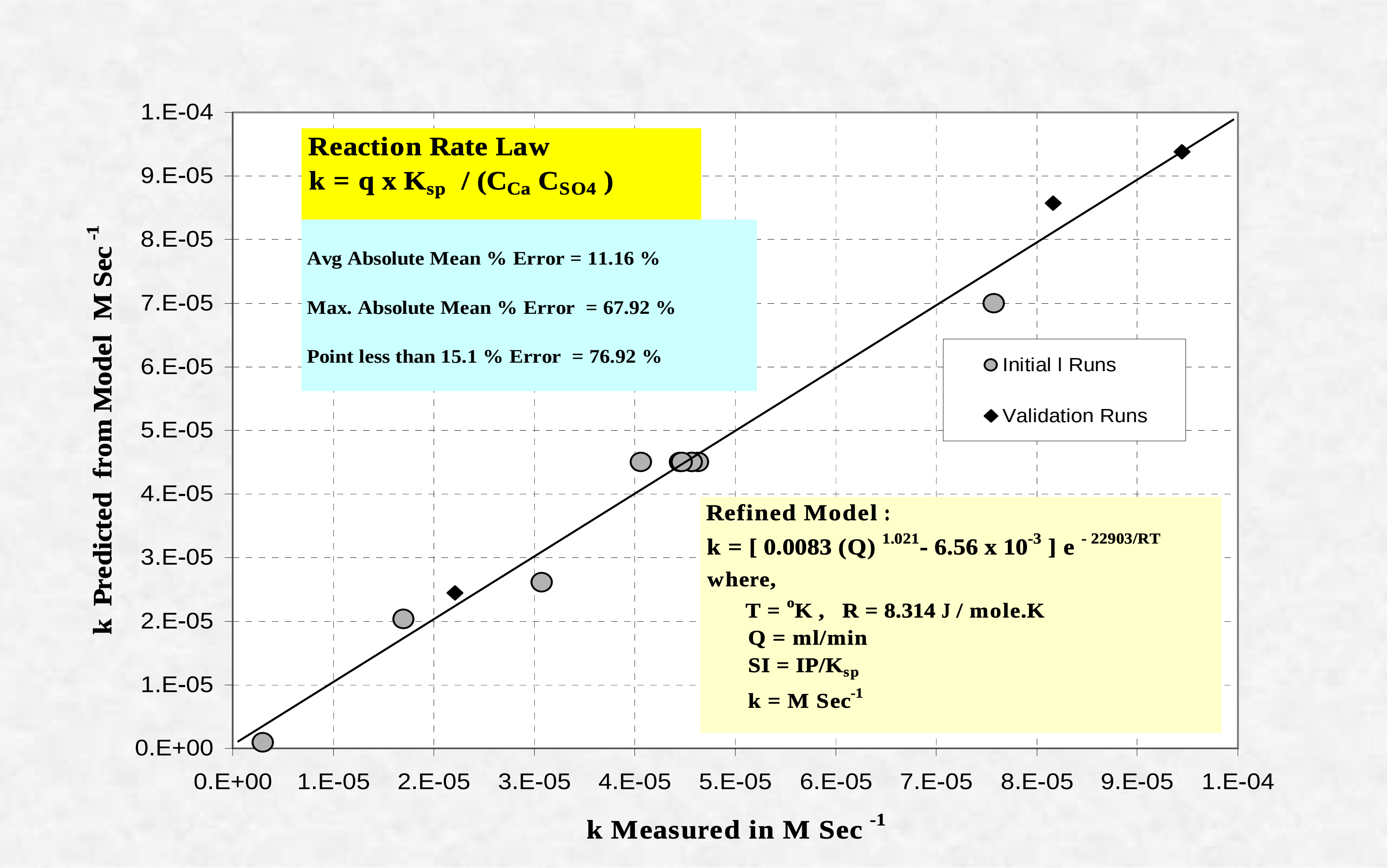

Figure 6.20: Comparison between Experimental & Predicted Kinetic Rate Constants for all 13 Runs

Chapter 7

CONCLUSIONS AND RECOMMENDATIONS

This study was aimed at obtaining a general reaction rate equation to predict the formation of $CaSO_4$ scale in porous media. Calcium sulphate scale is one of the most common oil field scales encountered in oil field operations. Laboratory core flooding experiments were conducted in which a supersaturated synthetic brine containing Ca^{++} and SO_4^{--} ions had been injected through Berea sandstone core samples. Experiments were conducted at various sets of conditions such as temperature, pressure, brine ionic strength (scaling index) and injection flow rate.

The developed reaction rate equation incorporated some kinetic and hydrodynamic parameters. The equation has been validated with the results of additional experimental runs with randomly selected parameters.

7.1 Conclusions

Based on the results presented, the following conclusions can be drawn:

- A simple and sound methodology for laboratory determination of the reaction rate of scale precipitation in porous media has been devised.

For $CaSO_4$ precipitation reaction in Berea Sandstone:

- The reaction rate constant (k) varies with temperature (in the range of 45 to 95^{o}C) according to the Arrhenius equation. The reaction's activation energy was determined at 22.9 kJ / mole.
- A slightly increasing trend was observed in the reaction rate constant with increase in pressure.
- Brine supersaturation level was found to have no conclusive influence on the reaction rate constant.
- The reaction rate constant increased nearly linearly with the total brine flow rate through the core sample.
- The following kinetic rate constant equation for $CaSO_4$ scale precipitation in Berea sandstone cores fitted the experimental data rater well:

$$k = \left[\, 0.0083\, Q^{\,1.021} - 6.56 \times 10^{\,-3} \,\right] e^{-22903/RT}$$

This equation yielded a mean absolute % error of 11.16%.

- Among the different reaction law equations proposed in the literature, the following law appears to be the most appropriate for $CaSO_4$ scale precipitation:

$$q = k\, \frac{C_{Ca}\, C_{SO_4}}{K_{sp}}$$

7.2. Recommendations

Due to the wide scope of this study, the following suggestions for future work in the same area are recommended:

- Analysis of coreflood effluent can be much improved by using an in-line ion analyzer or some other analytical device.
- Parameters such as permeability and porosity of the porous medium may be investigated, and included in the reaction model, by varying the range of porosity and permeability of Berea core samples.
- Instead of synthetic brines, real oil field brines can be employed in the study by mixing field disposal water and sea water.
- Other core materials like limestone and dolomite can be investigated.
- The effect of residual oil saturation on the precipitation reaction can be investigated.

REFERENCES

1. Peter A.R. and Jon K.R.: “The Use of Laboratory Tests to Evaluate Scaling Problems During Water Injection”, *paper* SPE 10593, 1982.

2. Tidwell V.C.: “Laboratory Investigation of Constitute Property Scaling Behavior”, *paper SPE* 28456, 1994.

3. Bayona, H.J.: “A Review of Well Injectivity Performance in Saudi Arabia’s Ghawar Field Seawater Injection Program”, *paper* SPE 25531, 1993.

4. Vatter O.G., Phillips R.C.: “Prediction of Deposition of Calcium Sulphate Scale Under Down-Hole Conditions, *Journal of Petroleum Technology*, 1299-1308, October 1970.

5. Paige R.W., Murray L.R., Martins J.P. and Marsh S.M.: “Optimizing Water Injection Performance”, *paper* SPE 29774, 1995.

6. Asghari K. and Kharrat R.: “Alteration of Permeability by Fine Particle Movement – A Water Injectivity Problem”, paper SPE 29006, 1995.

7. Mackay E.J., Coolins I.R., Jordan M.M. and Feassey N.: “PWRI: Scale Formation Risk Assessment and Management”, paper SPE 80385, 2003.

8. Voloshin A.I., Ragulin V.V.,Tyabayeva N.E., Diakonov I.I. and Mackay E.J.: “Scaling Problems in Western Siberia”, paper SPE 80407, 2003.

9. Moghadasi J., Jamilahmadi M., Muller-Steinhagen H. and Sharif A.: “Scale Formation in Iranian Oil Reservoir and Production Equipment during Water Injection”, *paper* SPE 80406, 2003.

10. Stalker R., Collins R.I. and Graham G.M.: “The Impact of Chemical Incompabilities in Commingled Fluids on the Efficiency of a Produced Water Reinjection System: A North Sea Example”, paper 80257, 2003.

11. Kohler N., Courbin G. and Ropital F.: “Static/Dynamic Evaluation of Calcium Carbonate Scale Formation and Inhibition”, *Journal of Petroleum Technology*, May 2002.

12. Bedrikovistsky P., Marchesin D., Shecaira F., Serra A.L., Marchesin A., Reszende E. and Hime G.: “Well Impairment During Sea/Produced Water Flooding: Treatment of Laboratory Data”, paper SPE 69546, 2001.

13. Paulo J., Mackay E.J., Menzies N. and Poynton N.: “Implications of Brine Mixing in the Reservoir for Scale Management in the Alba Field”, paper SPE 68310, 2001.

14. Andersen K.I., Havorsen E., Saelensminde T. and Ostbye N.O.: “Water Management in a Closed Loop – Problems and Solutions at Barage Field”, *paper* 65162, 2000.

15. Yuan M.D. and Todd A.C.: “Prediction of Sulfate Scaling Tendency in Oil Operations”, SPE paper 18484, *SPE Production Engineering*, February 1991.

16. Yeboah Y.D., Somuah S.K. and Saeed M.R.: “A New and Reliable Model for Predicting Oilfield Scale Formation”, paper SPE 25166, 1993.

17. Mauzzollnl E.J., Bertero L. and Truefllt G.S.: “Scale Prediction and Laboratory Evaluation of BaSO4 Scale Inhibitors for Seawater Flood in a High-Barium Environment”, *SPE Production Engineering*, May 1992.

18. Thomas L.G., Albertsen M., Perdeger A., Konoke H.H.K, Hosrstmann B.W. and Schenk D.: “Chemical Characterization of Fluids and Their Modeling with Respect to Their Damage Potential in Injection on Production Processes Using an Expert System”, paper SPE 28981, 1995.

19. Rousseau G., Hurtevent C.,Azaroual M., Kervevan C. and Durance M.V.: “Application of a Thermo-Kinetic Model to the Prediction of Scale in Angola Block 3 Field”, paper SPE 80387, 2003.

20. Katsanis E.P., Krumrine P.H. and Faclcone J.S.: “Chemistry of Precipitation and Scale Formation in Geological Systems”, paper SPE 11802, 1983.

21. Mitchel R.W., Grist D.M. and Boyle M.J.: “Chemical Treatment Associated with North Sea Projects”, *Journal of Petroleum Technology*, May 1980.

22. Betero L., Chierici G.L., Gottardi G. and Mesini E.: “Chemical Equilibrium Models: Their Use in Simulating of Incompatible waters”, paper SPE 14126, March 1986.

23. Lindlof J.C., and Stoffer K.J.: “A Case Study of Seawater Injection Incompatibility”, *Journal of Petroleum Technology*, July 1983.

24. Vatter O.G., Kandrapa V. and Harouaka A.: “Prediction of Scale Problems Due to Injection of Incompatible Waters”, *Journal of Petroleum Technology*, 273-284, February 1982.

25. Miller D.G., Piwinskii A.J. and Yamauchi R.: “Geochemical Equilibrium Codes: A Means of Modeling Precipitation and Reinjection Phenomenon in the Salton Sea Geothermal Field”, *paper* SPE 6604, 1977.

26. Al-Mumen A.A.: “The Effect of Injected water Salinity on Oil Recovery”, M.S. thesis, K.F.U.P.M., May 1990.

27. Mirza M. S. and Parasad V.: “Scale Removal in Khuff Gas Wells”, *paper* SPE 53345, February 1999.

28. Kabir A.H. and Haron J.: “Scaling Challenges in Tinggi Operation – A Case History of Scaling Management”, *paper* SPE 60199, January 2000.

29. Zhang Y. and Farquhar R.: “Laboratory Determination of Calcium Carbonate Scaling for Oilfield Wellbore Environments”, *paper* SPE 68329, January 2001.

30. Azaroul M., Hurtevent C., Kervevan C. and Brochot S.: “Quantitative Prediction of Scale Depostions Induced by Oil Production; Application of the Thermo-kinetic Software SCALE2000”, *paper* SPE 68303, January 2001

31. McElhiney J.E., Sydansk R.D., Lintelmann K.A., Benzel W.M. and Davidson K.B.: “Determination of In-Situ Precipitation of Barium Sulphate During Coreflooding”, *paper* SPE 68309, January 2001.

32. Marshall, W. L. and Slusher, R.: “Thermodynamics of Calcium Sulfate Dihydrate in Aqueous Sodium Chloride Solutions, 0-110^{O}”, The Journal of Physical Chemistry, Vol. 70(12), 44015-4027, December 1966.

33. Ostroff, A.G. and Metler, A.V.: “Solubility of Calcium Sulfate Dihydrate in the System NaCl-$MgCl_2$-H_2O from 28^{O} to 70^{O} C”, Journal of Chemical and Engineering Data, Vol. 11(3), 346-350, July 1966.

34. Power W.H., Fabuss, B.M. and Satterfield, C.N.: “Transient Solubilites in the Calcium Sulfate-Water System”, Journal of Chemical and Engineering Data, Vol. 9(3), 437-442, July 1966.

35. Power W.H., Fabuss, B.M. and Satterfield, C.N.: “Transient Solute Concentration and Phase Changes of Calcium Sulfate in Aqueous Sodium Chloride”, Journal of Chemical and Engineering Data, Vol. 9(3), 437-442, July 1966.

36. Madgin, W.M. and Swales, D.A.: “Solubilities In The System $CaSO_4$-NaCl-H_2O At 25^0 and 35^0”, Journal of Applied Chemistry, Vol. 6, 482-487, November 1956.

37. Raju, K.U., Nasr-El-Din, H.A. and Al-Shafai, T.A.: “A Feasibility Study of Mixing Disposal Water with Aquifer Water for Downhole Injection”, *paper* SPE 81449, April 2003.

38. Mackay, E.J.: “Modeling In-Situ Scale Deposition: The Impact of Reservoir and Well Geometries and Kinetic Reaction Rates”, *SPE Production & Facilities*, pp.45-56, February 2003.

39. Bezerra, M.C.M., Khalil, C.N. and Rosario, F.F.: “Barium and Strontium Sulfate Scale Formation Due to Incompatible Water in the Namorado Field, Campos Basin, Brazil”, *paper* SPE 21109, October 1990.

40. Sorbie, K.S. and Mackay, E.J.: “Mixing of injected, connate and aquifer brines ni waterflooding and its relevance to oilfield scaling”, *Journal of Petroleum Science and Engineering*, Vol. 27 (2000), pp. 85-106.

41. Hardy, J.A., Barthrope, R.T., Plummer, M.A. and Rhudy, J.S.: “Scale Control in the South Brae Field”, *SPE Production & Facilities*, pp.127-131, May 1994.

42. Lee, A.K.K., Saeed, M.R., Shalabi, M.A. and Rahman F.: “Kinetics of Crystal Growth of Sparingly Soluble Sulfates”, The Proceedings of the 4th Middle East Corrosion Conference, pp.259-273, January 1988, Bahrain.

43. Bertero, L., Chierici, G.L., Gottardi, G. and Mormino, G.: “Chemical Equilibrium Models: Their Use in Simulating the Injection of Incompatible Waters”, *paper* SPE 14126, March 1986.

44. Oddo, J.E. and Tomson, M.B.: “Why Scale Forms in the Oil Field and Methods To Predict it”, *paper* SPE 21710, April 1991.

45. Raju, K.U.G. and Atkinson, G.: “The Thermodynamics of Scale Mineral Solubilities. 3. Calcium Sulfate in Aqueous NaCl”, Journal of Chemical and Engineering Data, Vol. 35(3), 361-367, 1990.

46. Atkinson, G., Raju, K.U.G. Howell, R.D. and Mecik, M.: “A Comprehensive Scale Prediction Program for Oil and Gas Production”, paper *276, The NACE Annual Conference and Corrosion Show,* 1993.

47. Atkins, P.W.: “Physical Chemistry”, 4th Ed., Oxford University Press, London, 1995.

48. Becker, R. and Doring, W.: “Kinetiche Behandlung der Keinbildung in Ubersattigten Danpfen”, Ann. Physik., 24(719), 1935.

49. Campbell, J.R. and Nancollas, G.H.: “The Crystallization and Dissolution of Strontium Sulfate in Aqueous Solution”, Journal of Physical Chemistry, Vol.75 (6), pg. 1735-1740, 1969.

50. Cowan, J. and Weintritt, D.J.: “Water Formed Scale Deposits”, Gulf Publishing Company, Houston, Texas, 1976.

51. Davies, C.W. and Jones, A.L.: “The Precipitation of Silver Chloride from Aqueous Solutions, Part I”, Discussion, Faraday Society, 5, *pp. 103-111*, 1949.

52. Davies, C.W. and Nancollas, G.H.: “The Precipitation of Silver Chloride from Aqueous Solutions, Part 2”, Trans. Faraday Society, 5, *pp. 1-812*, 1955.

53. Garside, J.: “Industrial Crystallization from Solution”, Chemical Engineering Science, Vol. 40(1), *pp. 3-26*, 1985.

54. Gordon, L., Salutsky, M.L. and Willard, H.H.: “Precipitation from Homogenous Solutions”, Wiley, New York, 1959.

55. Horvath, A.L.: “Handbook of Aqueous Electrolyte Solutions”, Physical Properties Estimation and Correlation Methods, Ellis Horwood, UK Publishers, 1985.

56. Khamskii, E.V.: “Crystallization from Solutions”, Consultants Bureau, New York, A division of Plenum Publishing Corporation, 1969.

57. Konak, A.R.: “A New Model for Surface Reaction Controlled Growth of Crystals from Solutions”, Chemical Engineering Science, Vol. 29, *pp.1537-1543,* 1974.

58. Liu, S.T. and Noncollas G.H. “The Crystal Growth of Calcium Sulfate Dihydrate in the Presence of Additives”, Journal of Colloid and Interface Science, Vol. 44(3), *pp. 422-429*, 1973.

59. Mina-Mankarios, G. and Pinder, K.L.: “Salting out Crystallization of Sodium Sulfates”, The Canadian Journal of Chem. Eng., Vol. 69, *pp. 308-310*, 1991.

60. Mullin, J.W.: “Crystallization”, Butterworths, London, 1972.

61. Mullin, J.W.: Crystal Growth, Chapter 14, Bulk crystallization, Ed. B.R. Pamptin, Pergamon Press, *pp. 521-565*, 1980.

62. Noncollas, G.H. and Purdie, N.: “The Kinetics of Crystal Growth”, Quarterly Rev., Chem. Soc., London. Vol. 18, *pp. 1-20*, 1964.

63. Nielsen, A.E.: “Kinetics of Precipitation”, Pergomaon Press, London, 1964.

64. Nielsen, A.E.: “Kinetics of crystal growth during precipitation of a Binary Electrolyte”, Industrial Crystallization 78, Eds. E.J. Jong and S.J. Jancici, pp.159-168, 1979.

65. Pytkowicz, R.M.: “Thermodynamics of Aqueous Systems with Industrial Applications”, S. A. Newman Ed., American Chemical Society Symposium, No. 133, pp. 561-567, 1980.

66. Sohnel, O., Mullin, J.W. and Jones, A.G.: “Crystallization and Agglomeration Kinetics in the Batch Precipitation of Strontium Molybdate”, Ind. Eng. Chem. res., 27, pp.1721-1728, 1988.

67. Van Hook, A. “Crystallization”, Reinhold, New York, 1961.

68. Walton, A.G.: “The Formation and Properties of Precipitates”, Interscience.

69. Yeboah, Y.D., Saeed, M.R. and Lee, A.K.K.: “Strontium Sulfate Precipitation from Electrolyte Solutions”, AICHE Journal, Vol. 40(8), pp. 1422-1425, 1994.

70. Smith, J.M.: “Chemical Engineering Kinetics.” 3rd Edition, McGraw-Hill Company, Singapore, 1981.

71. Collins, A.G.: “Geochemistry of Oilfield Waters.” Chapter 12, Elsevier Scientific Publishing Company, USA, 1975.

72. Bedrikovetsky, P.G. et. al: “Oilfield Scaling - Part 1: Mathematical and Laboratory Modeling.” paper SPE 81127, April 2003.

73. Bedrikovetsky, P.G., Loper Jr. R.P. et. al.: “Barium Sulphate Oilfield Scaling: Mathematical and Laboratory Modeling.” *paper* SPE 87457, May 2004.

74. Patton, C.C.: “Oil Field Water Systems” Campbell Petroleum Series, 1974.

75. Denman, W.L. “Industry and Engineering chemistry”, 1961.

76. Fogler, H.S.: “Elements of Chemical Reaction Engineering.” 3rd Edition, Prentice-Hall, New Jersey, 1999.

APPENDICES

Appendix A

Solubility Data of $CaSO_4$ available in the Literature

- *For calculation of solubilities at different Ionic strengths of Brines at various temperatures*
- *To determine the values of K_{sp} indirectly based on the available solubilities*

- **Table A-1** *&* **Figure A-1** *based on the data available in* **Ostroff and Metler (1966)** [6] *at temperature = 70^{o}C*

- **Table A-2** *&* **Figure A-2** *based on the data available in* **Marshall and Slusher (1966)** [13] *at temperature = 40^{o}C*

- **Table A-3** *&* **Figure A-3** *based on the data available in* **Marshall and Slusher (1966)** [13] *at temperature = 95^{o}C*

- **Table A-4** *&* **Figure A-4** *based on the data available in* **Denmann W.L. (1961)** [75] *at temperature = 50^{o}C*

- **Table A-5** *&* **Figure A-5** *based on the data available in* **Denmann W.L. (1961)** [75] *at temperature = 85^{o}C*

- **Table A-6** *&* **Figure A-6** *based on the data available in* **Ostroff and Metler (1966)** [6] *at temperature = 90^{o}C*

- **Table A-7** *&* **Figure A-7** *based on the data available in* **Marshall and Slusher (1966)** [13] *at temperature = 110^{o}C*

Table A-1: Solubility Data at T = 70^{o}C (Ostroff & Metler)

Temp = 70 C [Source : Ostroff & Metler (1966)]	
Ionic Strength of	**Solubility of**

NaCl	$CaSO_4$
0.0000	0.01418
0.0890	0.0212
0.5660	0.0363
0.8900	0.0427
0.9880	0.0433
1.0000	0.0444
1.5500	0.0508
2.0400	0.0535
2.5300	0.0569
2.6000	0.0572
2.8000	0.0577
3.0100	0.0580
3.3100	0.0583
3.4000	0.0584
3.8000	0.0579
4.1500	0.0561

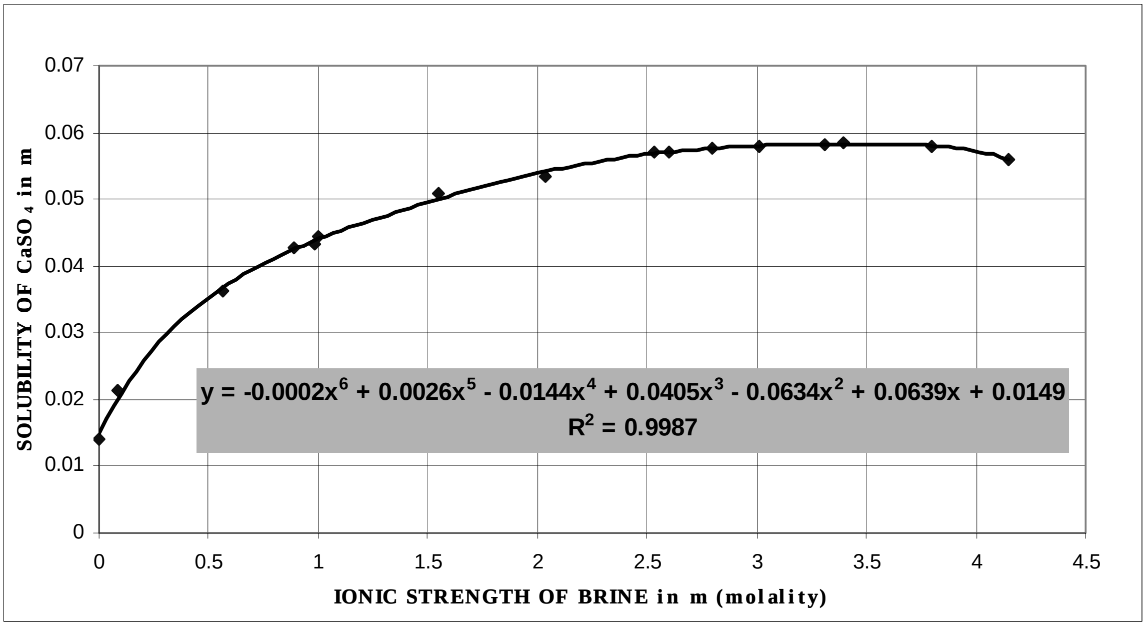

Figure A-1: Solubility Profile of $CaSO_4$ at T = 70^oC

Table A-2: Solubility Data at T = 40°C (Marshal & Slusher)

Temp = 40 C [Source : Marshal & Slusher (1966)]	
Ionic Strength of NaCl	**Solubility of $CaSO_4$**
0.0000	0.0154
0.2500	0.0291
1.0000	0.0458
0.0516	0.0195
0.0967	0.0228
0.1000	0.0227
0.1148	0.0238
0.1923	0.0270
0.2321	0.0282
0.2430	0.0292
0.5060	0.0378
0.5480	0.0371
0.7620	0.0430
0.8340	0.0427
0.9830	0.0461
1.0050	0.0461
2.8100	0.0572
3.6300	0.0563
4.4800	0.0532
5.3700	0.0492
6.2400	0.0480

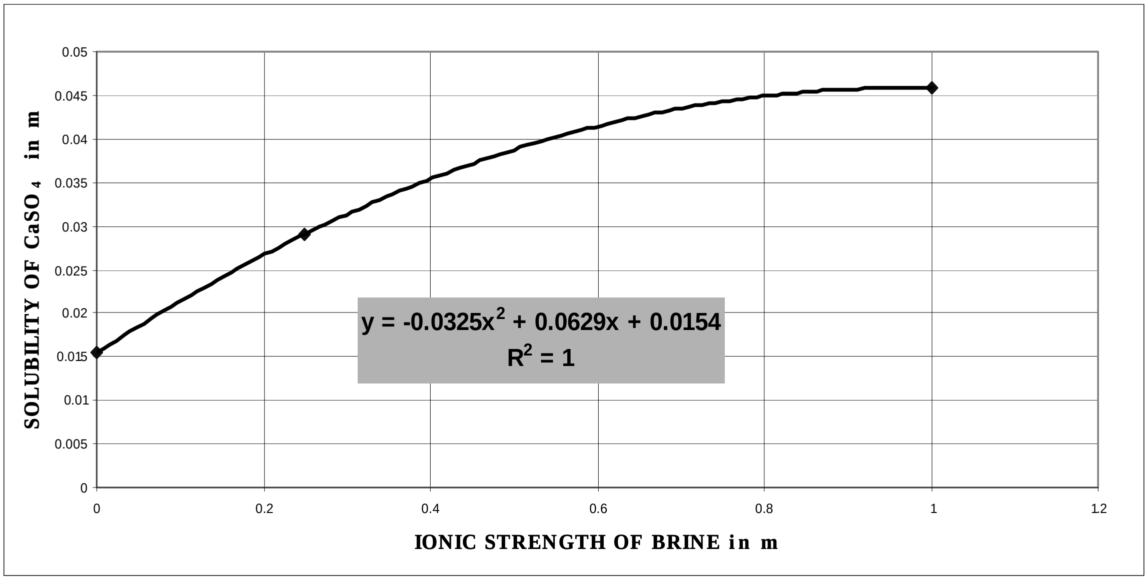

Figure A-2: Solubility Profile of $CaSO_4$ at T = 40°C

Table A-3: Solubility Data at T = 95^{o}C (Marshal & Slusher)

Temp = 95 C [Source : Marshal & Slusher (1966)]	
Ionic Strength of NaCl	**Solubility of CaSO$_4$**
0.0001	0.0123
0.1045	0.0194
0.3892	0.0295
0.9730	0.0427
2.0430	0.0538

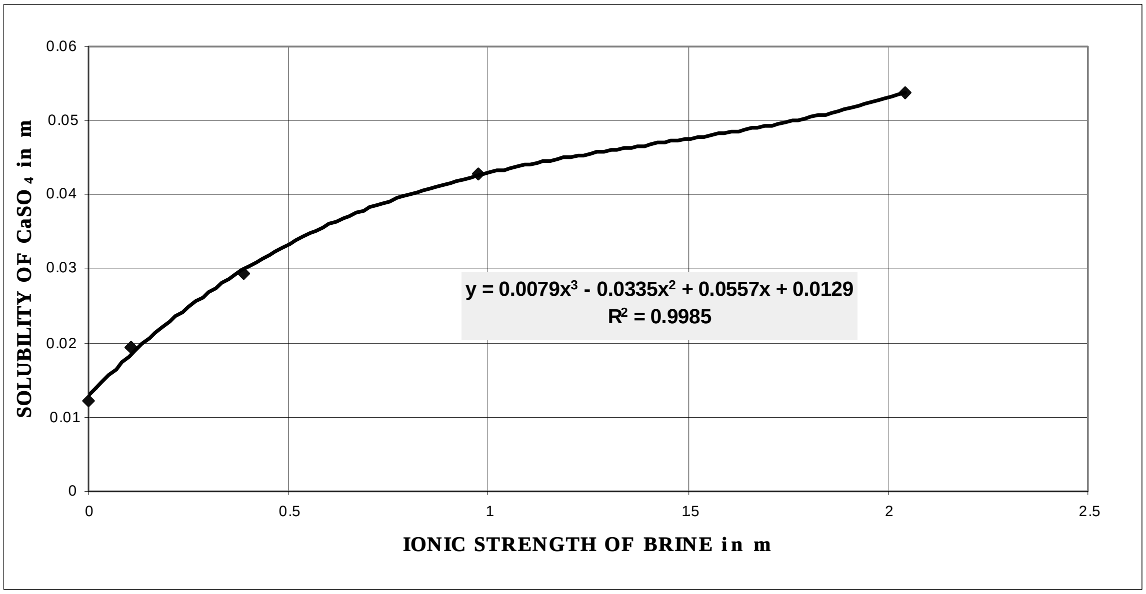

Figure A-3: Solubility Profile of CaSO$_4$ at T = 95^{o}C

Table A-4: Solubility Data at T = 50^{o}C (Denmann W.L.)

Temp = 50 C [Source : Denmann W.L. (1961)]	
Ionic Strength of NaCl	**Solubility of $CaSO_4$**
0.0000	0.01315
0.2470	0.0255
0.2570	0.0263
0.4840	0.0326
0.5120	0.0333
0.9670	0.0422
1.0190	0.0433
1.5600	0.0488

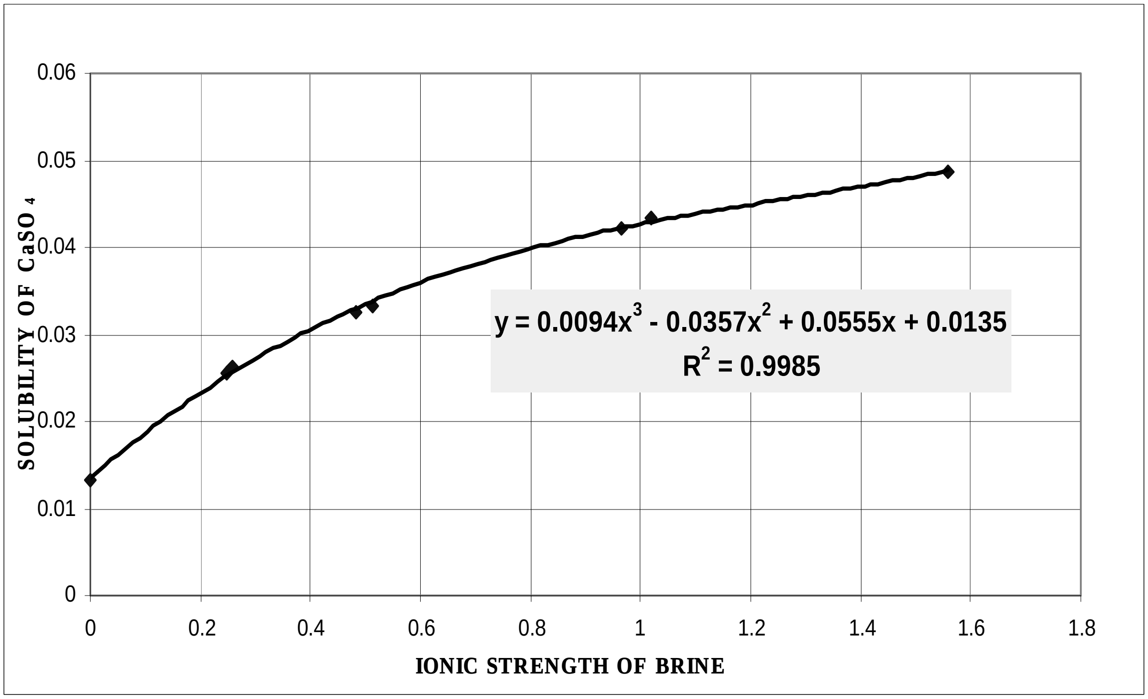

Figure A-4: Solubility Profile of $CaSO_4$ at T = 50^{o}C

Table A-5: Solubility Data at T = 85°C (Denmann W.L.)

Temp = 85 C [Source : Denmann W.L. (1961)]	
Ionic Strength of NaCl	**Solubility of $CaSO_4$**
0.0000	0.0134
0.2500	0.0268
1.0000	0.0439

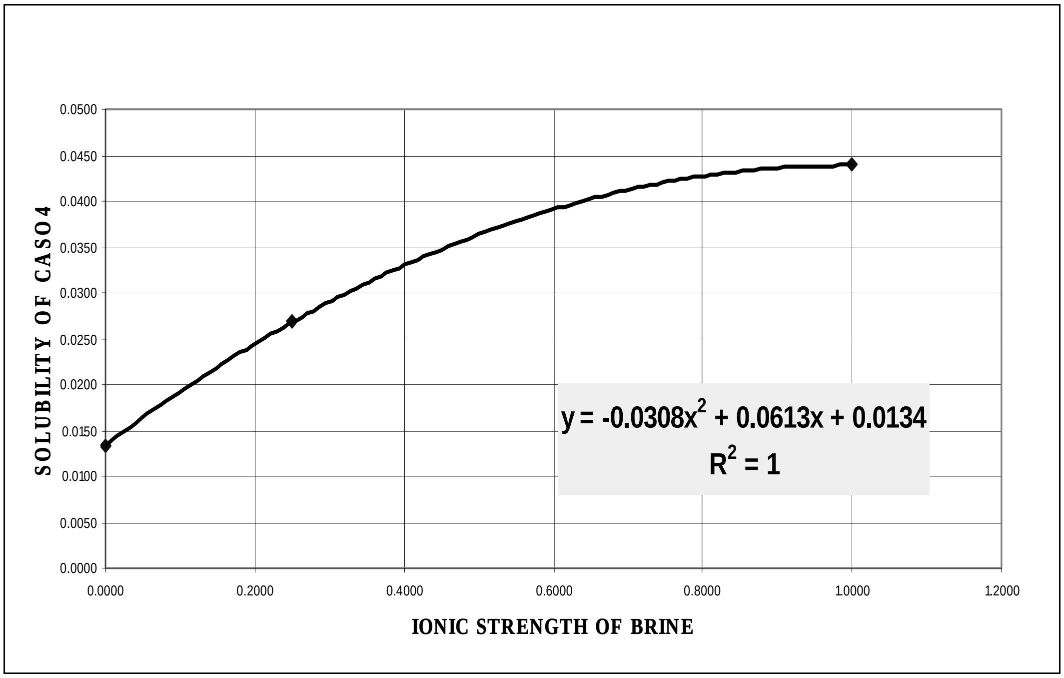

Figure A-5: Solubility Profile of $CaSO_4$ at T = 85°C

Table A-6: Solubility Data at T = 90°C (Ostroff & Metler)

Temp = 90 C [Source : Ostroff & Metler (1966)]	
Ionic Strength of NaCl	**Solubility of $CaSO_4$**
0.0000	0.01315
0.2470	0.0255
0.2570	0.0263
0.4840	0.0326
0.5120	0.0333
0.9670	0.0422
1.0190	0.0433
1.5600	0.0488

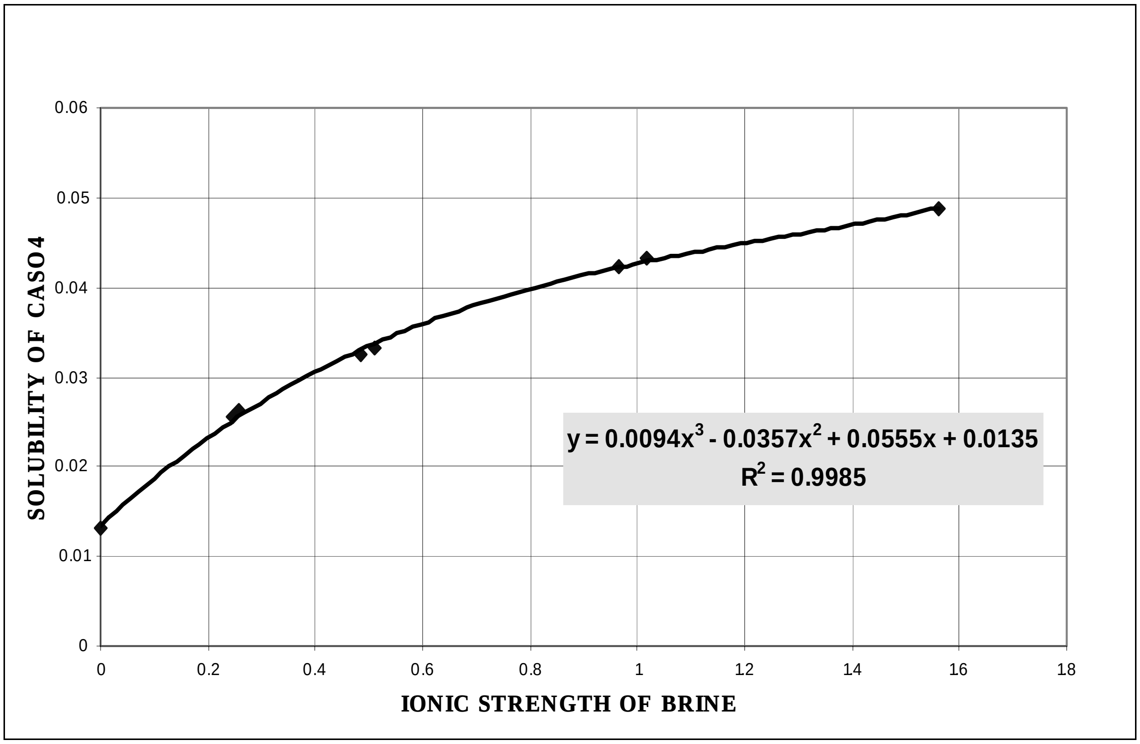

Figure A-6: Solubility Profile of $CaSO_4$ at T = 90°C

Table A-7: Solubility Data at T = $110^{o}C$ (Marshal & Slusher)

Temp = 110 C [Source : Marshal & Slusher (1966)]	
Ionic Strength of NaCl	**Solubility of $CaSO_4$**
0.0000	0.0100
0.1011	0.0161
0.3642	0.0308
3.5000	0.0619
4.1000	0.0719
4.6200	0.0672
5.1800	0.0734

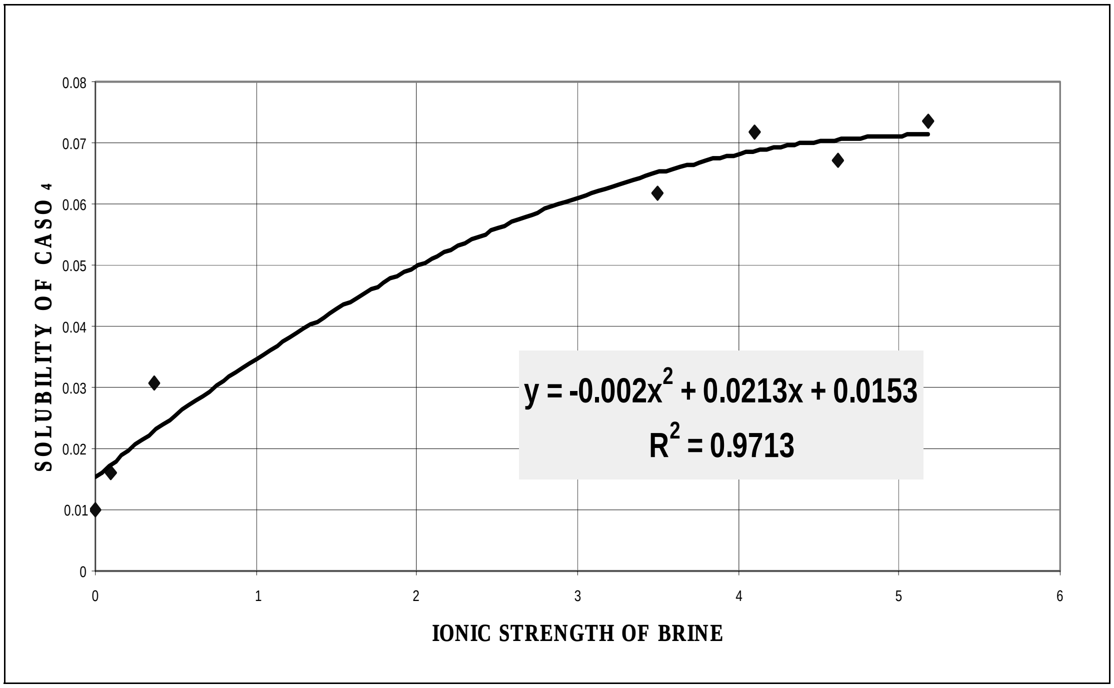

Figure A-7: Solubility Profile of $CaSO_4$ at T = $110^{o}C$

Appendix B

Experimental Data and Results for Flood Runs

In this appendix, the raw and calculated experimental data are presented. The abbreviations used in the tables are as follows:

A total of **21** runs were performed out of which **4** were preliminary, **2** failed due to plugging of tubing, **11** were considered as successful and **4** were validation runs.

Table B-1: Experimental Data of Core Flood Run # 1

Sample #	Date	Time	Cumulative Time (hrs)	ΔP	T	Pinlet	P_{Back}	Pob	Ca^{++} Conc.	
		am / pm		psia	C	psia	psia	psia	PPM	Mole/lit
1	26 / 11 / 2003	12:35 PM	0.0	1.38	95	3100	3000	4200	5200	0.1300
2	26 / 11 / 2003	2:30 PM	2.1	1.39	95	3120	3000	3600	4350	0.1088
3	26 / 11 / 2003	8:50 PM	8.2	1.39	95	3120	3000	3700	4300	0.1075
4	27 / 11 / 2003	1:30 AM	11.4	1.36	95	3120	3000	3700	4200	0.1050
5	27 / 11 / 2003	3:00 PM	24.9	1.37	95	3120	3000	3700	3150	0.0788
6	27 / 11 / 2003	8:00 PM	29.9	1.37	95	3120	3000	3600	2850	0.0713
7	28 / 11 / 2003	1:30 PM	47.4	0.99	95	3150	3000	3600	2600	0.0650
8	28 / 11 / 2003	10:00 PM	54.9	0.97	95	3120	3000	3500	2150	0.0538
9	29 / 11 / 2003	12:45 AM	69.3	1.4	95	3120	3000	3300	2250	0.0563
10	29 / 11 / 2003	12:00 PM	80.5	1.36	94	3060	3000	3300	2300	0.0575
11	30 / 11 / 2003	11:15 AM	91.6	2.12	94	3060	3000	3600	2250	0.0563
12	30 / 11 / 2003	4:00 PM	96.1	2.61	95	3100	3000	3600	2150	0.0538
13	30 / 11 / 2003	10:00 PM	102.1	2.22	95	3200	3000	3650	2200	0.0550
14	1 / 12 / 2003	12:00 AM	116.1	1.716	95	3080	3000	3600	2300	0.0575
15	1 / 12 / 2003	4:10 PM	120.2	1.732	95	3100	3000	3500	2250	0.0563
16	1 / 12 / 2003	11:45 PM	131.5	1.743	95	3100	3000	3450	2150	0.0538
17	2 / 12 / 2003	10:15 AM	142.0	2.347	95	3050	3000	3500	2300	0.0575
18	2 / 12 / 2003	5:30 PM	149.2	1.653	95	3000	3000	3500	2250	0.0563
19	2 / 12 / 2003	10:15 PM	153.4	1.626	95	3100	3000	3700	2250	0.0563
20	3 / 12 / 2003	11:15 AM	166.6	1.693	95	3154	3000	3400	2200	0.0550

Table B-2: Experimental Data of Core Flood Run # 2

Sample #	**Date**	**Time**	**Cumulative Time (hrs)**	**No. of PV Injected**	**Conductivity in ms**	**ΔP**	**T**	**Pinlet**	**P_{Back}**	**Pob**	**Ca^{++} Conc.**	
		am / pm				**psia**	**C**	**psia**	**psia**	**psia**	**PPM**	**Mole/lit**
1	31-1-04	2:15 AM	0	0.000	8.2	0.74	90	3047	3000	3800	5500	0.138
2	31-1-04	7:15 AM	5	0.134	8.2	0.915	92	3053	3000	4300	4000	0.100
3	31-1-2004	6:15 PM	16	0.428	7.9	0.742	92	3017	3000	4600	3100	0.078
4	1/2/2004	12:15 AM	22	0.588	7.8	0.775	92	3018	3000	4200	3300	0.083
5	1/2/2004	3:15 AM	25	0.669	7.6	0.707	93	3021	3000	4300	2250	0.056
6	1/2/2004	6:15 AM	28	0.749	7.6	0.69	93	3043	3000	4300	2700	0.068
7	1/2/2004	4:15 PM	38	1.016	7.4	0.816	92	3029	3000	4200	2050	0.051
8	1/2/2004	8:15 PM	42	1.123	7.5	1.213	93	3044	3000	3800	2200	0.055
9	2/2/2004	12:15 AM	46	1.230	7.7	1.68	92	3168	3000	4200	2100	0.053
10	2/2/2004	3:15 AM	49	1.310	6.6	2.76	93	3448	3050	4200	2300	0.058
11	2/2/2004	6:15 AM	51	1.364	5.9	3.68	95	3063	3000	3700	2150	0.054
12	2/2/2004	10:15 AM	55	1.471	5.8	4.117	95	3075	3000	4400	1950	0.049
13	2/2/2004	7:45 PM	64.5	1.725	5.7	4.325	94	3300	3050	4800	2650	0.066
14	3/2/2004	1:45 AM	70.5	1.885	5.4	4.221	95	3253	3000	4200	2600	0.065
15	3/2/2004	3:45 PM	84.5	2.260	4.2	4.394	95	3170	3000	4100	500	0.013
16	3/2/2004	7:15 PM	88	2.353	4.3	4.601	95	3077	3000	3800	1700	0.043
17	3/2/2004	11:15 PM	92	2.460	4.2	5.272	94	3081	3000	4100	1050	0.026

Table B-3: Experimental Data of Core Flood Run # 3

Date	Time	Cumulative Time (hrs)	No. of PV Injected	Conductivity in ms	ΔP	T	Pinlet	P_{Back}	Pob	Ca⁺⁺ Conc.	
	am / pm				psia	C	psia	psia	psia	PPM	Mole/lit
20 / 2 / 2004	5:00 PM	0.25	0.12	11.2	5.2	93	3047	3000	5000	7187.5	0.180
20 / 2 / 2004	10:00 PM	5.25	1.12	7.6	5.34	94	3048	3000	5100	3187.5	0.080
21 / 2 / 2004	10:00 AM	17.25	3.59	7.7	5.35	95	3058	3000	5100	3562.5	0.089
21 / 2 / 2004	5:00 PM	24.25	6.70	8.3	5.52	95	3101	3000	4400	4187.5	0.105
21 / 2 / 2004	10:00 PM	29.25	7.68	6.8	5.38	95	3050	3000	5200	3000	0.075
22 / 2 / 2004	11:00 AM	42.25	10.30	5.6	5.38	95	3050	3000	4900	3000	0.075
22 / 2 / 2004	5:00 PM	48.25	11.36	5.2	5.48	95	3110	3000	5100	3062.5	0.077
22 / 2 / 2004	10:00 PM	53.25	12.42	4.9	5.84	95	3107	3000	5200	3062.5	0.077
23 / 2 / 2004	11:00 AM	66.25	14.99	4.4	10.01	95	3117	3000	5200	2812.5	0.070
23 / 2 / 2004	3:00 PM	70.25	15.69	4	33.97	95	3122	3000	5200	3062.5	0.077
23 / 2 / 2004	6:00 PM	73.25	16.31	3.9	40	95	3128	3000	5200	3062.5	0.077
23 / 2 / 2004	7:15 PM	74.5	16.36	3.8	55.2	95	3155	3000	5200	3062.5	0.077

Table B-4: Experimental Data of Core Flood Run # 4

Sample #	Date	Time	Cumulative Time (hrs)	No. of PV Injected	Conductivity in ms	ΔP	T	Pinlet	P_{Back}	Pob	Ca^{++} Conc.	
		am / pm				psia	C	psia	psia	psia	PPM	Mole/lit
1	8/3/2004	4:15 PM	1	0.13	11.8	6.52	93	3042	3000	4800	250	0.006
2	8/3/2004	8:15 PM	4	0.47	9.9	6.3	92	3046	3000	5000	250	0.006
3	8/3/2004	10:15 PM	6	0.71	6.3	6.21	92	3055	3000	5200	1812.5	0.045
4	9/3/2004	1:15 AM	9	0.94	6	6.11	92	3022	3000	5300	2375	0.059
5	9/3/2004	1:15 PM	21	2.27	4.9	6.11	93	3044	3000	5200	3000	0.075
6	9/3/2004	5:15 AM	25	2.42	4.8	6.09	93	3058	3000	5200	3187.5	0.080
7	9/3/2004	10:15 PM	29	2.89	4.3	6.13	93	3057	3000	5300	3187.5	0.080
8	10/3/2004	12:30 PM	43.15	4.22	3.3	5.93	94	3054	3000	5400	3187.5	0.080
9	10/3/2004	4:15 PM	47	4.57	3.3	5.9	94	3048	3000	5400	3187.5	0.080
10	10/3/2004	7:15 PM	50	4.83	3.3	14.2	94	3055	3000	5400	3187.5	0.080
11	11/3/2004	10:15 PM	53	5.12	3.3	24.5	95	3063	3000	5400	3250	0.081
12	11/3/2004	1:15 AM	56	5.38	3.4	29.16	95	3084	3000	5400	3312.5	0.083
13	11/3/2004	2:45 AM	57.5	5.53	3.3	115	95	3118	3000	5400	3312.5	0.083
14	11/3/2004	3:30 AM	58.25	5.60	3.3	230	95	3246	3000	5400	3312.5	0.083
15	11/3/2004	5:00 AM	59.75	5.74	3.2	228.7	95	3277	3000	5400	3187.5	0.080
16	11/3/2004	7:00 AM	61.75	5.93	3	271.4	95	3319	3000	5400	3187.5	0.080
17	11/3/2004	10:00 AM	64.75	6.25	2.8	300	95	3340	3000	5400	3125	0.078
18	11/3/2004	12:00 PM	66.75	6.38	2.7	430	95	3503	3000	5400	3062.5	0.077
19	11/3/2004	1:30 PM	68.25	6.52	2.6	530	95	3582	3000	5400	3000	0.075
20	11/3/2004	7:15 PM	74	6.88	2.4	776	95	3635	3000	5400	2875	0.072

Table B-5: Experimental Data of Core Flood Run # 5

Sample #	**Date**	**Time**	**Commulative Time (min)**	**No. of PV Injected**	**Conductivity in ms**	**ΔP**	**T**	**Pinlet**	**P_{Back}**	**Pob**
		am / pm				**psia**	**C**	**psia**	**psia**	**psia**
1	17 / 4 / 2004	2:16 AM	1	2.47	6.8	21.5	89	3086	3000	5600
2	17 / 4 / 2004	2:45 AM	30	9.33	6.6	21.5	90	3107	3000	5600
3	17 / 4 / 2004	3:15 AM	60	19.84	3.6	332	92	3452	3000	5600
4	17 / 4 / 2004	3:30 AM	75	Stopped due to HP (Output ports Plugged)						

Table B-6: Experimental Data of Core Flood Run # 6

6

Sample #	Date	Time	Commulative Time (min)	No. of PV Injected	Conductivity in ms	ΔP	T	Pinlet	P_{Back}	Pob
		am / pm				psia	C	psia	psia	psia
1	25/4/2004	7:49 AM	1	0.88	9.1	7.3	91	3061	3000	4500
2	25/4/2004	8:00 AM	9	4.34	9.5	5.2	90	3062	3000	4500
3	25/4/2004	8:10 AM	19	61.12	9.6	6.2	92	3192	3000	4500
4	25/4/2004	8:20 AM	High Pressure due to plugging in the outlet tube							

Table B-5: Experimental Data of Core Flood Run # 7

Sample #	**Date**	**Time**	**Cumulative Time (min)**	**No. of PV Injected**	**Conductivity in ms**	**ΔP**	**T**	**Pinlet**	**P_{Back}**	**Pob**	**Ca^{++} Conc.**	
		am / pm				**psia**	**C**	**psia**	**psia**	**psia**	**PPM**	**Mole/lit**
1	6 / 5 / 2004	4:45 PM	5	4.65	9	1.5	93	3042	3000	5000	3000	0.075
2	6 / 5 / 2004	4:55 PM	15	10.78	8.6	2.8	90	3060	3000	5000	3750	0.094
3	6 / 5 / 2004	5:05 AM	25	16.70	8.8	3.1	91	3054	3000	5200	3750	0.094
4	6 / 5 / 2004	5:15 AM	35	22.98	8.6	5	90	3065	3000	5300	3750	0.094
5	6 / 5 / 2004	5:23 PM	38	29.12	8.5	20.9	91	3080	3000	5200	3562.5	0.089
6	6 / 5 / 2004	5:27 AM	42	31.53	8.4	80	92	3124	3000	5200	3312.5	0.083
7	6 / 5 / 2004	5:30 PM	45	34.04	8.3	250	92	3289	3000	5300	3312.5	0.083
8	6 / 5 / 2004	5:32 PM	47	34.11	8.4	320	92	3356	3000	5400	3250	0.081

Table B-8: Experimental Data of Core Flood Run # 8

Sample #	Date	Time	Cumulative Time (min)	No. of PV Injected	Conductivity in ms	ΔP	T	P_{inlet}	P_{Back}	P_{OB}	Ca^{++} Conc.	
		am				psia	C	psia	psia	psia	PPM	Mole/lit
1	16/5/2004	5:51 AM	1	0.78	8.8	7.2	89	3068	3000	4500	1625	0.041
2	16/5/2004	6:00 AM	10	3.54	4.7	7.4	90	3073	3000	4500	1750	0.044
3	16/5/2004	6:10 AM	20	6.68	4.5	7.6	92	3079	3000	4500	2000	0.050
4	16/5/2004	6:20 AM	30	10.09	4.4	7.8	92	3082	3000	4500	2000	0.050
5	16/5/2004	6:30 AM	40	12.91	4.2	7.8	92	3087	3000	4500	1937.5	0.048
6	16/5/2004	6:40 AM	50	16.28	4.1	7.9	92	3092	3000	4500	1875	0.047
7	16/5/2004	6:50 AM	60	19.49	3.9	8	92	3096	3000	4500	2062.5	0.052
8	16/5/2004	7:00 AM	70	23.05	3.9	8.1	92	3099	3000	4500	2062.5	0.052
9	16/5/2004	7:10 AM	80	26.87	3.9	8.3	92	3112	3000	4500	2000	0.050
10	16/5/2004	7:20 AM	90	29.83	3.8	8.4	92	3122	3000	4500	1750	0.044
11	16/5/2004	7:30 AM	100	32.82	3.9	8.5	92	3122	3000	4500	1875	0.047
12	16/5/2004	7:40 AM	110	36.41	4.3	8.6	92	3126	3000	4500	1937.5	0.048
13	16/5/2004	7:50 AM	120	39.75	4.4	8.7	92	3130	3000	4500	2125	0.053
14	16/5/2004	8:00 AM	130	42.95	4.3	8.8	92	3134	3000	4500	2000	0.050
15	16/5/2004	8:10 AM	140	46.29	4	8.9	92	3139	3000	4600	2000	0.050
16	16/5/2004	8:20 AM	150	50.30	4.2	9	92	3143	3000	4600	2000	0.050
17	16/5/2004	8:28 AM	158	53.11	4.2	9	92	3151	3000	4800	2000	0.050
18	16/5/2004	8:35 AM	165	55.18	4.2	9.1	92	3157	3000	4800	2000	0.050
19	16/5/2004	8:42 AM	172	57.52	4.2	9.2	92	3160	3000	4800	2062.5	0.052
20	16/5/2004	8:49 AM	179	59.92	4.3	9.3	92	3162	3000	4800	2125	0.053
21	16/5/2004	8:57 AM	187	62.99	4.2	9.4	92	3167	3000	4800	1812.5	0.045
22	16/5/2004	9:08 AM	198	66.40	3.8	9.4	92	3173	3000	4800	1875	0.047

Table B-9: Experimental Data of Core Flood Run # 9

Sample #	**Date**	**Time**	**Comulative Time (min)**	**No. of PV Injected**	**Conductivity in ms**	**ΔP**	**T**	**Pinlet**	**P_{Back}**	**Pob**	**Ca^{++} Conc.**	
		am / pm				**psia**	**C**	**psia**	**psia**	**psia**	**PPM**	**Mole/lit**
1	23/5/2004	5:25 PM	5	5.49	5.3	6.7	92	3068	3000	4500	3000	0.075
2	23/5/2004	5:33 PM	13	11.60	4.4	7	93	3073	3000	4500	2875	0.072
3	23/5/2004	5:41 PM	21	16.94	4.5	7.4	92	3079	3000	4500	2937.5	0.073
4	23/5/2004	5:50 PM	30	24.19	4.5	7.6	92	3082	3000	4500	2875	0.072
5	23/5/2004	6:00 PM	40	31.63	4.6	7.9	92	3087	3000	4500	2750	0.069
6	23/5/2004	6:10 PM	50	39.50	4.6	8.3	92	3092	3000	4500	2750	0.069
7	23/5/2004	6:20 PM	60	46.62	4.5	8.7	92	3096	3000	4500	2875	0.072
8	23/5/2004	6:30 PM	70	54.19	4.5	9.2	92	3099	3000	4500	2500	0.063
9	23/5/2004	6:40 PM	80	61.32	4.4	9.6	92	3112	3000	4500	2875	0.072
10	23/5/2004	6:50 PM	90	68.60	4.1	10	94	3122	3000	4500	2875	0.072
11	23/5/2004	7:00 PM	100	76.32	3.6	10.5	93	3122	3000	4500	3062.5	0.077
12	23/5/2004	7:10 PM	110	84.04	3.1	11	92	3126	3000	4500	2812.5	0.070
13	23/5/2004	7:20 PM	120	91.91	4.9	11.7	90	3130	3000	4500	2625	0.066
14	23/5/2004	7:30 PM	130	98.89	4.7	12	91	3134	3000	4500	2812.5	0.070
15	23/5/2004	7:45 PM	145	109.73	4.2	12.6	91	3139	3000	4600	2812.5	0.070
16	23/5/2004	7:55 PM	155	118.04	3.9	13.1	91	3143	3000	4600	2750	0.069
17	23/5/2004	8:05 PM	165	125.61	3.1	14.2	91	3151	3000	4800	2762.5	0.069
18	23/5/2004	8:15 PM	175	131.55	2.7	14.6	92	3157	3000	4800	2731.25	0.068
19	23/5/2004	8:25 PM	185	139.27	5.4	15	92	3160	3000	4800	2762.5	0.069
20	23/5/2004	8:30 PM	190	143.13	5.1	15.5	91	3162	3000	4800	2756.25	0.069

Table B-10: Experimental Data of Core Flood Run # 10

Sample #	Date	Time	Comulative Time (min)	No. of PV Injected	Conductivity in ms	ΔP	T	Pinlet	P_{Back}	Pob	Ca^{++} Conc.	
		am / pm				psia	C	psia	psia	psia	PPM	Mole/lit
1	27 / 5 / 2004	9:56 AM	0	2.14	3.6	9.2	68	3079	3000	4500	0	0.000
2	27 / 5 / 2004	10:03 AM	7	5.21	3.9	9.4	68	3086	3000	4500	3056.25	0.076
3	27 / 5 / 2004	10:09 AM	13	9.22	4.2	9.5	72	3091	3000	4500	2625	0.066
4	27 / 5 / 2004	10:13 AM	17	12.02	4.4	9.6	74	3097	3000	4500	2937.5	0.073
5	27 / 5 / 2004	10:20 AM	24	16.70	4.5	9.7	72	3101	3000	4500	2937.5	0.073
6	27 / 5 / 2004	10:28 AM	32	22.04	4.4	9.8	71	3105	3000	4500	2937.5	0.073
7	27 / 5 / 2004	10:35 AM	38	26.85	4.3	9.9	70	3106	3000	4500	3000	0.075
8	27 / 5 / 2004	10:45 AM	48	33.40	3.6	10	70	3109	3000	4500	3000	0.075
9	27 / 5 / 2004	10:53 AM	56	38.88	3.5	10	70	3115	3000	4500	2937.5	0.073
10	27 / 5 / 2004	11:00 AM	63	42.89	3.5	10.2	70	3117	3000	4500	3062.5	0.077
11	27 / 5 / 2004	11:10 AM	73	50.10	3.3	10.3	71	3122	3000	4500	2875	0.072
12	27 / 5 / 2004	11:20 AM	83	56.91	3.2	10.4	70	3134	3000	4500	2875	0.072
13	27 / 5 / 2004	11:30 AM	93	63.59	3.2	10.5	70	3138	3000	4500	2812.5	0.070
14	27 / 5 / 2004	11:40 AM	103	70.27	3	10.7	70	3140	3000	4500	2750	0.069
15	27 / 5 / 2004	11:50 AM	113	76.42	2.8	10.8	70	3142	3000	4500	2875	0.072
16	27 / 5 / 2004	12:00 PM	123	83.50	2.5	10.9	70	3144	3000	4500	2812.5	0.070
17	27 / 5 / 2004	12:10 PM	133	90.71	5.1	11.1	70	3148	3000	4500	2937.5	0.073
18	27 / 5 / 2004	12:20 PM	143	97.26	5.2	11.2	70	3150	3000	4500	2937.5	0.073
19	27 / 5 / 2004	12:32 PM	155	105.14	5.1	11.4	70	3153	3000	4500	2875	0.072
20	27 / 5 / 2004	12:40 PM	163	110.43	5.1	11.6	70	3160	3000	4500	2875	0.072
21	27 / 5 / 2004	12:47 PM	170	116.09	4.9	11.8	71	3160	3000	4500	2812.5	0.070
22	27 / 5 / 2004	12:53 PM	176	118.93	4.8	12	71	3164	3000	4500	2812.5	0.070
23	27 / 5 / 2004	1:00 PM	183	123.58	4.7	12.2	71	3173	3000	4500	2875	0.072
24	27 / 5 / 2004	1:05 PM	188	127.19	4.7	12.3	70	3175	3000	4500	2875	0.072

Table B-11: Experimental Data of Core Flood Run # 11

Sample #	Date	Time	Cumulative Time (min)	No. of PV Injected	Conductivity in ms	ΔP	T	Pinlet	P_{Back}	Pob	Ca^{++} Conc.	
		am / pm				psia	C	psia	psia	psia	PPM	Mole/lit
1	31 / 5 / 2004	10:47 PM	0	1.72	7.3	0.1	44	3074	3000	4500	0	0.000
2	31 / 5 / 2004	10:48 PM	1	2.58	3.9	0.3	45	3078	3000	4500	125	0.003
3	31 / 5 / 2004	10:56 PM	9	6.87	3.7	0.5	44	3081	3000	4500	500	0.013
4	31 / 5 / 2004	11:05 PM	18	12.46	3.6	0.8	45	3088	3000	4500	3043.75	0.076
5	31 / 5 / 2004	11:15 PM	28	20.19	3.4	1.1	45	3098	3000	4500	3050	0.076
6	31 / 5 / 2004	11:25 PM	38	27.34	2.7	1.3	45	3100	3000	4500	3047.5	0.076
7	31 / 5 / 2004	11:35 PM	48	34.65	2.3	1.4	45	3101	3000	4500	3056.25	0.076
8	31 / 5 / 2004	11:45 PM	58	41.66	2	1.5	45	3105	3000	4500	3056.25	0.076
9	31 / 5 / 2004	11:50 PM	63	48.96	4.3	1.7	45	3109	3000	4500	3000	0.075
10	31 / 5 / 2004	12:05 AM	73	67.50	4	1.5	44	3113	3000	4500	3000	0.075
11	31 / 5 / 2004	12:26 AM	84	78.60	3.6	1.6	43	3115	3000	4500	3012.5	0.075
12	31 / 5 / 2004	12:41 AM	99	87.62	3.5	2	44	3119	3000	4500	3018.75	0.075
13	31 / 5 / 2004	12:53 AM	111	96.21	3.2	2.3	45	3114	3000	4500	3031.25	0.076
14	31 / 5 / 2004	1:05 AM	123	111.22	2.3	2.5	45	3117	3000	4500	3031.25	0.076
15	31 / 5 / 2004	1:26 AM	144	118.83	2	2.8	45	3122	3000	4500	3043.75	0.076
16	31 / 5 / 2004	1:37 AM	155	128.70	4.3	2.9	45	3123	3000	4500	3037.5	0.076
17	31 / 5 / 2004	1:50 AM	168	136.29	3.8	3	45	2125	3000	4500	3043.75	0.076
18	31 / 5 / 2004	2:01 AM	179	140.01	3.6	3.2	45	2130	3000	4500	3043.75	0.076

Table B-12: Experimental Data of Core Flood Run # 12

Sample #	**Date**	**Time**	**Cumulative Time (min)**	**Volume Injected**	**Conductivity in ms**	**ΔP**	**T**	**Pinlet**	**P_{Back}**	**Pob**	**Ca^{++} Conc.**	
		am / pm		**ml**		**psia**	**C**	**psia**	**psia**	**psia**	**PPM**	**Mole/lit**
1	2 / 6 / 2004	5.55 am	0	30	2.8	3.8	92	633	500	1000	187.5	0.005
2	2 / 6 / 2004	6:00 am	5	59	2.4	4.1	93	635	500	1000	2750	0.069
3	2 / 6 / 2004	6.23 am	28	175	2.2	4.4	94	637	500	1000	3031.25	0.076
4	2 / 6 / 2004	6.30 am	35	208	3.5	4.5	95	638	500	1000	3059.375	0.076
5	2 / 6 / 2004	6.40 am	45	261	3.4	4.6	94	639	500	1000	2875	0.072
6	2 / 6 / 2004	6.51 am	56	315	3	4.8	95	640	500	1000	3000	0.075
7	2 / 6 / 2004	7:00 am	66	366	2.7	4.9	95	641	500	1000	2812.5	0.070
8	2 / 6 / 2004	7.10 am	75	415	4.2	15.5	95	655	500	1000	2750	0.069
9	2 / 6 / 2004	7.24 am	89	483	3.6	140.6	95	700	500	1000	2562.5	0.064
10	2 / 6 / 2004	7.28 am	93	580	3.2	350	95	754	500	1000	2562.5	0.064

Table B-13: Experimental Data of Core Flood Run # 13

Sample #	Date	Time	Cumulative Time (min)	No. of PV Injected	Conductivity in ms	ΔP	T	Pinlet	P_{Back}	Pob	Ca^{++} Conc.	
		am / pm				psia	C	psia	psia	psia	PPM	Mole/lit
1	31 / 8 / 2004	7:54 AM	0	0.19	4.7	4	92	110	100	500	0	0.000
2	31 / 8 / 2004	7:55 AM	1	1.66	2.9	3.9	93	115	100	500	1437.5	0.036
3	31 / 8 / 2004	8:01 AM	7	6.16	3	3.8	94	117	100	500	2562.5	0.064
4	31 / 8 / 2004	8:05 AM	11	9.59	3.2	3.5	95	120	100	500	3062.5	0.077
5	31 / 8 / 2004	8:10 AM	16	12.01	3.2	3.3	95	123	100	500	2625	0.066
6	31 / 8 / 2004	8:15 AM	21	15.55	3.3	3.3	95	124	100	500	2750	0.069
7	31 / 8 / 2004	8:20 AM	26	18.75	3.4	3.3	95	126	100	500	2687.5	0.067
8	31 / 8 / 2004	8:30 AM	36	25.48	3.4	3.4	95	127	100	500	2750	0.069
9	31 / 8 / 2004	8:40 AM	46	32.07	3.5	3.5	95	130	100	500	2687.5	0.067
10	31 / 8 / 2004	8:50 AM	56	39.51	3.5	3.9	95	134	100	500	2687.5	0.067
11	31 / 8 / 2004	9:00 AM	66	46.53	3.5	4.2	95	136	100	500	2625	0.066
12	31 / 8 / 2004	9:10 AM	76	53.54	3.5	4.6	95	139	100	500	2750	0.069
13	31 / 8 / 2004	9:17 AM	83	59.56	4.7	10.5	95	150	100	500	2562.5	0.064
14	31 / 8 / 2004	9:25 AM	91	65.00	3.8	11.5	95	167	100	700	2750	0.069
15	31 / 8 / 2004	9:33 AM	99	70.87	3.5	189	95	292	100	1000	2687.5	0.067
16	31 / 8 / 2004	9:37 AM	103	75.02	3.1	343.9	95	456	100	1000	2375	0.059

Table B-14: Experimental Data of Core Flood Run # 14

Sample #	**Date**	**Time**	**Cumulative Time (min)**	**No. of PV Injected**	**Conductivity in ms**	**ΔP**	**T**	**Pinlet**	**P_{Back}**	**Pob**	**Ca^{++} Conc.**	
		am / pm				**psia**	**C**	**psia**	**psia**	**psia**	**PPM**	**Mole/lit**
1	5/9/2004	8:25 AM	0	2.47	3.3	3.6	92	3162	3000	4500	0	0.000
2	5/9/2004	8:27 AM	2	3.39	2.7	3.7	93	3165	3000	4500	2375	0.059
3	5/9/2004	8:30 AM	5	6.32	2.9	3.9	92	3173	3000	4500	3562.5	0.089
4	5/9/2004	8:35 AM	10	10.49	3	4.1	94	3174	3000	4500	3375	0.084
5	5/9/2004	8:45 AM	20	17.27	3.1	4.4	95	3184	3000	4600	3375	0.084
6	5/9/2004	8:55 AM	30	24.98	2.4	4.7	95	3187	3000	4700	3500	0.088
7	5/9/2004	9:03 AM	33	30.69	2	5	95	3191	3000	4800	3437.5	0.086
8	5/9/2004	9:10 AM	43	37.16	3.9	5.2	95	3194	3000	4800	3437.5	0.086
9	5/9/2004	9:20 AM	53	43.95	3.7	5.5	95	3197	3000	4800	3562.5	0.089
10	5/9/2004	9:30 AM	63	51.97	3.5	5.9	95	3201	3000	4800	3562.5	0.089
11	5/9/2004	9:40 AM	73	59.98	3.3	6.2	95	3204	3000	4800	3500	0.088
12	5/9/2004	9:50 AM	83	67.39	3.2	6.5	95	3207	3000	4800	3500	0.088
13	5/9/2004	10:00 AM	93	75.10	3	6.9	95	3217	3000	4800	3437.5	0.086
14	5/9/2004	10:10 AM	103	82.81	2.3	7.3	95	3224	3000	4800	3437.5	0.086
15	5/9/2004	10:20 AM	113	90.36	4.4	7.7	95	3227	3000	4800	3312.5	0.083
16	5/9/2004	10:30 AM	123	98.07	3.8	8.4	95	3236	3000	4800	3312.5	0.083
17	5/9/2004	10:40 AM	133	104.86	3.7	11.4	95	3243	3000	4800	3312.5	0.083
18	5/9/2004	10:50 AM	143	112.57	3.6	38.6	95	3278	3000	4800	3375	0.084
19	5/9/2004	10:54 AM	147	117.19	3.5	123.3	95	3356	3000	4800	3375	0.084
20	5/9/2004	10:57 AM	150	118.89	3.1	324.9	95	3547	3000	4800	3375	0.084

Table B-15: Experimental Data of Core Flood Run # 15

Sample #	**Date**	**Time**	**Cumulative Time (min)**	**No. of PV Injected**	**Conductivity in ms**	**ΔP**	**T**	**Pinlet**	**P_{Back}**	**Pob**	**Ca^{++} Conc.**	
		am / pm				**psia**	**C**	**psia**	**psia**	**psia**	**PPM**	**Mole/lit**
1	29/9/2004	10:40 PM	0	0.46	3.5	9.5	92	3143	3000	4800	62.5	0.002
2	29/9/2004	10:43 PM	3	2.00	1.3	9.7	93	3145	3000	4800	562.5	0.014
3	29/9/2004	10:50 PM	10	4.06	0.7	9.7	94	3101	3000	4800	2250	0.056
4	29/9/2004	11:00 PM	20	7.83	0.8	9.8	94	3113	3000	4800	2812.5	0.070
5	29/9/2004	11:21 PM	41	15.71	0.7	9.9	94	3124	3000	4800	2937.5	0.073
6	29/9/2004	11:40 PM	60	22.82	0.7	9.9	94	3131	3000	4800	2937.5	0.073
7	29/9/2004	12:00 AM	80	30.84	0.7	10	94	3138	3000	4800	2937.5	0.073
8	29/9/2004	12:21 AM	101	38.95	0.7	10.1	94	3145	3000	4800	2875	0.072
9	29/9/2004	12:40 AM	120	46.26	0.8	10.1	94	3152	3000	4800	2875	0.072
10	29/9/2004	1:00 AM	140	53.82	0.8	10.1	95	3157	3000	4800	2843.75	0.071
11	29/9/2004	1:20 AM	160	61.68	0.8	10.1	95	3164	3000	4800	2843.75	0.071
12	29/9/2004	1:41 AM	181	69.55	0.8	10.1	95	3168	3000	4800	2837.5	0.071
13	29/9/2004	2:00 AM	200	77.10	0.8	10.1	95	3177	3000	4800	2840.625	0.071
14	29/9/2004	2:23 AM	223	84.81	0.8	10.1	95	3185	3000	4800	2850	0.071
15	29/9/2004	2:40 AM	240	92.52	0.8	10.2	95	3192	3000	4800	2850	0.071
16	29/9/2004	3:00 AM	260	100.23	0.8	10.2	95	3198	3000	4800	2837.5	0.071
17	29/9/2004	3:20 AM	280	107.79	0.8	10.3	95	3205	3000	4800	2837.5	0.071
18	29/9/2004	3:41 AM	301	116.11	0.8	10.3	95	3215	3000	4800	2843.75	0.071
19	29/9/2004	4:04 AM	324	124.75	0.8	10.4	95	3224	3000	4800	2843.75	0.071
20	29/9/2004	4:20 AM	340	130.45	0.6	10.5	95	3232	3000	4800	2825	0.071

Table B-16: Experimental Data of Core Flood Run # 16

Sample #	Date	Time	Cumulative Time (min)	No. of PV Injected	Conductivity in ms	ΔP	T	Pinlet	P_{Back}	Pob	Ca^{++} Conc.	
		am / pm				psia	C	psia	psia	psia	PPM	Mole/lit
1	4 / 10 / 2004	12:23 AM	1	15.42	4.3	7.9	92	3103	3000	4500	62.5	0.002
2	4 / 10 / 2004	12:24 AM	2	24.67	3.6	8.1	93	3106	3000	4900	750	0.019
3	4 / 10 / 2004	12:29 AM	7	33.00	1.6	8.2	94	3109	3000	4900	2812.5	0.070
4	4 / 10 / 2004	12:35 AM	12	38.55	1.8	8.3	95	3118	3000	4900	2875	0.072
5	4 / 10 / 2004	12:40 AM	17	44.72	1.8	8.3	95	3124	3000	4900	2875	0.072
6	4 / 10 / 2004	12:45 AM	22	50.73	1.6	8.4	95	3128	3000	4900	2875	0.072
7	4 / 10 / 2004	12:52 AM	29	58.91	1.3	8.4	95	3136	3000	4900	2875	0.072
8	4 / 10 / 2004	1:00 AM	37	68.93	1.3	8.4	95	3142	3000	4900	2937.5	0.073
9	4 / 10 / 2004	1:07 AM	44	75.56	2.2	8.5	95	3149	3000	4900	2875	0.072
10	4 / 10 / 2004	1:15 AM	52	84.81	2	8.6	95	3154	3000	4900	2862.5	0.072
11	4 / 10 / 2004	1:23 AM	60	95.14	2.1	8.7	95	3160	3000	4900	2862.5	0.072
12	4 / 10 / 2004	1:30 AM	67	103.01	2	8.8	95	3168	3000	4900	2793.75	0.070
13	4 / 10 / 2004	1:37 AM	74	111.18	1.9	8.9	95	3175	3000	4900	2762.5	0.069
14	4 / 10 / 2004	1:45 AM	82	120.43	1.8	9	95	3181	3000	4900	2781.25	0.070
15	4 / 10 / 2004	1:53 AM	90	130.15	1.7	9.2	95	3186	3000	4900	2750	0.069
16	4 / 10 / 2004	2:00 AM	97	137.39	1.5	9.3	95	3192	3000	4900	2812.5	0.070
17	4 / 10 / 2004	2:07 AM	104	145.41	1.4	9.5	95	3200	3000	4900	2750	0.069
18	4 / 10 / 2004	2:15 AM	112	155.74	1.3	9.7	95	3213	3000	4900	2750	0.069
19	4 / 10 / 2004	2:20 AM	117	160.37	2.3	9.7	95	3222	3000	4900	2768.75	0.069
20	4 / 10 / 2004	2:25 AM	122	166.54	2.2	9.9	95	3233	3000	4900	2750	0.069
21	4 / 10 / 2004	2:30 AM	127	171.16	2	10.1	95	3250	3000	4900	2756.25	0.069

Table B-17: Experimental Data of Core Flood Run # 17

Sample #	**Date**	**Time**	**Cumulative Time (hrs)**	**No. of PV Injected**	**Conductivity in ms**	**ΔP**	**T**	**Pinlet**	**P_{Back}**	**Pob**	**Ca^{++} Conc.**	
		am / pm				**psia**	**C**	**psia**	**psia**	**psia**	**PPM**	**Mole/lit**
1	10/10/2004	11:55 PM	0	0.84	2.8	4.6	94	3184	3000	4600	187.5	0.005
2	10/10/2004	11:56 PM	0.02	3.16	2	3.8	93	3188	3000	4600	687.5	0.017
3	11/10/2004	12:20 AM	0.42	17.32	1.5	2.9	95	3193	3000	4600	3000	0.075
4	11/10/2004	1:02 AM	1.12	20.47	0.7	2.9	95	3197	3000	4600	2937.5	0.073
5	11/10/2004	2:00 AM	2.08	24.62	0.8	2.9	95	3215	3000	4600	3000	0.075
6	11/10/2004	3:06 AM	3.18	29.43	0.7	2.9	95	3236	3000	4600	3000	0.075
7	11/10/2004	4:10 AM	4.25	33.96	0.7	2.9	95	3255	3000	4600	3000	0.075
8	11/10/2004	5:00 AM	5.08	37.54	0.7	2.9	95	3270	3000	4600	2937.5	0.073
9	11/10/2004	8:53 AM	8.97	54.26	0.6	2.8	95	3274	3000	4600	2937.5	0.073
10	11/10/2004	11:53 AM	11.97	67.00	0.5	1.7	95	3319	3000	4600	2875	0.072
11	12/10/2004	1:35 PM	13.67	74.30	0.5	1.7	95	3293	3000	4600	2875	0.072
12	12/10/2004	4:00 PM	16.08	84.75	0.5	1.7	95	3289	3000	4600	2937.5	0.073
13	12/10/2004	5:55 PM	18.00	93.06	0.4	1.7	95	3299	3000	4600	2875	0.072
14	12/10/2004	8:43 PM	20.80	104.94	0.4	1.7	95	3303	3000	4600	2812.5	0.070
15	12/10/2004	10:15 PM	22.33	111.38	0.4	1.6	95	3308	3000	4600	2812.5	0.070
16	12/10/2004	11:30 PM	23.58	116.96	0.4	1.5	95	3335	3000	4600	2812.5	0.070
17	13/10/2004	12:50 AM	24.92	122.55	0.4	1.4	95	3355	3000	4600	2812.5	0.070
18	13/10/2004	1:45 AM	25.83	126.70	0.4	1.4	95	3372	3000	4600	2812.5	0.070
19	13/10/2004	3:15 AM	27.25	132.93	0.4	1.4	95	3383	3000	4600	2812.5	0.070

Table B-18: Experimental Data of Core Flood Run # 18

Sample #	**Date**	**Time**	**Cumulative Time (min)**	**No. of PV Injected**	**Conductivity in ms**	**ΔP**	**T**	**Pinlet**	**P_{Back}**	**Pob**	**Ca^{++} Conc.**	
		am / pm				**psia**	**C**	**psia**	**psia**	**psia**	**PPM**	**Mole/lit**
1	25 / 10 / 2004	1:23 AM	1	0.12	3	0.5	89	3126	3000	4500	62.5	0.0016
2	25 / 10 / 2004	1:24 AM	2	0.87	2.5	0.8	90	3150	3000	4600	187.5	0.0047
3	25 / 10 / 2004	1:29 AM	7	14.96	1.8	1.5	90	3168	3000	4600	2875	0.0719
4	25 / 10 / 2004	1:38 AM	16	30.30	1.8	2.9	89	3171	3000	4600	2750	0.0688
5	25 / 10 / 2004	1:45 AM	23	39.94	1.8	3.7	90	3184	3000	4600	2750	0.0688
6	25 / 10 / 2004	1:50 AM	28	48.84	1.8	4.5	90	3192	3000	4600	2813	0.0703
7	25 / 10 / 2004	2:00 AM	38	63.05	1.7	6	90	3210	3000	4600	2875	0.0719
8	25 / 10 / 2004	2:07 AM	45	74.63	1.6	7.5	90	3222	3000	4600	2875	0.0719
9	25 / 10 / 2004	2:16 AM	54	88.33	1.5	9.4	90	3236	3000	4600	2844	0.0711
10	25 / 10 / 2004	2:22 AM	60	97.15	1.5	10.6	90	3241	3000	4600	2863	0.0716
11	25 / 10 / 2004	2:30 AM	68	110.08	1.4	11.9	90	3251	3000	4600	2850	0.0713
12	25 / 10 / 2004	2:39 an	77	122.74	1.3	13.8	90	3265	3000	4600	2850	0.0713
13	25 / 10 / 2004	2:45 AM	83	132.31	2.5	14.9	90	3277	3000	4600	2850	0.0713
14	25 / 10 / 2004	2:50 AM	88	140.85	2.3	16.2	90	3288	3000	4600	2850	0.0713
15	25 / 10 / 2004	2:55 AM	93	148.77	2.3	16.9	90	3299	3000	4600	2850	0.0713
16	25 / 10 / 2004	3:00 AM	98	154.97	2.1	17.5	90	3315	3000	4600	2854	0.0714

Table B-19: Experimental Data of Core Flood Run # 19

Sample #	**Date**	**Time**	**Cumulative Time (min)**	**No. of PV Injected**	**Conductivity in ms**	**ΔP**	**T**	**Pinlet**	**P_{Back}**	**Pob**	**Ca^{++} Conc.**	
		am / pm				**psia**	**C**	**psia**	**psia**	**psia**	**PPM**	**Mole/lit**
1	27 / 10 / 2004	12:11 AM	1	1.36	4.4	31.8	50	3082	3000	4500	250	0.006
2	27 / 10 / 2004	12:12 AM	2	3.73	2.3	33.3	50	3086	3000	4500	1938	0.048
3	27 / 10 / 2004	12:15 AM	5	8.55	2	35.2	50	3095	3000	4500	6375	0.159
4	27 / 10 / 2004	12:20 AM	10	16.03	1.9	37.7	50	3098	3000	4800	6375	0.159
5	27 / 10 / 2004	12:25 AM	15	24.58	1.5	40.3	50	3100	3000	4800	6438	0.161
6	27 / 10 / 2004	12:30 AM	20	32.82	1.3	43	50	3106	3000	4800	6444	0.161
7	27 / 10 / 2004	12:35 AM	25	40.08	2.2	45.5	50	3109	3000	4800	6438	0.161
8	27 / 10 / 2004	12:40 AM	30	49.62	1.9	47.8	50	3111	3000	4800	6441	0.161
9	27 / 10 / 2004	12:45 AM	35	57.85	1.7	50.3	50	3114	3000	4800	6440	0.161
10	27 / 10 / 2004	12:50 AM	40	66.13	1.5	52.7	50	3116	3000	4800	6440	0.161
11	27 / 10 / 2004	12:57 AM	47	77.76	2.5	55.9	50	3119	3000	4800	6440	0.161
12	27 / 10 / 2004	1:05 AM	55	91.32	2.4	59.6	50	3122	3000	4800	6440	0.161
13	27 / 10 / 2004	1:15 AM	65	107.76	1.8	64.5	50	3128	3000	4800	6440	0.161
14	27 / 10 / 2004	1:20 AM	70	116.37	1.7	66.9	50	3132	3000	4800	6440	0.161
15	27 / 10 / 2004	1:25 AM	75	125.05	1.6	69.1	50	3137	3000	4800	6440	0.161

Table B-20: Experimental Data of Core Flood Run # 20

Sample #	Date	Time	Cumulative Time (min)	No. of PV Injected	Conductivity in ms	ΔP	T	Pinlet	P_{Back}	Pob	Ca⁺⁺ Conc.	
		am / pm				psia	C	psia	psia	psia	PPM	Mole/lit
1	27 / 10 / 2004	11:20 PM	0	1.34	5.5	5.3	85	3040	3000	4500	125	0.003
2	27 / 10 / 2004	11:21 PM	1	3.61	1.6	6.1	85	3056	3000	4500	2875	0.0719
3	27 / 10 / 2004	11:25 PM	5	8.78	1.2	6.9	85	3065	3000	4500	2875	0.0719
4	27 / 10 / 2004	11:40 PM	20	19.66	1.3	7.6	85	3078	3000	4800	2813	0.0703
5	27 / 10 / 2004	11:51 PM	31	24.72	1.2	8.1	85	3090	3000	4800	2688	0.0672
6	28 / 10 / 2004	12:05 AM	40	31.38	0.9	7.9	85	3101	3000	4800	2750	0.0688
7	28 / 10 / 2004	12:20 AM	55	38.34	1.9	8.9	85	3109	3000	4800	2781	0.0695
8	28 / 10 / 2004	12:36 AM	71	45.70	1.9	9.5	85	3111	3000	4800	2794	0.0698
9	28 / 10 / 2004	12:53 AM	88	53.65	1.8	10.5	85	3114	3000	4900	2794	0.0698
10	28 / 10 / 2004	1:15 AM	111	64.25	1.7	11.6	85	3116	3000	4900	2794	0.0698
11	28 / 10 / 2004	1:31 AM	127	71.82	1.6	12.5	85	3119	3000	4900	2794	0.0698
12	28 / 10 / 2004	1:50 AM	146	80.39	1.4	13.9	85	3122	3000	4900	2795	0.0699
13	28 / 10 / 2004	2:05 AM	161	87.59	1.3	14.7	85	3128	3000	4900	2795	0.0699
14	28 / 10 / 2004	2:20 AM	176	94.32	1.2	15.5	85	3132	3000	4900	2794	0.0698
15	28 / 10 / 2004	2:35 AM	191	101.40	1.2	16.1	85	3137	3000	4900	2795	0.0699
16	28 / 10 / 2004	2:50 AM	206	108.64	1.1	16.9	85	3154	3000	4900	2795	0.0699
17	28 / 10 / 2004	3:06 AM	222	115.83	2	17.3	85	3178	3000	4900	2795	0.0699
18	28 / 10 / 2004	3:15 AM	231	119.97	2	17.5	85	3184	3000	4900	2795	0.0699
19	28 / 10 / 2004	3:25 AM	241	123.98	2	17.4	85	3196	3000	4900	2795	0.0699

Table B-21: Experimental Data of Core Flood Run # 21

Sample #	Date	Time	Cumulative Time (min)	No. of PV Injected	Conductivity in ms	ΔP	T	Pinlet	P_{Back}	Pob	Ca^{++} Conc.	
		am / pm				psia	C	psia	psia	psia	PPM	Mole/lit
1	28 / 10 / 2004	2:31 PM	1	14.37	4.3	1.3	112	3167	3000	5000	188	0.005
2	28 / 10 / 2004	2:33 PM	2	15.54	2.6	1.8	111	3179	3000	5200	2188	0.0547
3	28 / 10 / 2004	2:38 PM	7	23.56	1.5	2.1	110	3193	3000	5500	2125	0.0531
4	28 / 10 / 2004	2:45 PM	14	31.75	1.7	2.3	110	3211	3000	5500	2094	0.0523
5	28 / 10 / 2004	2:55 PM	24	44.11	1.8	2.6	110	3210	3000	5500	2105	0.0526
6	28 / 10 / 2004	3:15 PM	44	69.47	1.2	8	110	3220	3000	5500	2106	0.0526
7	28 / 10 / 2004	3:30 PM	59	88.55	1.5	9.4	110	3229	3000	5500	2104	0.0526
8	28 / 10 / 2004	3:45 PM	74	106.43	1.2	10.7	110	3251	3000	5500	2105	0.0526
9	28 / 10 / 2004	4:00 PM	89	125.48	1.9	12	110	3277	3000	5500	2105	0.0526
10	28 / 10 / 2004	4:10 PM	99	137.84	1.8	12.6	110	3300	3000	5500	2105	0.0526
11	28 / 10 / 2004	4:20 PM	109	150.54	1.6	12.9	110	3329	3000	5500	2105	0.0526
12	28 / 10 / 2004	4:25 PM	114	156.73	1.4	13	110	3367	3000	5500	2105	0.0526

VITAE

NAME: Syed Jawwad Ahmed

ADDRESS: A-13, Haroon Heights, Sector 11-K,
North Karachi, Karachi,
PAKISTAN.

E-MAIL: sjawwad@kfupm.edu.sa

DATE OF BIRTH: July, 8 1974

NATIONALITY: Pakistani

EDUCATIONAL QUALIFICATION:

M.S ***(Petroleum Engineering)***
December 2004
King Fahd University of Petroleum and Minerals
Dhahran, Saudi Arabia.

B.E. ***(Mechanical Engineering)***
December 1998.
NED University of Engineering & Technology, Karachi,
Pakistan.